ST. ANTHONY FALLS HYDRAULIC LABORATORY
UNIVERSITY OF MINNESOTA

Project Report No. 44

EXPERIMENTAL STUDIES OF WAVE FILTERS AND ABSORBERS

Submitted by
LORENZ G. STRAUB
Director

Prepared by
JOHN B. HERBICH

January 1956

Prepared for the
DAVID TAYLOR MODEL BASIN
Department of the Navy
Washington, D.C.

Office of Naval Research Contract Nonr-710(05)

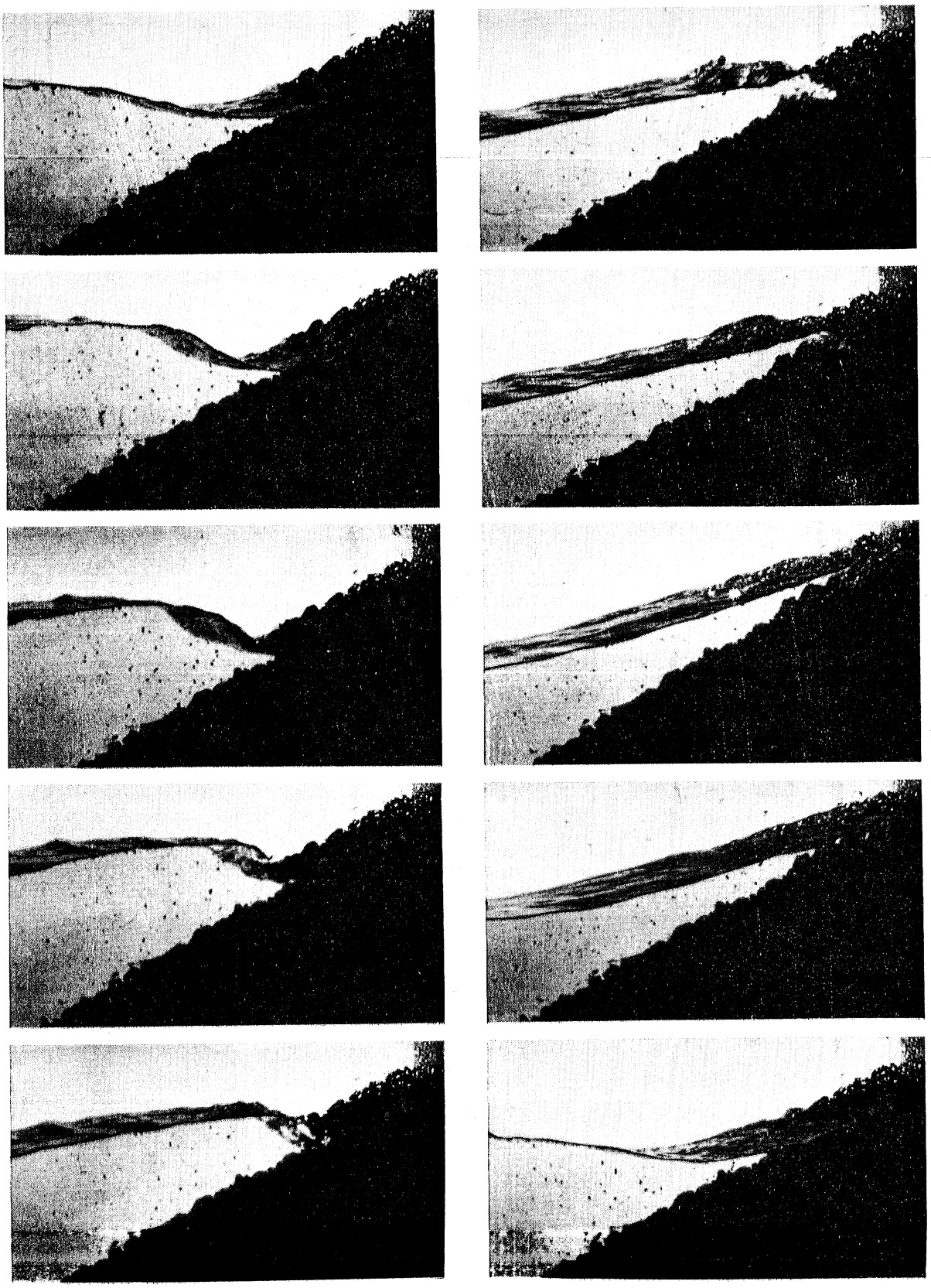

Wave Breaking on a Crushed-Rock Absorber

PREFACE

Contract Nonr-710(05) between the University of Minnesota, St. Anthony Falls Hydraulic Laboratory and David Taylor Model Basin, Bureau of Ships, Department of the Navy, provides for an experimental investigation of certain types of laboratory equipment necessary for studies involving gravity waves.

Initially three items in particular were suggested for detailed study, namely:

(1) wave absorbers
(2) wave filters
(3) wave generators.

In accordance with the expressed interest of the Sponsor, the studies under the initial proposal were largely restricted to an investigation of wave absorbers. A limited number of tests were conducted on wave filters, primarily to obtain information which would contribute to the study of absorbers. Studies of wave generators were confined to a review of available literature on this subject. Under the initial proposal one project report, "Laboratory Surface Wave Equipment, A Summary of Literature," was prepared; and a second project report, a translation of selected articles on wave generators, was made available for the use of the Sponsor [13] [3]*.

The program under the second proposal has been restricted to wave absorbers with the primary objective of providing experimental data to assist in the design of an efficient, inexpensive absorber of minimum length for the proposed Maneuvering Basin.

Initial, comprehensive experiments were conducted in a small wave channel and later tests were performed in a large wave channel. The main object of large-scale tests was a check on possible scale effect which might exist in extrapolating the small-scale data to larger facilities.

The present Project Report describing studies performed at the St. Anthony Falls Hydraulic Laboratory is intended to provide a summary of results of studies in the small facility, a channel 6 in. wide and 40 ft long. The primary experiments involved measurements of wave characteristics (such

*Numbers in brackets refer to bibliography on p. 81.

as wave height, length, profile) and coefficient of reflection for various types of filters and absorbers. The more important experimental results are presented to show the relationship between wave attenuation and wave length and filter length for wave filters, and the relationship between coefficient of reflection and wave steepness and wave length for wave absorbers.

The main body of the report is devoted to a summary description of the most important variables affecting wave absorption which might be of help in designing a filter or an absorber. As tests of filters were limited to those which would contribute to the study of absorbers, the filter data are not as comprehensive as might be desired.

In the final part of the body of the report under the heading "Applied Study," a summary of tests is given which led to the preliminary design of the prototype absorber. This design was later modified after completion of large-scale tests.

More detailed analysis of the experimental data of wave attenuation and coefficient of reflection for various filters and absorbers, as well as other pertinent information, is included in the Appendixes. Thus, Appendix A describes the "artificial viscosity" theoretical development; Appendix B, the experimental apparatus; Appendix C, the testing technique; Appendix D, the measurement of wave reflection; Appendix E, the photographic comparison of wave energy dissipation on impermeable and permeable absorbers; Appendix F, the experimental data grouped under various subheadings.

The project was under the general direction of Dr. Lorenz G. Straub, Director of the St. Anthony Falls Hydraulic Laboratory. C. E. Bowers, as project leader, supervised the studies and reviewed this report. Edward Silberman initiated the "artificial viscosity" theoretical development. The study was conducted and the report written by John B. Herbich. James A. Ross made significant contributions to the project in early stages of the work, particularly with regard to test procedures and the preliminary program. Most of the experimental work was done by Jurgen Ziegler, R. Baumeister, and D. Husby. Manuscript preparation was performed by Nancy D. Nyrop, under the general direction of Loyal A. Johnson.

A B S T R A C T

Laboratory wave studies are of importance in explaining the natural phenomena, determining the remedial measures for harbor protection and beach erosion, and providing design information for various laboratory wave installations.

The objective of the research reported here was to investigate the basic equipment and methods associated with laboratory wave studies. Of particular interest was the investigation of wave absorbers. A limited study was conducted on wave filters, primarily to obtain information which would contribute to the study of absorbers. Studies of absorbers included impermeable-beach types, as well as permeable types such as gravel, crushed rock, wire-mesh, perforated plate, round-rod, triangular wedge and rectangular bar, or a combination of these. Observations and analysis indicated that the wave absorption depends on wave characteristics, such as steepness (H_I/L) and depth-to-length ratio (d/L), as well as the absorber characteristics, such as surface slope and shape in the case of impermeable absorbers; and surface slope, shape, volume, and porosity in case of permeable absorbers. For selected wave conditions absorbers with reflection coefficients (H_R/H_I) as low as 0.02 were developed during the studies. Filters were developed which produced severe attenuation of the incident wave without causing excessive reflection. However, additional studies will be necessary to provide adequate design information for wave filters.

The absorber studies in a small channel led to a preliminary design of an efficient, inexpensive absorber of minimum length for the proposed Maneuvering Basin at the David Taylor Model Basin. The preliminary design will be checked in a large test channel.

CONTENTS

LIST OF ILLUSTRATIONS

LIST OF SYMBOLS

a, b - Wave amplitudes.

a_I - Incident wave amplitude.

C - Wave celerity.

C_g - Group celerity.

d - Water depth.

g - Acceleration of gravity.

H - Wave height.

H_I - Incident wave height.

H_ℓ - Wave envelope height at the loop.

H_n - Wave envelope height at the node.

H_R - Reflected wave height.

H_T - Transmitted wave height.

ℓ - Length of filter or absorber.

L - Wave length.

m - $\frac{2\pi}{L}$

N - Dissipation of energy per cycle per unit length of channel

p - Pressure.

P - Power.

R - Measured coefficient of reflection.

R' - Theoretical coefficient of reflection.

t - Time.

u - Horizontal component of particle orbital velocity; positive in the direction of wave velocity.

v - Vertical component of particle orbital velocity.

w - Complex potential function.

w_i - Rate of energy dissipation per unit volume.

T - Period.

V - Velocity.

x, y - Variables, coordinate axes.

α - Angle.

β - Damping coefficient.

Δ - Change.

δ - Wave steepness.

δ_0 - Wave steepness, deep water.

δ_{0I} - Incident wave steepness, deep water.

δ_{0M} - Maximum wave steepness, deep water.

η - Surface elevation.

η_I - Surface elevation for incident wave.

η_R - Surface elevation for reflected wave.

λ - Permeability coefficient.

μ - Absolute viscosity.

ν' - Artificial viscosity.

ρ - Intrinsic coefficient.

ρ_f - Density of fluid.

σ - $\frac{2\pi}{T}$.

ϕ - The real part of complex velocity potential.

$\nabla\phi$ - Gradient of $\phi = \frac{\partial\phi}{\partial x} + \frac{\partial\phi}{\partial y}$ (for two-dimensional flow).

$\overline{m}$ - Model dimensions.

$\overline{p}$ - Prototype dimensions.

EXPERIMENTAL STUDIES OF WAVE FILTERS AND ABSORBERS

I. INTRODUCTION

Because of the large number of uncontrolled variables affecting ocean waves, it is very difficult, if not impossible, to study the nature, behavior, and effect of waves in the field. Therefore, laboratory investigations are of great importance in providing explanations for natural phenomena, determining the remedial measures for harbor protection and beach erosion, and facilitating design for larger laboratory installations. In the laboratory the variables can be isolated and studied systematically in two- or three-dimensional models.

The objective of the present study was to investigate basic equipment and methods associated with laboratory wave studies. Three items were suggested for detailed study: wave generators, wave filters, and wave absorbers. In the study of the absorbers the special emphasis was on the procurement of information to assist in the design of wave absorbers for various David Taylor Model Basin installations, in particular, the Main Towing Basin and the proposed Maneuvering and Rotating-Arm Basins. In the initial study a limited investigation was conducted on wave filters, primarily to obtain information contributing to the study of absorbers. Studies of wave generators were confined to a review of available literature on the subject.

A survey of the available literature on filters and generators revealed that published information is quite limited. Some types of wave filters and absorbers were either installed or briefly investigated at various research establishments, but very little quantitative information on their performance is available. The results of the survey were prepared in the form of two project reports, one covering the summary and bibliography of literature and another describing laboratory wave generators [13][3]*.

Limited experimental studies of filters indicated that wave attenuation depended upon wave characteristics, such as steepness, depth-of-channel to length-of-wave ratio; and filter characteristics, such as length, density, and roughness. Filters were developed which produced severe attenuation of

---

*Numbers in brackets refer to the bibliography on p. 81.

the incident wave without causing excessive reflected waves. However, the study of filters was not as comprehensive as desired and has not provided adequate design information.

Studies of wave absorbers indicated that the efficiency also depended upon wave and absorber characteristics. Wave steepness and depth-to-length ratio are important, as well as shape and surface slope in case of impermeable absorbers; and shape, surface slope, volume and porosity in case of permeable absorbers. After determining the primary variables, the study was directed toward the development of an efficient absorber of minimum length for proposed installations. A preliminary design was developed using building materials of reasonable cost. This design, based on the tests in the 6-in. channel, is considered preliminary, as a possible scale effect might exist in scaling up the small model. Tests in the large facility 9 ft wide, 250 ft long, and 6 ft deep will determine the scale effect and should provide a sound basis for the design of a prototype absorber.

II. WAVE FILTERS

A. General Remarks

One of the main differences between laboratory waves and prototype waves is that in the laboratory, waves are produced at a finite distance from the model structure, while the prototype waves may be considered generated an infinite distance from the prototype structure. Similarly, in the laboratory, waves reflected from the model travel toward the wave-generating device which in turn acts as a reflector and returns the reflected wave to the model structure. The reflected wave superimposes on the generated wave to form a wave profile which might be very different from that desired. This condition does not exist in the prototype because the reflected wave, propagated seaward, has a large expanse of water in which to decay.

In the laboratory the difficulty due to reflection might be avoided or diminished through the use of a wave filter between the model and the generating device. An efficient filter would absorb part of the wave energy and reflect little or not at all. Filters might also be used to improve the quality of the incident or generated wave by reducing or eliminating harmonics of the main wave. In addition, it is possible that filters may be beneficial in reducing transverse waves which sometimes develop in laboratory wave channels.

A review of available literature [13] revealed that published information pertaining to wave filters is quite limited. The following types of filters have been investigated at various research establishments:

1. Perforated plates parallel to channel walls at Neyrpic Laboratory [2] and Vicksburg Waterways Experiment Station [9].
2. Cellular wire mesh at Vicksburg Waterways Experiment Station.
3. Vertical, circular cylinders tested by Costello at the University of California [4].
4. Plate filters tested by Meyer at Louisiana State College [9].

The only experimental data were reported by Costello and Meyer. Costello was primarily interested in the effect of various configuration of vertical, circular cylinders (piling) upon oscillatory waves. While the data obtained are of interest in the study of filters, their application is quite limited because the spacing of cylinders was so small that considerable reflection occurred. The data obtained by Meyer were for relatively short filters with very low damping characteristics; it appears that these filters were too short to yield satisfactory results. For a more detailed review of these studies, the reader is referred to SAF Project Report No. 38 [13].

B. Theoretical Considerations

At present, two published theories are available which are of interest in the analysis of filters. One was proposed by O'Brien and Chaffin [12] and another developed by Biésel [2]. O'Brien and Chaffin's theory can be used in computing the energy loss of a wave in a channel of finite depth and width. The energy loss due to friction against the bottom and sides of the channel is calculated and deducted from the wave energy. Dissipation of energy through viscous action is assumed. The velocity distribution in the boundary layer is adapted from a development by Lamb for a case of an infinite plate oscillating parallel to itself with periodic motion in an infinite fluid. The velocities outside the boundary layer are obtained from the theory of gravity waves on the surface of a frictionless liquid, and it is assumed that the wall friction has no other effect than to reduce wave heights and energies.

Taking the origin of coordinates at the intersection of the still-water surface, and one wall with x measured in the direction of wave advance,

y downward, and z perpendicular to direction of wave advance, the theory of frictionless waves to a first approximation yields as the maximum velocities at any depth, y,

$$\text{maximum horizontal velocity} = \bar{u}_y = \pm \left(\frac{\pi H}{T}\right)\left\{\frac{\cosh\left[(2\pi/L)\ (d - y)\right]}{\sinh\ (2\pi d/L)}\right\} \quad (1)$$

$$\text{maximum vertical velocity} = \bar{v}_y = \pm \left(\frac{\pi H}{T}\right)\left\{\frac{\sinh\left[(2\pi/L)\ (d - y)\right]}{\sinh\ (2\pi d/L)}\right\} \quad (2)$$

where T is the wave period, L is the wave length, d is the depth of water measured from still-water level to the bottom, and H is the height of wave from crest to trough. The dissipation of energy per cycle per unit length of channel is

$$N = \left(\frac{\rho_w}{2}\right)\sqrt{\pi \nu T}\left[\int_0^b (\bar{u}_y - d)^2\ dz + 2\int_0^d (\bar{u}_y^{\,2} + \bar{v}_y^{\,2})\ dy\right] \quad (3)$$

where ρ_w is the density of water, ν is the kinematic viscosity, and b is the breadth of channel.

The total energy dissipation occurring in a channel of length ℓ, per unit of time, is equated to the difference between power entering the reach at $x = 0$ and the power leaving at $x = \ell$.

$$\Delta P = P_o - P_\ell = \int_0^\ell \frac{N}{T}\ dx \quad (4)$$

where P_o is the power transported into the reach at $x = 0$ and P_ℓ is the power leaving the reach at $x = \ell$.

From the above equations both H_ℓ and P_ℓ, or wave height and power leaving the filter, can be calculated; however, the application of this theory is restricted to plate filters.

The second theory was developed by Biesel for computing the damping characteristics of filters. Biesel employs Euler's equations for irrotational motion of an ideal incompressible fluid and he assumes that the forces acting on a fluid are due to gravity and viscous friction. He develops a

solution for the following boundary conditions of wave motion in a channel of finite depth:

$$\text{(a)} \quad \nabla^2 \phi = 0$$

$$\text{(b)} \quad \frac{\partial \phi}{\partial y} = 0 \qquad \text{for } y = -d$$

$$\text{(c)} \quad p = \text{constant} \qquad \text{for } y = \eta(x) \tag{5}$$

or

$$\frac{\partial \phi}{\partial t} + \lambda \phi + g \int_0^T \frac{\partial \phi}{\partial y} \, dt = 0$$

where ϕ is the velocity potential, λ the permeability coefficient ($\lambda > 0$) and g the acceleration of gravity.

These boundary conditions must be satisfied by the complex potential developed to represent the damped wave motion. Biesel shows that the velocity potential function for the flow passing through a wave filter,

$$\phi = \frac{a_I \sigma e^{-\beta mx}}{m \sinh md} \cos \beta m (y + d) \cosh m (y + d) \sin (mx - \sigma t)$$

$$+ \frac{a_I \sigma e^{-\beta mx}}{m \sinh md} \sin \beta m (y + d) \sinh m (y + d) \cos (mx - \sigma t) \tag{6}$$

does satisfy the boundary conditions if the following relationships exist:

$$\lambda = \beta \sigma \, \frac{1 + \dfrac{\sin 2 \beta md}{\beta \sinh 2md}}{1 - \dfrac{\beta \sin 2 \beta md}{\sinh 2md}} \tag{7}$$

and

$$\sigma^2 = mg \tanh md \, \frac{1 - \dfrac{\beta \sin 2 \beta md}{\sinh 2md}}{1 + \dfrac{\sin^2 \beta md}{\cosh^2 md}} \tag{8}$$

where a_I is the incident amplitude, $\sigma = 2\pi/T$, $m = 2\pi/L$, and β the damping coefficient. From these equations it is possible to determine m and λ when σ and β are known.

It seems apparent that the form of the surface profile may also be determined by making use of the potential function developed by Biesel.

$$\eta = \frac{1}{g}\frac{\partial \phi}{\partial t} = \frac{-a_I \sigma^2 e^{-\beta mx}}{gm \sinh md} \cos \beta m (y + d) \cosh m(y + d) \cos(mx - \sigma t)$$

$$+ \frac{a_I \sigma^2 e^{-\beta mx}}{gm \sinh md} \sin \beta m (y + d) \sinh m (y + d) \sin (mx - \sigma t) \qquad (9)$$

where η is the surface elevation and the other terms are as previously defined.

It can be seen that the latter factor of Eq. (9) describes the variation of the profile with time and position. The first factor indicates the variation of the profile as a function of the filter-to-wave length ratio. For the case of the wave height this can be expressed as

$$\frac{H_T}{H_I} = e^{-\beta mx} \qquad (10)$$

where H_T is the wave height transmitted, and the other symbols are as previously defined.

If $m = \frac{2\pi}{L}$ and $x = \ell$ is the filter length,

$$\frac{H_T}{H_I} = e^{-2\pi\beta \frac{\ell}{L}} \qquad (11)$$

Hence, the value of β, the damping coefficient, can be calculated from the experimental data.

Biesel's theoretical development does not indicate the internal mechanism of wave attenuation, nor is it self-sufficient in the determination of damping when only filter geometry is known. Although the solution of Biesel's equations necessitates the use of experimental data, the theory provides a

method of comparing the general performance of various filters in terms of the damping coefficient β and possibly the permeability coefficient λ. The primary objection to the solution is that it assumes the resistance of a filter in the form of viscous friction, whereas wire-mesh filters exert a form drag on the flow. In this case, the energy loss may vary as a function of V^n (V = velocity) where n may not be the first power as assumed by Biesel.

An attempt was made during the present investigation to develop a theory pertaining to the damping of a wave by a permeable filter and reflection from such a filter. The ultimate objective was the applicability of the theory to permeable absorbers.

The difference in entrant and exit energy was equated to the rate of energy dissipation as computed from the dissipation function. From this, the damping rate was expressed as a function of known wave characteristics and an unknown apparent viscosity ν'. The detailed analytical development is given in Appendix A. It was presumed that ν' would be descriptive of the damping qualities of the device and constant for a particular filter. Therefore, once the value of ν' had been determined for the permeable medium, it was hoped that the rate of damping for the filter could be calculated for given wave characteristics. This theoretical study will be referred to hereafter as the "artificial viscosity" development. Consideration was given to wave reflection produced by the filter but no satisfactory theory has been developed.

C. Experimental Studies

The brief experimental studies have been restricted to plate-type and wire-mesh filters. No tests have been conducted on perforated-plate filters which might be considered in a separate class. Plate-type filters were selected for comparison of the experimental data with O'Brien and Chaffin's theory and with Biesel's theory, and tests on wire-mesh filters were made in connection with the "artificial viscosity" development and Biesel's theory. Figures 1, 2, and 3 are the photographs of two types of filters which were subjected to limited tests. Wave attenuation was the primary measurement in these tests for various values of wave length, wave steepness, and filter characteristics. Variations in wave steepness were not as complete as desired because of the limited time available.

1. O'Brien and Chaffin's Theory

The effect of wave damping due to side-wall and bottom friction in a 6-in. channel is shown in Figs. 4 and 5. Theoretical curves, which are also indicated in the same graphs, were computed following O'Brien and Chaffin's theory. The results indicate that there is good agreement between experimental data and a theory developed by O'Brien and Chaffin for wave attenuation in a channel of finite width and depth.

2. Biesel's Theory

Tests were performed on plate filters designed to permit variations in the length of the filter from 2 to 6 ft and variations in the transverse spacing between plates from 1/2 to 3 inches. The damping coefficient β was calculated from the experimental data using Eq. (11) for various plate filters and was found to have not a constant but a variable value. Figure 6 indicates that β varied greatly with the wave length L (particularly for wave lengths below 3.5 ft) and varied only slightly with the length of filter. In Fig. 7 a comparison is made between experimental data and the damping coefficient. The theoretical curve was calculated using the damping coefficient β taken from the experimental data for L = 3.3 ft and assumed constant for all values of L. The agreement is considered good and it appears, within the limits of this study, that the wave damping can be predicted quite accurately for plate filters for longer wave lengths (3.5 to 5.5 ft in the model). However, the available data are not adequate to make definite conclusions, and it is also not known whether accurate predictions can be made for wave lengths shorter than L = 3.5 ft.

3. "Artificial Viscosity" Theory

In an attempt to verify the "artificial viscosity" theory (Appendix A), experimental data were collected for wire-mesh filters. The results indicated that the apparent viscosity ν' varies greatly with L, slightly with ℓ and H/L, and almost not at all with d/L. As ν' should be independent of all variables for a given material, it was concluded that the basic theory has received some support from these tests, but other tests, particularly in a larger model, are necessary to verify it.

As an alternative, an empirical expression was developed giving the relationship between wave attenuation and length of filter-to-wave length

ratio (ℓ/L). An empirical plotting is presented in Fig. 8 and it indicates an expression for wave attenuation of the form

$$\frac{H_I}{H_T} = e^{A\,(\ell/L) + B} \tag{12}$$

where A and B are constants. The constant appears to be determined by the filter material and B by the initial wave height. For the No. 8 wire-mesh filter the expression is

$$\frac{H_I}{H_T} = e^{3.084\,(\ell/L) - 0.062} \tag{13}$$

and for the No. 4 wire-mesh filter

$$\frac{H_I}{H_T} = e^{0.856\,(\ell/L) + 0.198} \tag{14}$$

4. Variables Affecting Wave Attenuation

Limited experimental and analytical studies have indicated that wave attenuation depends on the wave characteristics and filter characteristics.

a. Wave Characteristics

The primary variables are wave steepness H_I/L, and the ratio of depth of water to length of wave d/L. In most instances the wave attenuation was lower for low-steepness waves $(H_I/L = 0.03)$ than for high-steepness waves $(H_I/L = 0.06)$, but only limited experimental data were obtained. The effect of depth-to-length ratio on wave attenuation was briefly surveyed. Figure 9 indicates that the wave attenuation was higher for low wave lengths (or high values of d/L) than for high wave lengths (or low values of d/L). In Fig. 10 a comparison is made between wave attenuation for plate filters and wire-mesh filters. It appears that both plate and wire-mesh filters could be used to produce significant wave attenuation; values as high as 75 per cent and 30 per cent were measured for the wire-mesh and plate types, respectively. The mesh-type units appear to be advantageous where the filter length is limited and reflections from the filter are objectionable. However, the available data are not adequate for a thorough comparison of the two types.

b. Filter Characteristics

The variables affecting wave attenuation are the length of filter, the solidity ratio and plate spacing (in the case of plate filters), porosity of the filter (in case of a wire-mesh filter), and roughness. In general, the longer and denser the filter, the higher the energy loss. Figure 11 presents the effect of length of filter on wave attenuation for plate filters. A comparison is made on the same graph between experimental data and theoretical values computed following O'Brien and Chaffin's theory. Good agreement was obtained between theoretical and experimental values, particularly for L = 3.30 ft (d/L = 0.227).

In Fig. 12 comparison was made between wave attenuation as a function of wave length for plate filters and wire-mesh filters. It appears that for a given length the wire-mesh units are considerably more effective. Figure 13 presented additional data for wire-mesh filters for wave lengths 1.8 and 2.0 ft, respectively, and various values of wave steepness. The unit constructed of No. 8 wire mesh with 92.3 per cent porosity appeared to produce highest wave attenuation for a given wave length and wave steepness (Fig. 13b); however, it also caused highest reflection (H_R/H_I) of between 0.13 and 0.18 as compared with units constructed of No. 4 wire mesh for which H_R/H_I was observed between 0.048 and 0.075. Wave reflection is apparently a function of the density of the filter and the resultant rate of attenuation, as well as the solidity ratio of a typical transverse cross section.

D. Conclusions

The experimental studies of filters performed to date are not extensive enough to provide adequate design information. However, several general conclusions might be drawn:

a. Filters can be developed which will produce severe attenuation of the incident wave without excessive reflection.

b. Wire-mesh filters cause higher wave attenuation than plate-type filters.

c. The wave attenuation for wave filters depends on wave characteristics (steepness, length-to-depth ratio) and filter characteristics (length, density, roughness).

d. Within the limits of the studies performed to date, good agreement was obtained between experimental data for plate filters and a theory developed by O'Brien and Chaffin for wave attenuation in a channel of finite width and depth.

e. Limited experimental data prohibits definite verification of Biesel's theory.

f. Additional studies of mesh-type and other types, such as perforated plate filters are necessary for the determination of adequate design information.

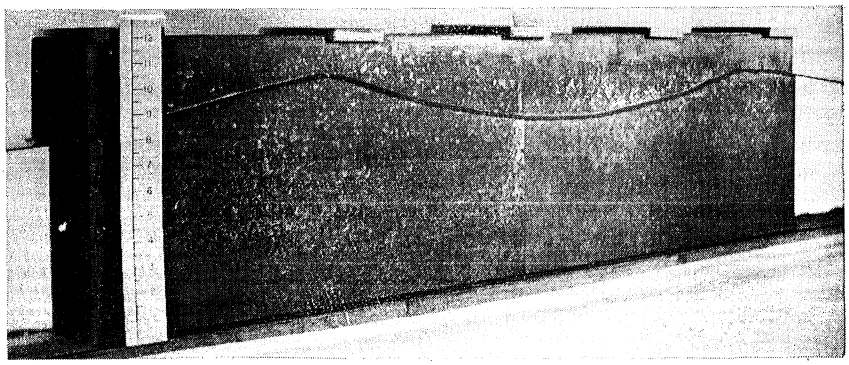

Fig. 1 - A View of a Plate Filter Installed in a 6-in. Wide Wave Channel

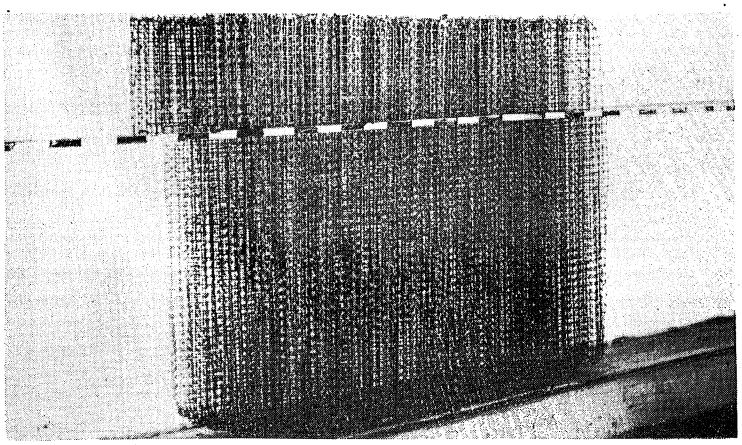

Fig. 2 - A View of a Wire-Mesh Filter Installed in a 6-in. Wide Wave Channel

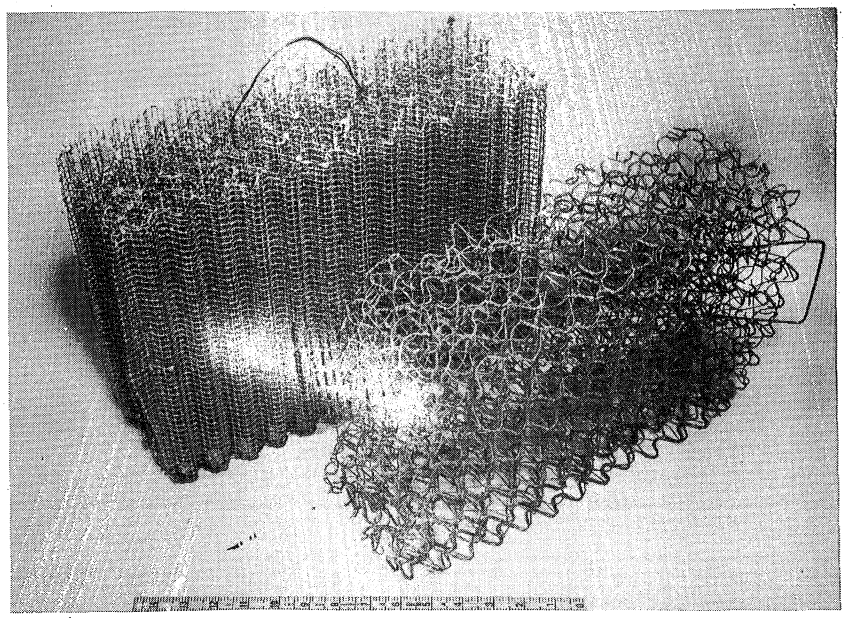

Fig. 3 - A Close-Up View of Wire-Mesh Filters. (On the left is No. 4 Wire-Mesh Filter, 1-in. Corrugations, on the right is No. 2 Wire-Mesh Filter, 1-in. Corrugations

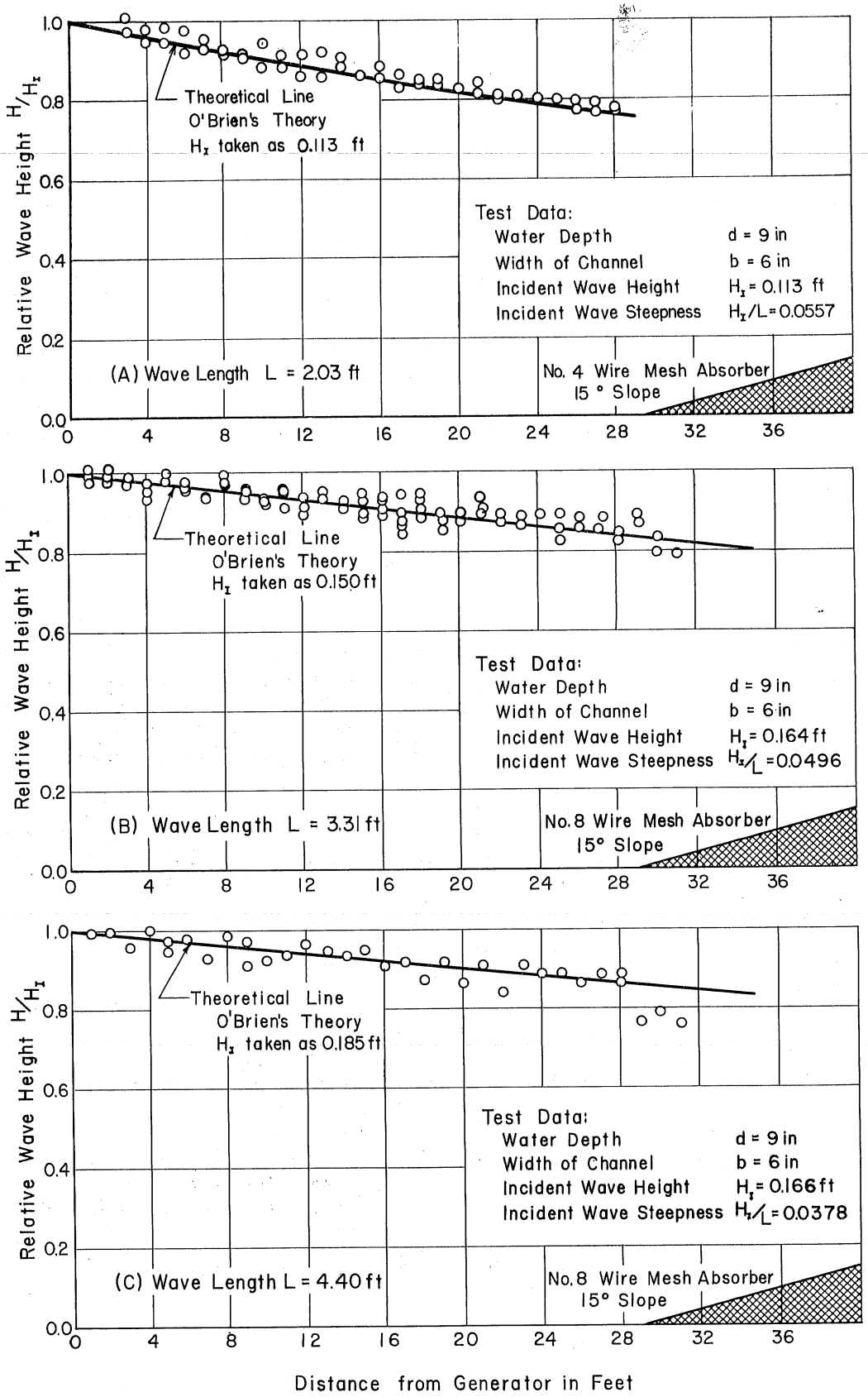

Fig. 4 - Wave Damping due to Wall and Bed Friction in a 6-in. Wide Channel. L = 2.03, 3.31, 4.40 ft

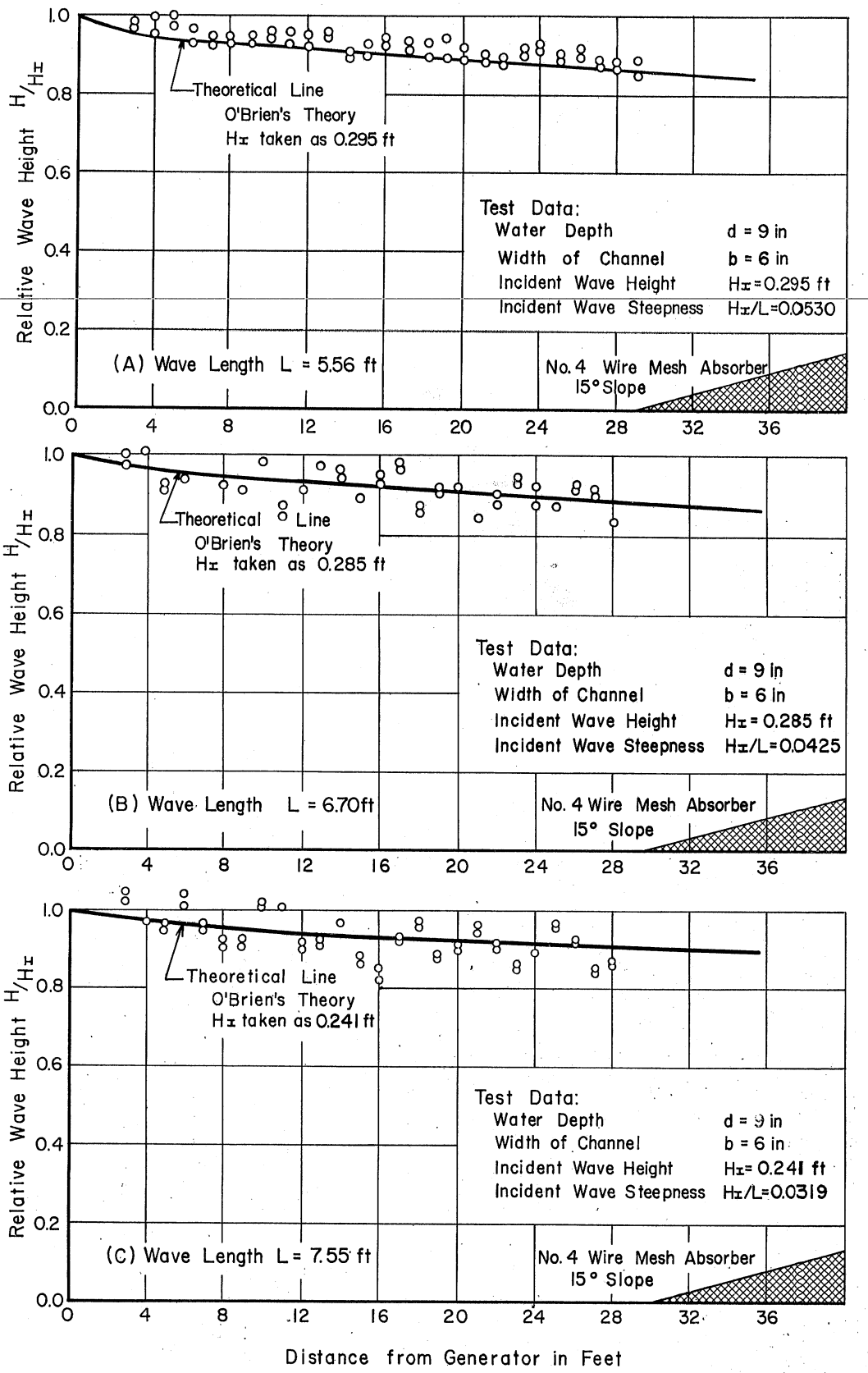

Fig. 5 - Wave Damping due to Wall and Bed Friction in a 6-in. Wide Channel. L = 5.56, 6.70, 7.55 ft

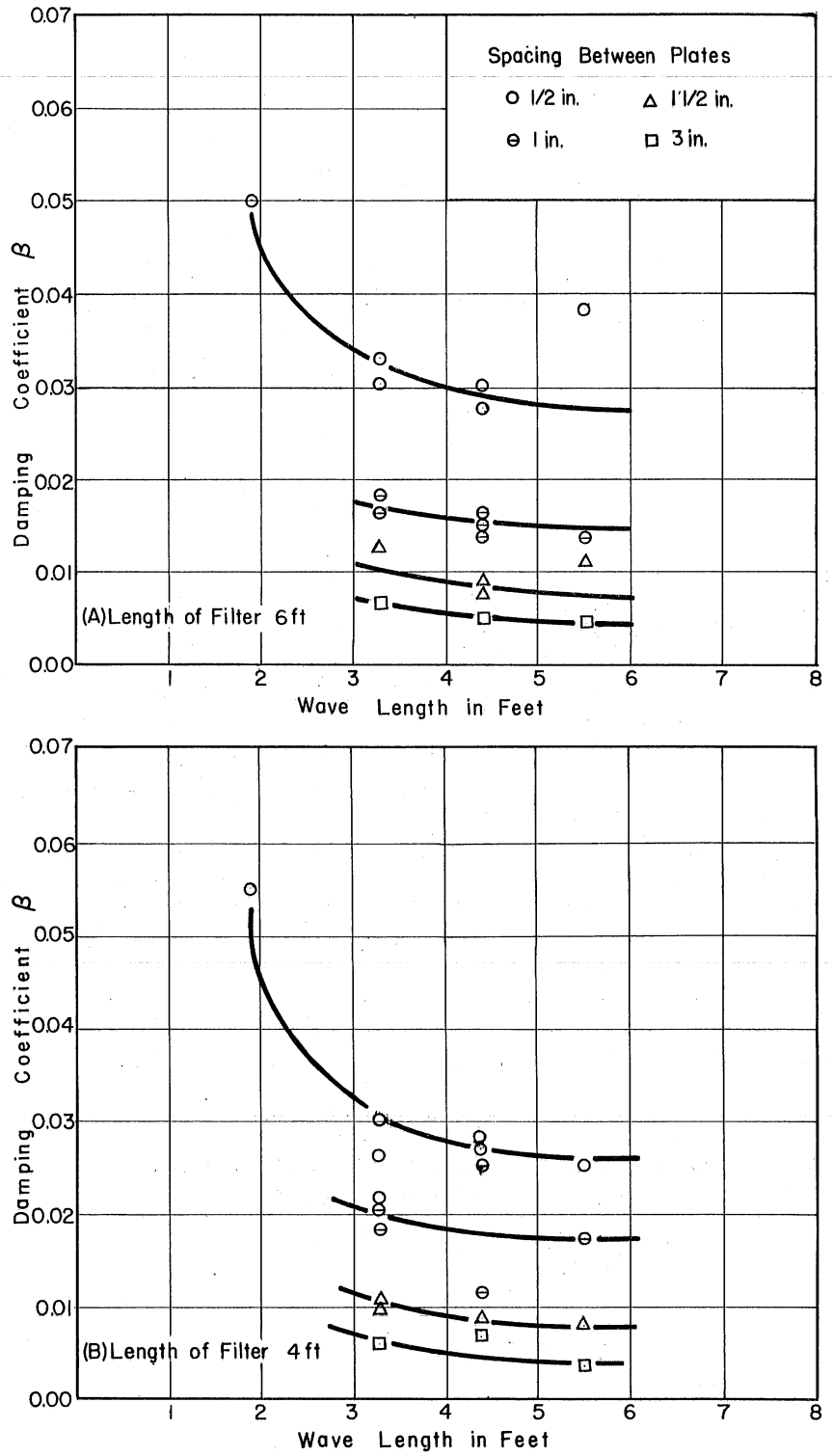

Fig. 6 - Effect of Wave Length on Damping Coefficient β for Plate Filters

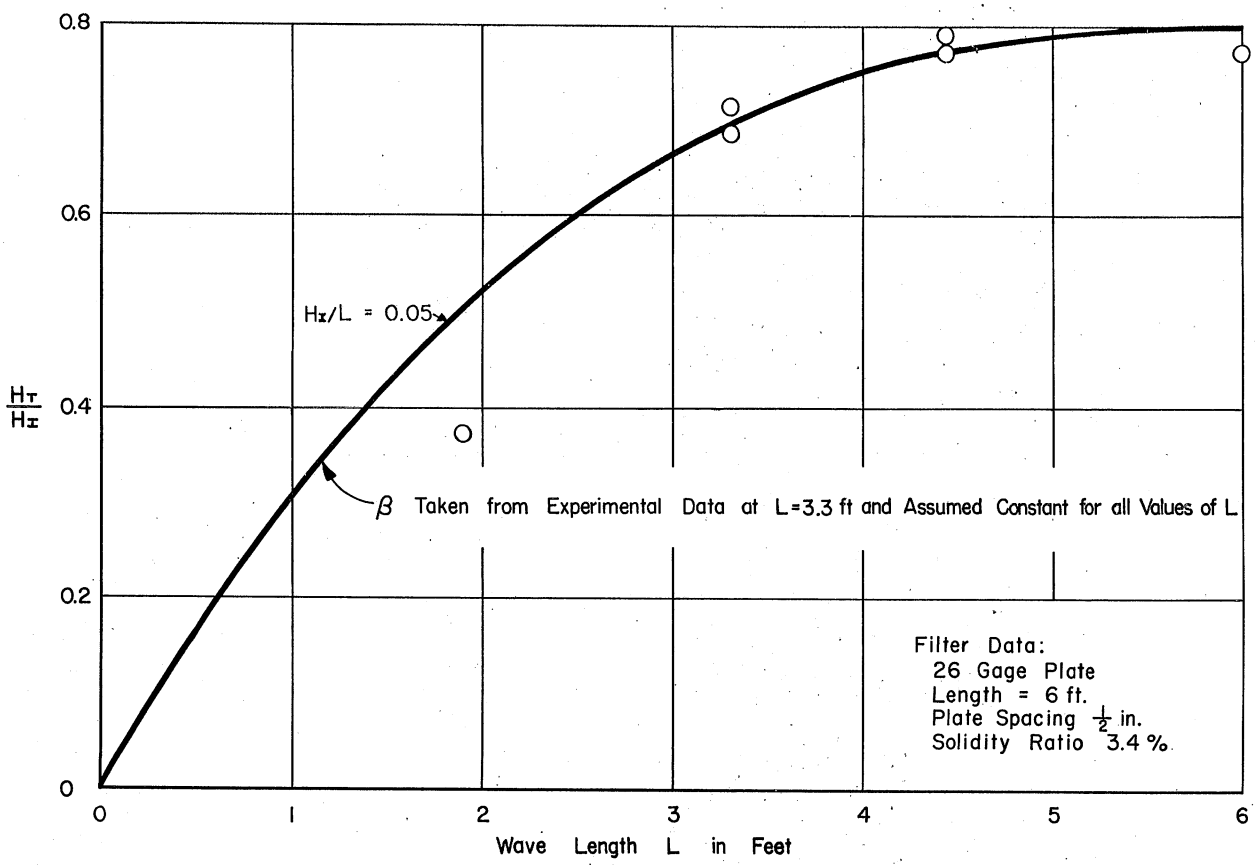

Fig. 7 – Comparison of Experimental and Computed Data for Plate Filters Using Damping Coefficient β

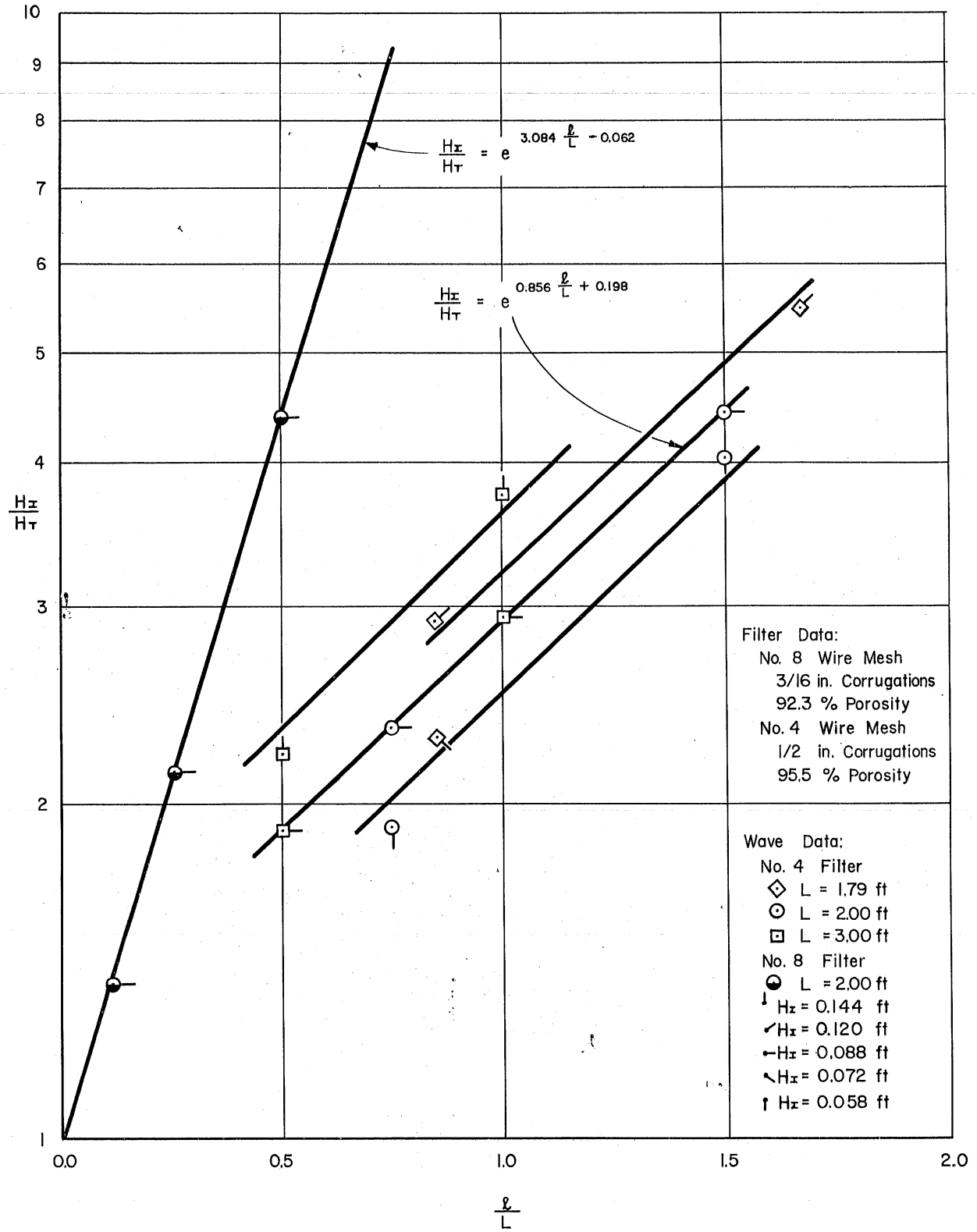

Fig. 8 – An Empirical Plot of Wave Attenuation for Wire-Mesh Filters

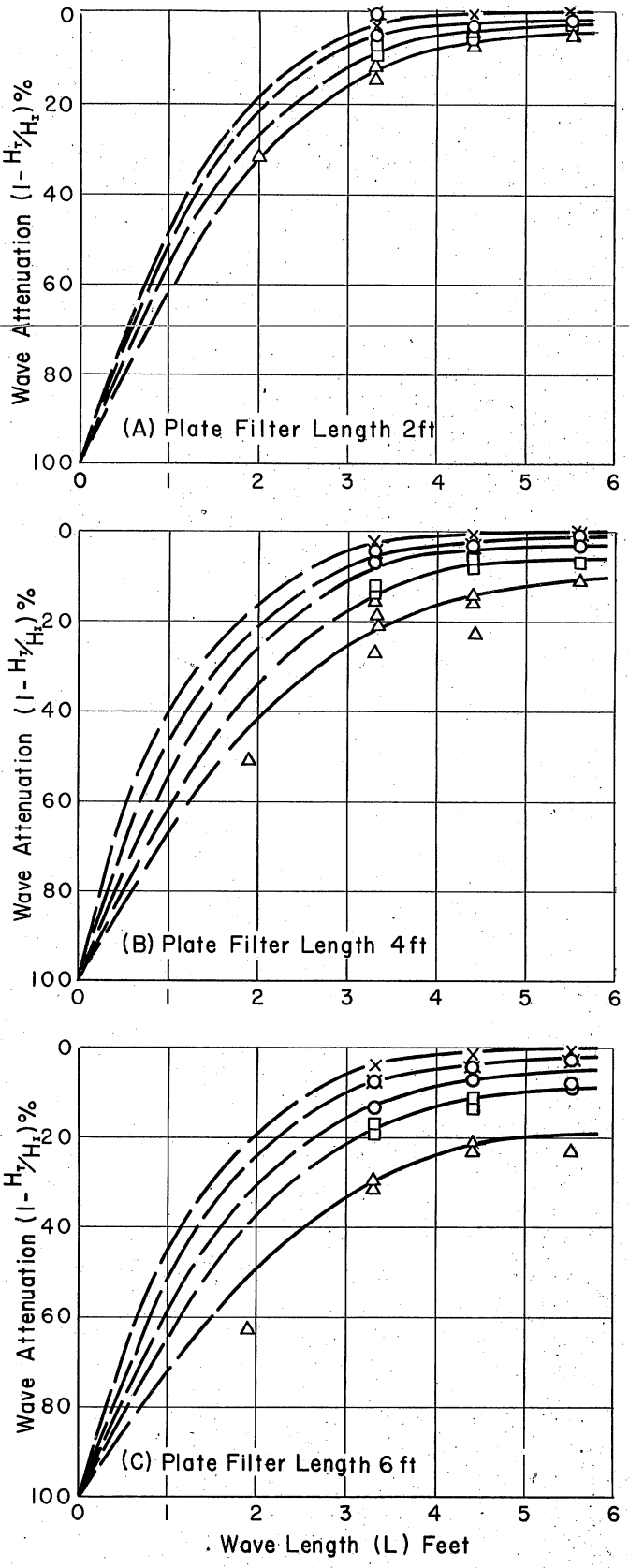

Test Data:
Wave Steepness H_I/L = 0.05
Depth of Channel d = 9 in

Legend:
Spacing between Plates
× 6 in (Glass Channel)
⊠ 3.0 in
○ 1.5 in
□ 1.0 in
△ 0.5 in

Fig. 9 – Effect of Wave Length on Wave Attenuation for Plate Filters

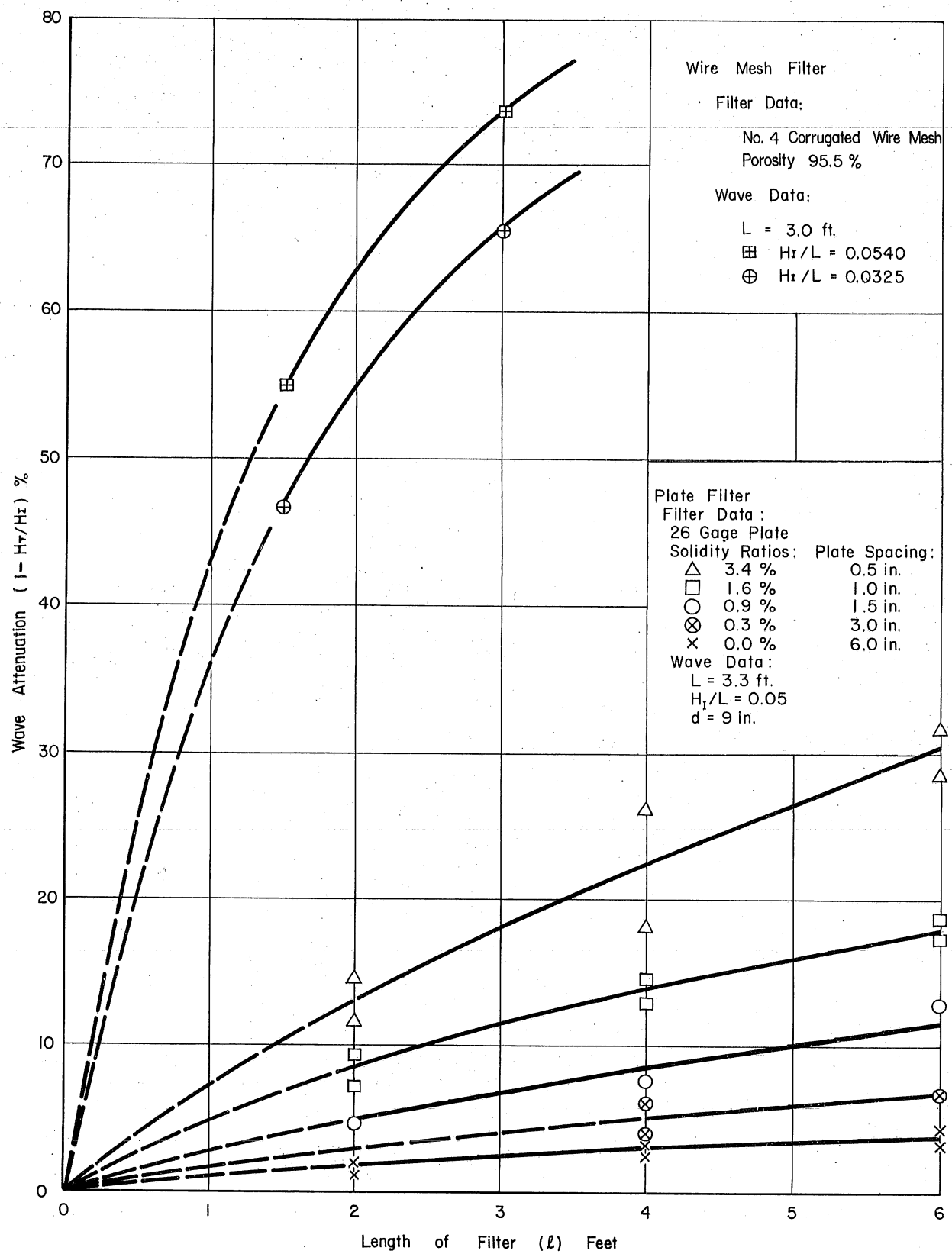

Fig. 10 - Typical Experimental Data for Wire-Mesh and Plate-Type Filters. The Coefficient of Reflection for these Filters Ranged from 5 to 7.5 per cent

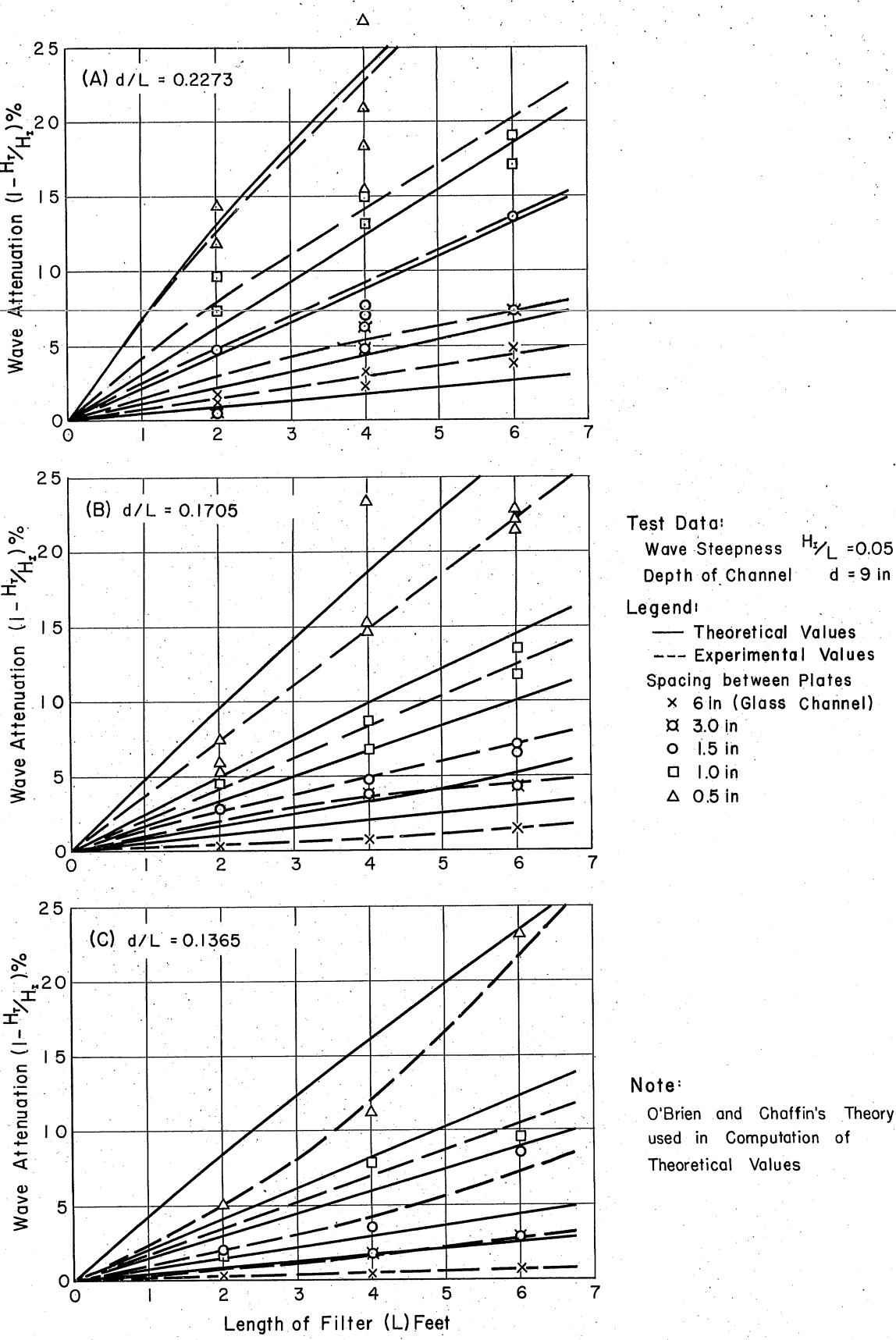

Fig. 11 - Comparison of Experimental and Computed Values of Wave Attenuation for Plate-Type Filters

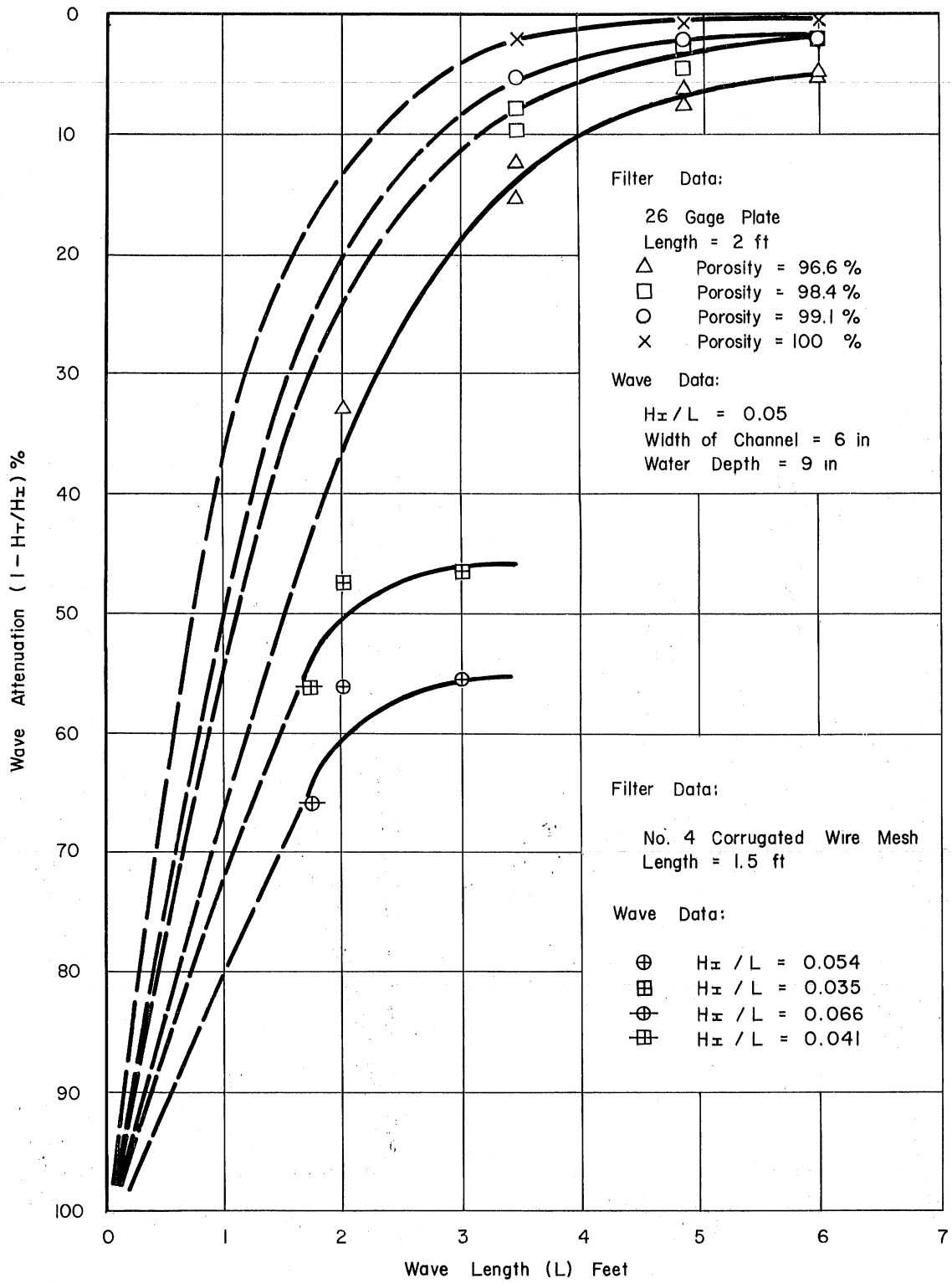

Fig. 12 – Effect of Wave Length on Wave Attenuation for Wire-Mesh and Plate-Type Filters

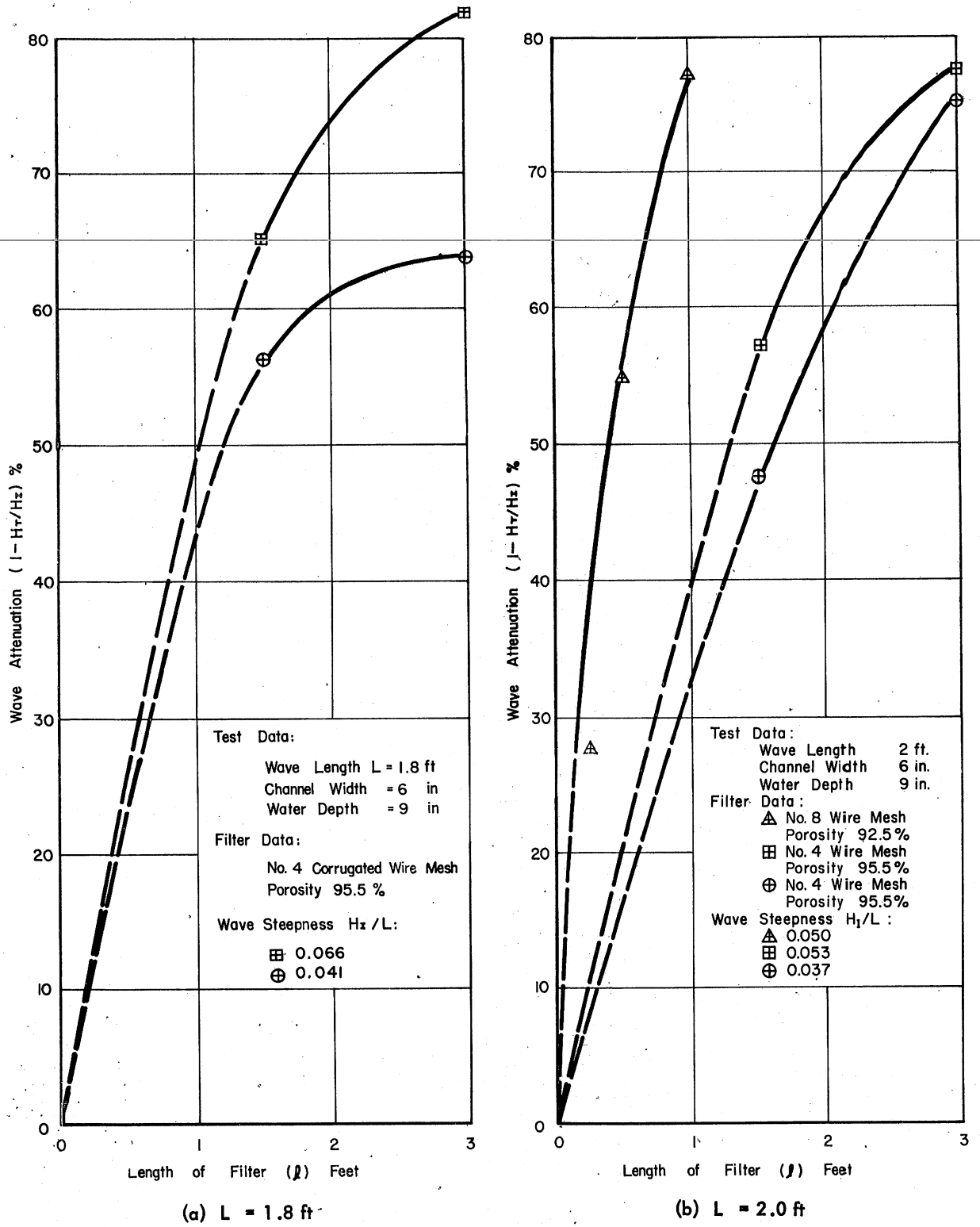

(a) L = 1.8 ft (b) L = 2.0 ft

Fig. 13 – Effect of Length of Filter on Wave Attenuation for Plate Filters

III. WAVE ABSORBERS

A. General Remarks

Wave absorbers are usually required in laboratory wave experiments to prevent reflection of the generated waves from the extremities of the test channel. Absorbers, as considered for laboratory use, may be of several types:

1. Impermeable beaches: Variables include the slope, shape, and roughness of the beach.

2. Permeable beaches: Variables include the slope, shape, volume, and porosity of permeable material.

3. A combination of (1) and (2).

4. Special devices: This classification might include items such as:

   a. partly submerged horizontal cylinders,

   b. overflow troughs,

   c. submerged barriers and similar devices, and

   d. rods of various shapes forming a sloping beach.

A survey of literature on the subject of absorbers reveals very little quantitative information. However, in recent years studies of the absorbing and reflecting properties of beaches have produced some information of interest in the design of laboratory absorbers. This work is concerned primarily with relatively impermeable beaches. Schoemaker and Thijsse [14] have published experimental data on smooth impermeable beaches with both continuous and discontinuous slopes. Their tests covered variations in the beach slope and length-to-depth ratio of the incident waves; however, the effect of variation in steepness of the incident wave was not studied. Laurent and Devimeux [8] have made investigations of three types of discontinuous slope impermeable absorbers. The conclusion reached from this study was that higher wave reflections occur for low-steepness waves. Healy [5] also studied impermeable beaches with a continuous slope for variations in steepness and length-to-depth ratio of the waves and for variations in beach slope. Some of the data from Schoemaker-Thijsse and Healy's studies, as well as from the present study, are reproduced in Figs. 14, 15, 16, and 17. The Beach Erosion Board [1] reported the results of tests on the reflection of solitary waves

from both permeable and impermeable beaches. The results indicated that the permeable beach is a much better absorber than an impermeable beach of the same slope. However, application of the results to the present study is somewhat limited because it is difficult to determine the magnitude of reflections which will result if a continuous train of waves is used in place of a solitary wave. Design studies of a rubble wave absorber by Straub and Hudson [15] in connection with a harbor study, indicate that for a constant surface slope the percentage of absorption of incident wave energy is a function of the volume of rock in the structure.

The reader is referred to St. Anthony Falls Hydraulic Laboratory Project Report No. 38 [13] for a more detailed review of available literature.

B. Theoretical Considerations

Several theories, which are at present available, were reviewed for their applicability to the analysis of absorber performance; these are the theories of O'Brien and Chaffin, Biesel, and Miche. Of these, Miche's is the only theory developed for conditions approximating a laboratory absorber.

Miche developed a theory to determine the reflective capacity of beaches by considering both the slope and beach roughness. He was concerned with essentially impermeable-type beaches. His theory did not take into account the vertical flow through permeable beaches; hence it could not be used in evaluating permeable absorbers. However, Miche's development is of value in evaluating impermeable absorbers and as a means of comparison of permeable absorbers with impermeable or permeable absorbers of the same shape. A short resumé of his theory follows.

Considering the ideal case of a perfectly smooth barrier forming an angle α with the horizontal, he developed analytically a formula for the maximum wave steepness in deep water which will be totally reflected by such a barrier

$$\delta_{CM} = \sqrt{\frac{2\alpha}{\pi}} \; \frac{\sin^2\alpha}{\pi} \qquad (15)$$

where δ_{CM} is the maximum wave steepness (in deep water) which will be totally reflected by a smooth barrier. From this he deduced that waves steeper

than δ_{OM} would be partially reflected and those flatter than δ_{OM} would be totally reflected.

The part theoretically reflected (R') has then the following value:

$$R' = \frac{\delta_{OM}}{\delta_{OI}} \text{ with } R' \leq 1 \tag{16}$$

where δ_{OI} = incident wave steepness in deep water.

To account for a rough or permeable barrier, Miche introduced an intrinsic coefficient ρ, apparently independent of the slope of the barrier, which varies from unity for perfectly smooth slopes to 0.33 for rough, permeable barriers. The effectively reflected part (R) will therefore be equal to

$$R = \rho R' = \frac{H_R}{H_I} \tag{17}$$

where H_R is the reflected wave height and H_I the incident wave height.

It was thought that the experimental evaluation of Miche's coefficient ρ might provide a means of comparing various absorbers, both permeable and impermeable. Permeable absorbers considered were made of No. 4, No. 8, and No. 16 corrugated wire mesh; perforated plate with 37 and 60 per cent voids; natural screened gravel, passing 1-1/2-in. and retained on 5/8-in. mesh; and crushed limestone rock, passing 3/4-in. and retained on 1/4-in. mesh, and passing 2-in. and retained on 3/8-in. mesh. Two impermeable absorbers were also considered, one of a flat sloping-beach type and another of parabolic beach type.

In all cases, both for permeable and impermeable absorbers, ρ was found to be a variable, dependent on wave steepness. To give an example, the values of ρ were plotted against the wave steepness in Figs. 18 and 19. Figure 18(a) shows the results obtained for an impermeable absorber; Fig. 18(b) for a corrugated wire-mesh absorber; Fig. 19(a) for a perforated-plate absorber; Fig. 19(b) for a screened-gravel absorber; and Fig. 19(c) for a crushed-rock absorber.

It is interesting to note that very low values of the intrinsic coefficient were obtained for highly permeable materials such as wire mesh or

perforated plates. The actual values were between 0.22 and 0.01 for some of the absorbers tested, as compared with Miche's lowest value of 0.33 for rough, permeable barriers, which is another indication of high absorption efficiency for wire-mesh or perforated-plate absorbers.

C. Experimental Studies

The general program followed can be divided into two parts.

(a) A basic study of variables affecting the wave reflection and wave absorption in order to procure general absorber design information.

(b) An applied study to facilitate design of a wave absorber for a proposed facility at the David Taylor Model Basin.

1. Basic Study

The experimental study has indicated that the reflection coefficient (ratio of reflected wave height to incident wave height H_R/H_I) depends on the wave characteristics and the absorber characteristics.

a. Wave Characteristics

The primary variables are wave steepness H_I/L and the ratio of depth of channel to length of wave d/L. In most instances the reflection coefficient was much higher for low-steepness waves ($H/L = 0.01$) than it was for high-steepness waves ($H/L = 0.07$). This may be partially explained by the fact that the high-steepness waves may break as they pass onto the absorber. The effect of depth-to-length ratio (d/L) on the coefficient of reflection was briefly surveyed. Figure 20 indicates that for a particular absorber, constructed of perforated plates, the coefficient was approximately constant for d/L values between 0.30 and 0.80, while it increased fairly rapidly for values below 0.30. It will be noticed that to obtain the data for higher d/L values, the depth of water in the channel was increased to 12 inches. In Fig. 21 a comparison is made for a particular absorber between tests in 9-in. and 12-in. depths of water for a 2-ft wave (d/L values of 0.375 and 0.50 or deep-water waves). Almost identical results were obtained in these tests.

Figure 22 presents tests on two other types of absorbers: an impermeable-beach, 22(a); and a square-bar absorber, 22(b). Based on the above

tests it appears that the d/L ratio does not have a significant effect on coefficient of reflection for higher d/L values (d/L > 0.3 or medium and deep-water waves). For lower d/L values the reflection coefficient increases with decreasing d/L values (d/L < 0.3 or shallow-water waves). It would be logical to assume that for shallow-water waves (d/L < 0.5) where the orbital particle motion extends to the bottom of the channel, the d/L ratio would have a significant effect on coefficient of reflection for discontinuous-type absorbers.

b. Absorber Characteristics

Variables affecting the efficiency of a permeable part of the absorber are the slope, volume, porosity, and shape of the absorber.

1) Effect of Volume of Absorber

Figures 23, 24, and 25 illustrate the effect of variations in the volume of a permeable absorber upon the reflection coefficient. The absorbers were constructed of corrugated wire mesh with a slope of 30 degrees. The slope, porosity, and depth remained constant throughout the test. The volume of the absorber was proportional to its length except for the shorter absorbers. The data were plotted as a function of volume of absorber, and the approximate length scale was also indicated.

It was anticipated that as the volume of absorber was decreased the reflection coefficient would increase, at first gradually and then rapidly for low values of volume. However, in most instances there was a pronounced dip in the curves, which resulted in better efficiencies for intermediate-length absorbers than for very long ones. As the length was decreased still further, the reflection coefficient increased very rapidly; the sharp increase in the coefficient occurred as the water-line length of the absorber approached zero. Figures 23, 24, and 25 represent the results obtained for wave steepnesses of 0.01, 0.03, and 0.07, respectively. Several wave lengths were tested for each steepness. It is expected that variations either in porosity or slope of absorber would produce different results. Figure 26 presents the results for absorbers of the same porosity as Figs. 23, 24, and 25 but with a surface slope of 45 degrees. A similar dip of the reflection coefficient was also

observed in this case for intermediate-length absorbers. Figures 27 and 28 are photographs of a wire-mesh-type absorber used in early tests of permeable absorbers.

2) Effect of Slope of Permeable Absorbers

Figures 29, 30, 31, and 32 illustrate the effect of variation in surface slope upon the reflection coefficient of a wire-mesh absorber. The porosity and volume of the absorber remained constant as the slope was varied. The computed reflection coefficient of an impermeable absorber, as well as experimental data for wire-mesh, crushed-rock, and impermeable absorbers, is shown for comparison purposes. The permeable absorber is far more efficient than the impermeable one, even though the porosity and volume of the permeable absorber do not represent optimum selections. Other tests of permeable absorbers with slopes of 12 to 30 degrees have resulted in lower coefficients than the corresponding absorbers in this series.

Variations in either porosity or volume would produce different curves; however, the data shown are indicative of the trends to be expected.

3) Effect of Porosity of Absorber

Early in the experimental program it was realized that porosity had a considerable effect on the coefficient of reflection for permeable absorbers. In order to show the effect of porosity on the coefficient of reflection, a general graph was prepared presenting the data for various permeable absorbers, such as screened gravel, crushed rock, perforated plates, and square bars (Figs. 33 and 34); on the same graphs the theoretical values for an impermeable beach are given. All absorbers, except a square-bar absorber, had a continuous slope of 22 degrees; the square-bar absorber had a discontinuous slope and consisted of a permeable layer backed with an impermeable beach. The porosity of screened gravel, crushed rock, and square bars was 40, 46 to 52, and 73 per cent, respectively, while for perforated plates the porosity was between 93 and 99 per cent. A single curve for one selected wave length (3.30 ft) was drawn through all the data. As no experimental data were available for porosities between 0 and 40 per cent, between 52 and 73 per cent,

and between 73 and 93 per cent, the shape of the curve is somewhat arbitrary. However, it appears that for a comparatively short absorber of a 22-degree slope (model length 2 ft 8 in.) porosities somewhere between 46 and 96 per cent are desirable if reflections are to be minimized.

An effort was made to determine the effect of porosity on the reflection coefficient in the range above 93 per cent porosity. Perforated plate was selected for these tests in preference to wire mesh because the porosity could be easily controlled and it was thought that the metal plate or concrete panel-type construction might be of value in the prototype installation. The porosity was varied by changing the size and spacing of holes, thus affecting the plate-void ratio as well as by altering the spacing between plates. Figures 36 and 37 present the results of tests in which the porosity was varied between 93 and 99 per cent. The reflection coefficient was a minimum for porosities between 93 and 99 per cent; however, it is possible that a minimum could very well be below the value of 90 per cent.

The optimum porosity depends on the other variables, such as slope and volume of absorber. However, the choice of slope and volume of absorber used in this series of tests was based to a considerable extent upon the prototype space limitations and as a result these data should be of interest. The data of Figs. 36 and 37 are for incident wave steepnesses of 0.01, 0.03, and 0.07, and for wave lengths varying from 1.25 to 4.40 ft.

In general, a higher reflection coefficient was obtained for flat waves than for steep waves; short waves produced less reflection than the long waves. For a specified porosity, the data can be plotted as a function of wave length or depth-to-length ratio to illustrate this effect. It will be noticed that two sets of curves are shown for the plate absorbers: one for absorbers made from plates with 60 per cent voids (solid lines), and another from plates with 37 per cent voids (broken lines) (Figs. 36 and 37). The shape of the curves is similar in each case, but units with 37 per cent plate voids caused lower reflections within the limits of this

study. It is difficult to explain why data for plates with 60 per cent voids do not agree with data for 37 per cent voids for the same porosity, except that the spacing of holes might be a significant factor. It is interesting to note that experimental data for one wire-mesh absorber with the same shape and volume agreed very well with the data for 37 per cent voids.

A photographic record of waves attacking various types of absorbers, both permeable and impermeable, is presented in Appendix F.

4) Effect of Shape of Absorber

It is a well-known fact that a long, flat, impermeable beach constitutes a good absorber, but due to a large space requirement such an absorber would not be practical for most laboratory installations.

A brief investigation during this study was made to determine the effect of shape of absorber, i.e., whether the length of absorber can be reduced, particularly for deep-water waves ($d/L > 0.5$) where the orbital particle motion near the bottom of the channel is negligible. Two types of absorbers were considered: absorbers with continuous slopes (e.g., parabolic in shape), and discontinuous slopes (e.g., units with a sudden break or change in slope). Parabolic, impermeable absorbers have sometimes been employed in laboratory wave facilities, but no data have been obtained on their efficiency. The main advantage of the parabolically shaped absorber is that for a specified length a flatter slope near the water surface can be achieved than would otherwise be possible with a single continuous slope. The parabolic slope can be approximated by a series of straight lines which may in some cases simplify construction. In a discontinuous-type unit, the toe of the absorber is removed; this type might be visualized as a very crude approximation of a parabolic type, but it is considerably easier to construct.

In the present study, tests were conducted on parabolic and discontinuous-slope units, both permeable and impermeable. Figure 39 illustrates data obtained for parabolic-type absorbers. An impermeable unit caused high reflections for the wave lengths tested and the addition of a layer of permeable material (wire mesh) to

the original unit proved to be very beneficial. With wave lengths shorter than those tested the parabolic shape would probably be somewhat more efficient, with the reflections dependent to a considerable extent on the nominal slope in the vicinity of the water surface.

Figure 40 illustrates discontinuous slope absorbers. A discontinuous permeable absorber, which produced fairly low reflections even though the length was quite short, is shown in Fig. 40(a). In an effort to reduce the amount of permeable material, a unit shown in Fig. 40(b) was tested. In this case the permeable material (wire mesh) is backed with an impermeable plate.

Further tests were made to determine whether the permeable material should be backed with an impermeable or perforated plate. A comparison of absorbers with an impermeable and perforated beach is presented in Fig. 41. The absorber backed with an impermeable beach is considerably more efficient.

2. Applied Study

The applied study was conducted to provide design information for an absorber for the Maneuvering Basin at David Taylor Model Basin. The information contained here is not as complete as might be desired for someone designing a discontinuous absorber of short length; however, this part of the report describes in a step-by-step fashion the study leading up to the preliminary design of the absorber.

It was specified by the Sponsor that the depth of water will be 20 ft and that the waves ranging in length from 3 to 40 ft ($d/L = 6.7$ to 0.5) with steepness of 1/100 (0.01) to 1/15 (0.067) were contemplated. An absorber efficiency corresponding to that of a 5-degree impermeable beach was considered desirable. It was further specified that the absorber length should be a minimum and preferably not in excess of 25 to 35 ft.

The specified length proved to be the most important limitation, and after a review of available literature and initial tests on both permeable and impermeable absorbers, it was concluded that an absorber of permeable type would be most satisfactory for the specified conditions.

The majority of tests of the applied study were conducted on permeable or partly permeable units constructed of crushed rock, wire mesh,

perforated plates, inclined rods, and square and rectangular bars. A number of tests were performed on an impermeable-type absorber to compare with available theory and to investigate the techniques used in experimental studies.

a. Porosity Effect

Wire mesh and perforated plate had been used in permeable absorbers in the basic tests. However, because of high prototype cost of such an absorber, other materials were considered which might be less expensive. Tests were performed on screened gravel, crushed rock, square and rectangular bars (representing slotted, precast, concrete panels in the prototype); some thought was given to other materials such as concrete blocks, building tile, and similar products. Permeable materials of this type were not fully investigated in the basic study; therefore, brief tests were conducted on the effect of porosity on reflection coefficient for a selected design of discontinuous-type permeable absorber shown in Fig. 40(b). To decrease prototype costs, the thickness of permeable layer was reduced to approximately one-half as shown in Fig. 42. The absorber tested consisted of a permeable layer backed with an impermeable beach of 12-degree slope. Two materials selected for the tests were crushed rock and square bars; thus the permeable layer consisted of crushed rock passing 1-1/4 in. and retained on 1/2-in. screen for one absorber, Fig. 42(a), and 0.1-in. square bars spaced to form a permeable medium of uniform porosity of 73 per cent for another absorber, Fig. 42(b). Figure 42 presents the data obtained for both absorbers. The low reflection coefficients observed for the wave lengths of interest ($L = 1.0$ and $L = 2.0$ ft) were the first indication that a short-length absorber constructed of comparatively low-cost materials might produce a satisfactory design for the prototype installation.

It will be noted in Fig. 42(a) that there was an increase of coefficient of reflection for wave lengths 3.3 and 4.4 ft for higher wave steepness ($H_I/L > 0.04$). This was due to the fact that waves of such length and steepness uprush over the sloping beach of the absorber and part of the wave breaks at the back wall. If such is the case, the absorber should be redesigned to prevent the crest of the wave reaching the back wall.

It might be appropriate at this time to raise an important point regarding the construction of crushed-rock absorbers. In order to obtain a porosity of between 50 and 52 per cent, a narrow-size gradation of crushed rock is required and failure to control the size and placement might result in higher reflections.

The porosity of a square-bar absorber was arbitrarily chosen as 73 per cent, and it was not known whether this represented the optimum value for this type of absorber. Since extensive study was not possible because of time limitations, only one more set of tests was performed with the porosity of the square-bar absorber increased to 79 per cent. Figure 44 presents the experimental data for the absorber of 79 per cent porosity and in comparing the data with that for an absorber of 73 per cent porosity, Fig. 42(b), it appears that the increase in porosity has not improved the absorber's efficiency.

b. Slope Effect

The effect of slope on coefficient of reflection for permeable absorbers was described earlier in the report (chapter II, p. 28). As the study covered only continuous-slope-type absorbers, there was a need for additional experiments for discontinuous-type units. The selected absorber consisted of a permeable layer, constructed of 0.1-in. square bars spaced to form a medium of 73 per cent porosity. Figure 45 summarizes the data obtained for slopes between 12 and 30 degrees. Within this range the absorber with a 12-degree slope produced lowest reflections. The complete data for a 12-degree slope absorber of this type are given in Fig. 42(b). It will be noticed that this absorber of comparatively short length produced reflections below 10 per cent ($H_R/H_I < 0.1$) for depth-to-length ratio (d/L) between 0.227 and 0.75.

c. Shape Effect

It appeared from the basic study that the most economical absorber for the specified wave characteristics of the David Taylor Model Basin installation would consist of a discontinuous- or of a parabolic-type unit in which the permeable layer is backed with an impermeable beach. The first question to be answered was whether the area under the upstream part of the sloping permeable absorber should be sealed off or not. The comparison of data presented in Figs. 44 and 46 indicated that there was little, if any, difference in the coefficient of reflection for the range of specified wave characteristics ($L < 2.0$ ft in the model) whether the area under the upstream part of the absorber was sealed off or not. With the objective of reducing the reflection coefficient, additional tests were performed with a layer of permeable material placed in front of the vertical seal plate. It appeared from Fig. 47 that slightly lower coefficient of reflection was recorded for

the model wave length of 2.0 ft (corresponding approximately to a prototype wave length of 40.0 ft) when the permeable layer was present in front of the sealing plate. As was expected, there was no difference for the shorter wave lengths (L_m = 1.0 and 1.5 ft).

Next the effect of location of the impermeable backing plate with respect to the water level was briefly studied. The square-bar type absorber was employed in these tests. The effect of raising the absorber was to decrease the reflection for the 1- and 2-ft long waves and increase the reflections for the 1.5-ft long wave. The results of the tests presented in Fig. 48 were not very conclusive, and it was felt that the exact location of the impermeable beach with respect to the water level could be recommended only after completion of tests in the large facility.

A test was also performed on an absorber having a semi-parabolic instead of a flat, discontinuous slope, but no improvement in the coefficient of reflection was observed (compare Fig. 47(b) with Fig. 49). A flat, discontinuous slope would be easier to construct.

The final experiments in the small-scale channel were performed with the principal objective being to determine the optimum value of thickness of a permeable part of the absorber as a basis for the large-scale tests.

The thickness of the permeable part of the absorber was varied and experimental data obtained for the following prototype thicknesses: 3-3/4 in., 7-1/2 in., 1 ft 3 in., 2 ft 6 in., 3 ft 9 in., and 5 ft 0 inch. The permeable layer in front of the absorber was eliminated in order to simplify the tests and to investigate the thickness parameter only. The data are presented in Figs. 50 and 51 for prototype wave lengths of 40.0 ft (L_m = 2.0 ft) and 24.4 ft (L_m = 1.22 ft), respectively. Individual graphs of reflection coefficient as a function of wave steepness for a given thickness of permeable layer and various wave lengths are presented in the Appendix F (Fig. F-20). An inspection of the data indicated that the choice of an optimum thickness of permeable layer was somewhat difficult because so many parameters would have to be considered. In addition, in some instances (Figs. 50 and 51) the curves have several reversals in slope and were, in general, not as consistent as might be expected. Some of the variations were probably due to reinforcement and cancellation of reflections from various parts of the absorber, in which case wave length and geometry of the absorber were important parameters.

Another variation was caused by the mechanism of energy loss at the absorber; thus for some values of wave steepness the wave was breaking, while for the flatter waves the primary loss was caused by an oscillatory flow through the permeable media. While the small-scale data indicated trends and approximate reflection coefficients, it appeared that they were not adequate for selection of thickness of permeable layer for the prototype absorber. For the longer waves (L_m = 2 ft, L_p = 20 ft) the data indicated that a prototype thickness of permeable layer of about 5 ft may be desirable. For intermediate-length waves (L_m = 1.22 ft, L_p = 24.4 ft) it appeared that a thickness of either 0.75 ft or 2.5 ft might be acceptable. In the latter case intermediate values of thickness did not produce as good results as the two values noted, particularly for low-steepness waves. On the basis of these tests and others with other materials it can be concluded that for the specified absorber length and for the anticipated range of wave characteristics the thickness of the permeable layer should not exceed 5 ft and the optimum value may be somewhat less than this value. The large-scale tests should be of great benefit in determining the optimum thickness, provided a sufficient number of wave lengths are tested.

D. Preliminary Prototype Design

Final recommendations can only be made after completion of tests in the large facility. However, it appears that the most efficient unit of minimum length (considering only building materials of reasonable cost) could be constructed of either crushed rock or slotted, precast, concrete panels resembling square or rectangular bars in the model. Because of difficulty in controlling the placement of crushed rock (and thus porosity of the absorber) which might result in high reflections, it might be desirable to use a unit constructed of precast, concrete panels for which the reflection could be predicted with greater certainty.

In general, the design should follow the sketches shown in Figs. 52 and 53 which have been developed in conjunction with the sponsor. The absorber would have a discontinuous surface slope of 12 degrees, the permeable part to be constructed on top of an impermeable, discontinuous beach of the same slope. Two items had not been settled on the basis of small-model data, the thickness of permeable layer and the necessity of permeable material in front of the absorber. However, the large-scale model should provide adequate design information.

The porosity of permeable material should be between 50 and 55 per cent for crushed rock and between 70 and 75 per cent for the rectangular bars. The size of crushed rock should probably be between 3 and 3-1/2 in.; rectangular-bar, precast units should consist of 2- by 2-1/2-in. bars in panels of convenient size (probably 7 by 12 ft).

A question might arise as to how much better a permeable absorber of this type will be than an impermeable absorber of the same shape and length. Some tests were performed in the 6-in. channel to determine this, and Fig. 54 indicates that reflections from an impermeable absorber would be very high for low-steepness waves ($H_I/L = 0.01$), but that the reflection would be high but not necessarily excessive for high-steepness waves ($H_I/L = 0.05$). It should also be emphasized that the prototype absorber was designed for the specific waves (d/L values 0.5 to 6.7) and such an absorber would cause considerable reflection in case of shallow-water waves ($d/L < 0.5$).

E. Scale Effect

All experiments covered by the present report have been conducted in a glass-wall channel 6 in. wide, 15 in. deep, and 40 ft long. Generally, a water depth of 9 in. was used, except for a limited number of tests with a water depth of 12 inches. With a channel of this size it has been possible to cover a fairly wide range of conditions quickly and economically. The final studies will be conducted in a much larger channel 9 ft wide, 6 ft deep, and 250 ft long to provide a sound basis for prototype recommendations. The results of these studies which would cover both crushed-rock and bar-type absorbers will be the subject of the next project report.

Some of the earlier tests were conducted without concern for scale ratio as the primary objective was the determination of the comparative importance of several variables involved. However, in some studies an approximate scale ratio was desired. For this purpose it was assumed, as an approximation, that gravity and inertia forces are of primary importance and, as a consequence, that the model and prototype can be related according to Froude's law. It is thought that the mechanism of energy loss in absorbers might be due to breaking, friction, form drag, or due to all three combined. In addition, part of the wave energy will be reflected. For impermeable absorbers the wave energy is dissipated by breaking and friction, or both. The proportion of energy dissipated by each action would depend on wave steepness and

beach slope. For example, steep waves would dissipate principally by breaking; flat waves, by friction in running up the beach slope.

For permeable absorbers wave energy is dissipated by breaking, friction, or form drag. The proportion of energy dissipated by each action would depend on wave steepness, beach slope, nature of permeable medium and its porosity. For example, the lower the value of porosity, the more a permeable absorber would approach an impermeable absorber and the form-drag loss would be less and loss by breaking and friction will be correspondingly greater. In the case of wire mesh, perforated plates, crushed rock, and bars, it is expected that form-drag loss will be predominant by far for low-steepness waves and that both breaking action and form-drag losses will be responsible for absorption in the case of high-steepness waves. If such is the case, the dimensions of absorbers would be scaled up according to the Froude's law to give prototype values.

The Froude number may be expressed as

$$F = \frac{V}{\sqrt{g\,L}} \tag{18}$$

where V = velocity, g = acceleration of gravity, and L = length.

In this case the most significant ratio is the depth of water, d.

Therefore,

$$F = \frac{C}{\sqrt{g\,d}} \tag{19}$$

where C = wave celerity.

If the Froude numbers of the model and prototype are to be the same

$$F = \frac{C_m}{\sqrt{g\,d_m}} = \frac{C_p}{\sqrt{g\,d_p}} \tag{20}$$

where subscript m describes model, and subscript p, prototype. And the length ratio is

$$L_r = \frac{d_m}{d_p} = \frac{1}{20} \tag{21}$$

The ratio may be used, with reservation, to estimate the prototype length of the absorber corresponding to some of the models tested.

F. Conclusions

1. Basic Study

a. The efficiency of a wave absorber is dependent upon the characteristics of the incident waves as well as the characteristics of the absorber.

b. The length and height of the incident wave and the water depth are important, but one of the most significant parameters is the incident wave steepness (wave height/wave length). The low-steepness waves ($H/L \approx 0.01$) are much more difficult to absorb than the high-steepness waves ($H/L \approx 0.07$). This can be explained in part by the fact that the steeper waves usually break, dissipating considerable energy; whereas, the flat waves may be reflected without breaking. In the latter case the energy loss and corresponding absorber efficiency are dependent upon frictional and turbulent losses on the surface and interior of the absorber.

c. The efficiency of an impermeable absorber is dependent upon the surface slope, roughness of the surface, and the shape of the absorber.

d. The efficiency of a permeable absorber is dependent upon the volume, surface slope, porosity, and shape of the absorber. Variations in each of these items were studied as part of this investigation, although not as comprehensively as may be desired. The four variables are interdependent and, as a result, optimum values of one variable are dependent upon predetermined values of the other three. The data obtained provide an indication of the general influence of each of the four variables upon absorber efficiency.

e. The effect of variations in volume of a permeable absorber was studied by varying the length of the absorber while using fixed values of surface slope and porosity (Figs. 23 to 25, inclusive). For the particular values of slope and porosity used, it was noted that a well-defined minimum volume (or length) existed; volumes less than this amount resulted in high reflections.

f. Similarly, for selected values of porosity and volume the surface slope was varied. It was noted that, in general, the reflection coefficient was a function of the slope, with high reflections resulting from steep slopes (Figs. 29 to 32, inclusive).

g. The effect of porosity was studied using two different materials: gravel and crushed rock (porosities from 40 to 52 per cent), and perforated plate (porosities from 93 to 99 per cent). In addition, limited tests were performed using wire mesh of 95 per cent porosity and square-bar units of 73 and 79 per cent porosity. A slope of 22 degrees was used, and the volume was a constant (Figs. 33, 34, 36, and 37). The lowest reflection coefficients, and corresponding best efficiencies, were obtained for the higher porosities, particularly in the region from 73 to 96 per cent.

h. In case of permeable absorbers for d/L values greater than 0.5, instead of a flat, continuous slope, a parabolic or a discontinuous slope can be employed to advantage. There will be no improvement in coefficient of reflection as compared with a flat, continuous slope (of the same slope as that of the parabolic or discontinuous absorber near the water line), but the length of absorber and the amount of permeable material will be greatly reduced.

2. Applied Study

a. If the length of the absorber is not restricted, it is possible to use a very flat, impermeable slope (slopes of the order of 5 degrees to 10 degrees). However, if the length is restricted, requiring much steeper slopes (say of the order of 10 to 30 degrees), it is necessary to construct the absorber of permeable materials, or a combination of permeable materials and an impermeable beach (i.e., permeable layer overlying the impermeable beach) if high reflections are to be avoided. A discontinuous-slope absorber of this type appears to be the most economical for the proposed prototype installation (Fig. 52).

b. For the conditions specified by the Sponsor a discontinuous-slope-type absorber consisting of a permeable layer backed with an impermeable beach, a 12-degree surface slope appears to be the most favorable (Fig. 45).

c. The reflection coefficient for absorbers made up of a layer of permeable material over an impermeable beach varies with the thickness or volume of the permeable layer. The minimum thickness for the proposed prototype absorber, as well as the necessity of permeable material in front of the absorber will be determined by tests in the large facility. On the basis of the small-scale tests it appears that the maximum thickness to be considered should be 5 ft.

d. The permeable layer can be constructed from either crushed rock or slotted, precast, concrete panels; however, a narrow size gradation of crushed rock would be required, and failure to control the size and placement might result in high reflections. Therefore, it might be desirable to build a unit employing precast, concrete panels for which the reflections could be predicted with greater certainty.

e. In addition to variables discussed under section 1-d of the conclusions, the location of the impermeable beach underlying the permeable part of the absorber is important. The exact location of the impermeable beach can be recommended only after completion of tests in the large facility; however, it appears that for the range of wave characteristics of interest to the Sponsor (d/L = 6.7 to 0.5 and H_I/L = 1/15 to 1/100), the location indicated in Fig. 52 would be most favorable.

f. The tests in the large facility will cover the most promising absorber design (Fig. 52). Both crushed rock and a wooden model of precast, concrete panel beach will be employed in these tests. The final absorber design will be based on tests in the large facility.

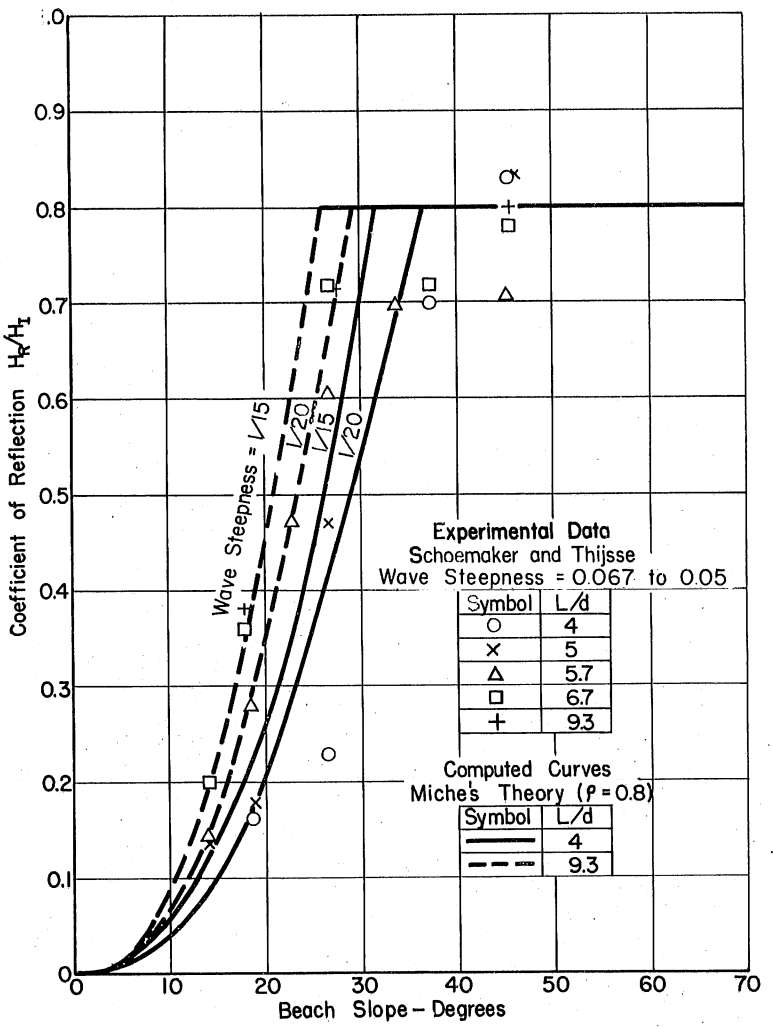

Fig. 14(a) – Comparison of Experimental and Theoretical Results for Impermeable Absorbers. Schoemaker and Thijsse's Data

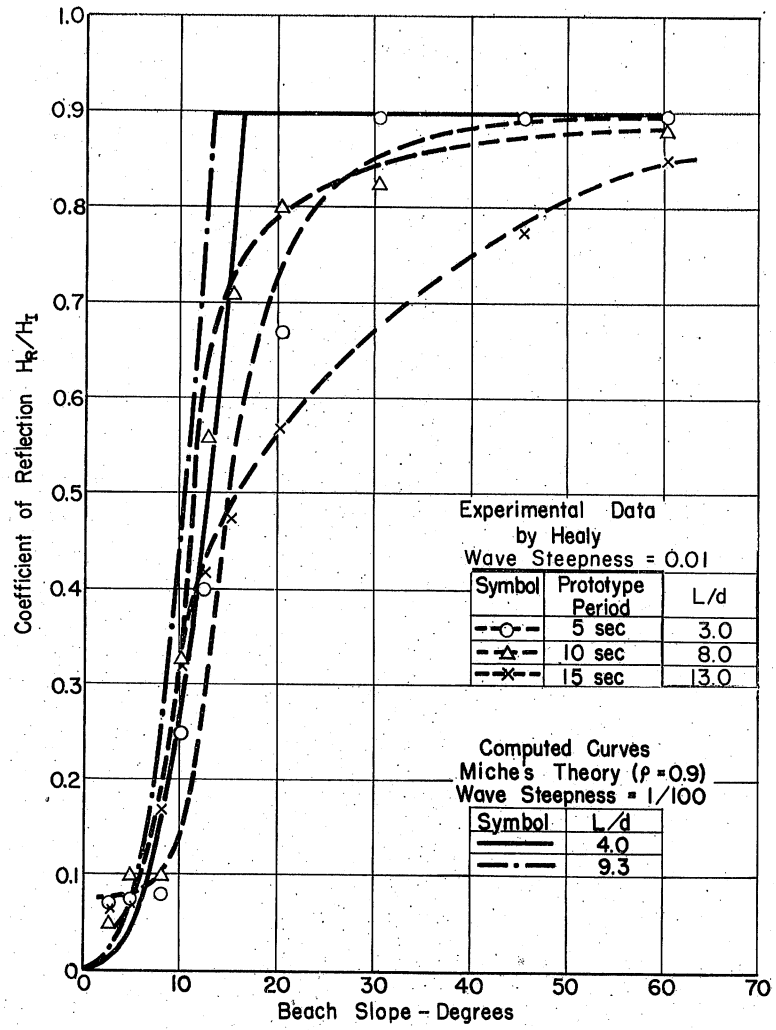

Fig. 14(b) – Comparison of Experimental and Theoretical Results for Impermeable Absorbers. Healy's Data

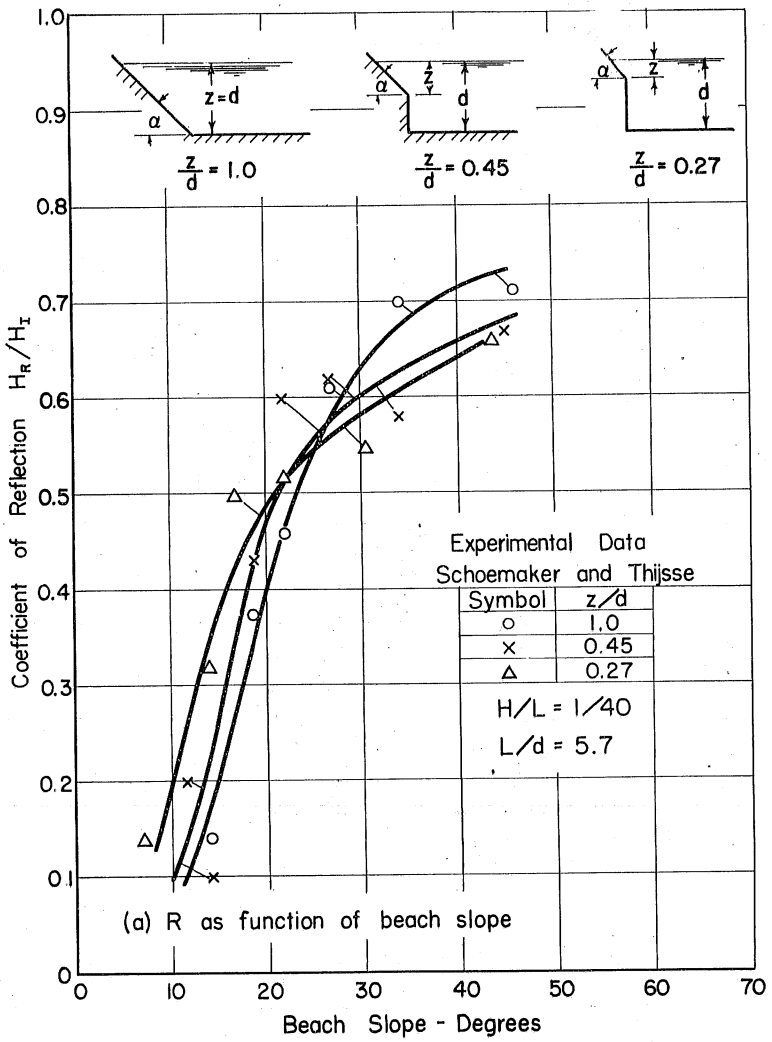

Fig. 15(a) – Experimental Data for Impermeable Beaches with a Discontinuous Slope. R as a Function of Beach Slope

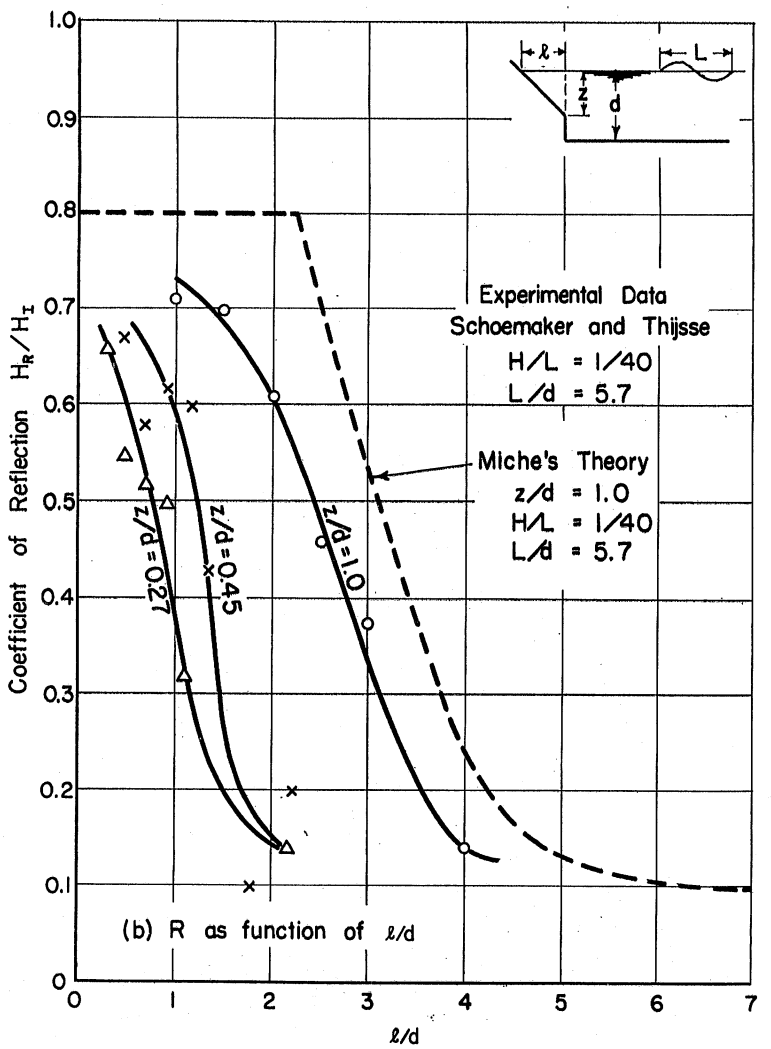

Fig. 15(b) – Experimental Data for Impermeable Beaches with a Discontinuous Slope. R as a Function of ℓ/d

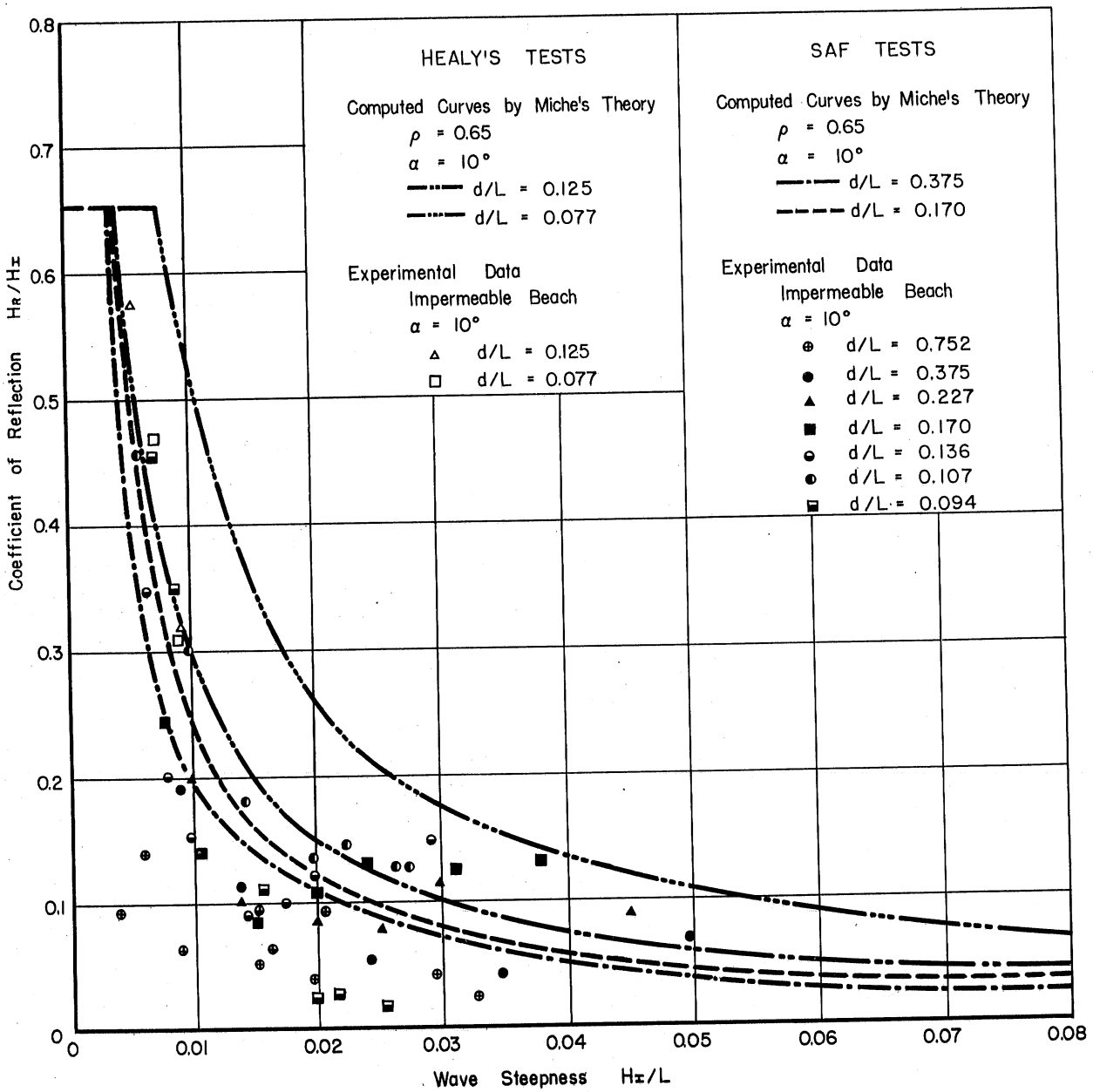

Fig. 16 – Comparison of Experimental and Theoretical Results for Impermeable Absorbers. Theoretical Curves Computed Following Miche's Theory

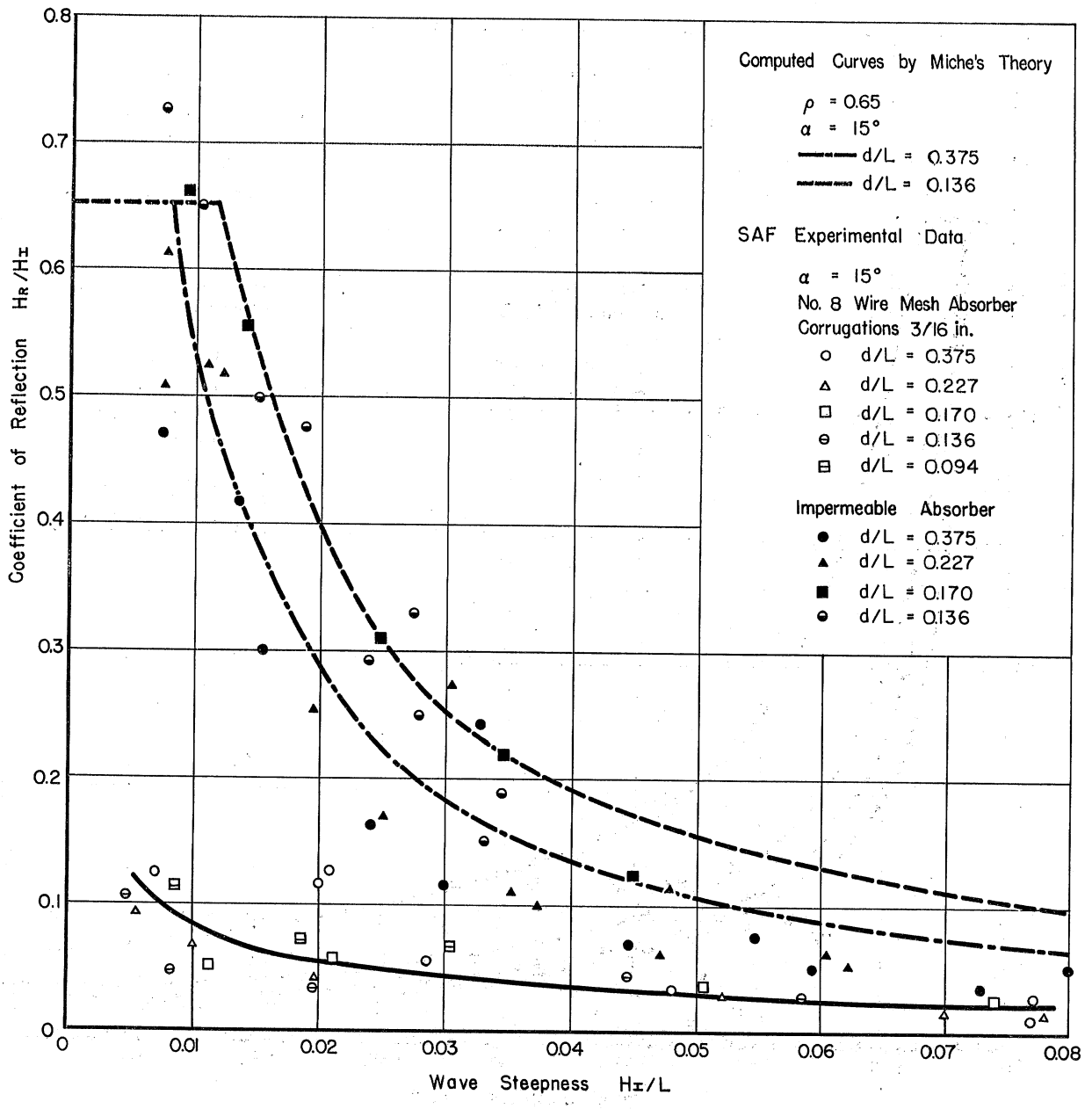

Fig. 17 – Comparison of Experimental and Theoretical Results for Impermeable and Permeable Absorbers

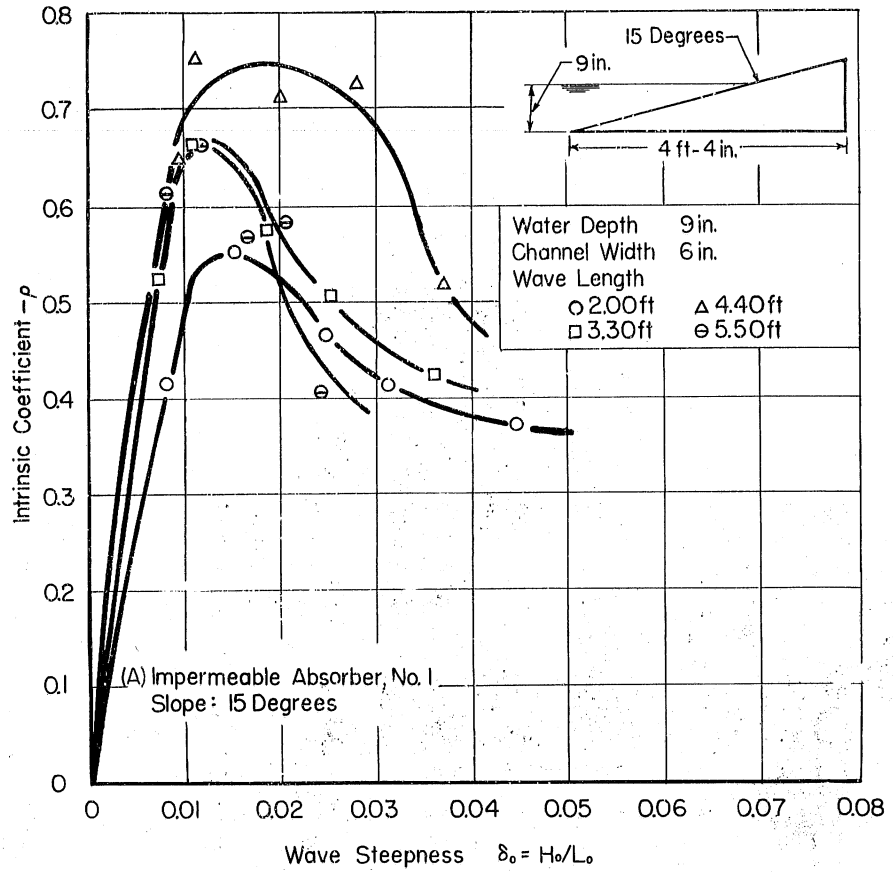

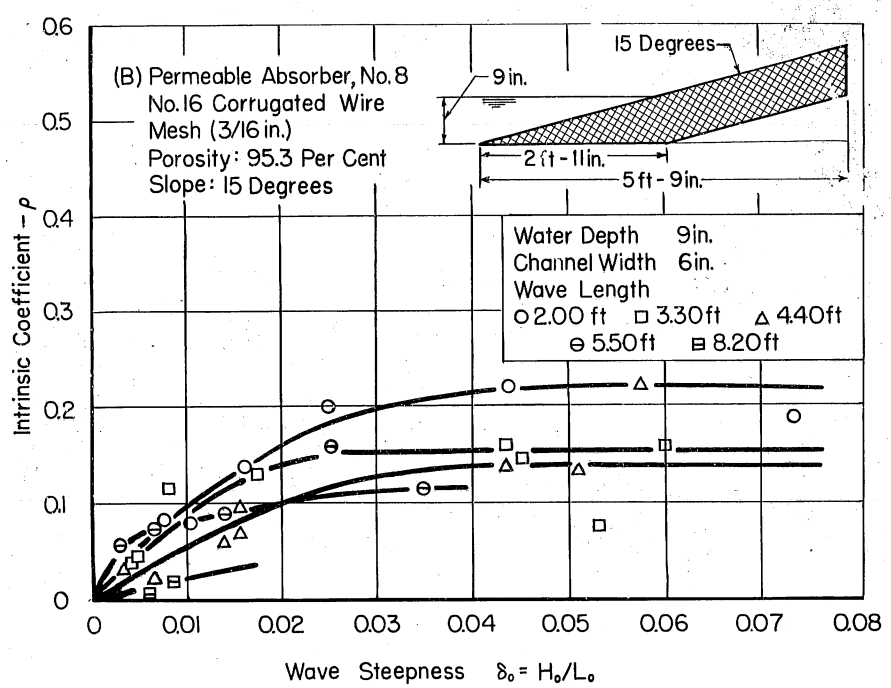

Fig. 18 – Miche's Intrinsic Coefficient ρ for Various Absorbers

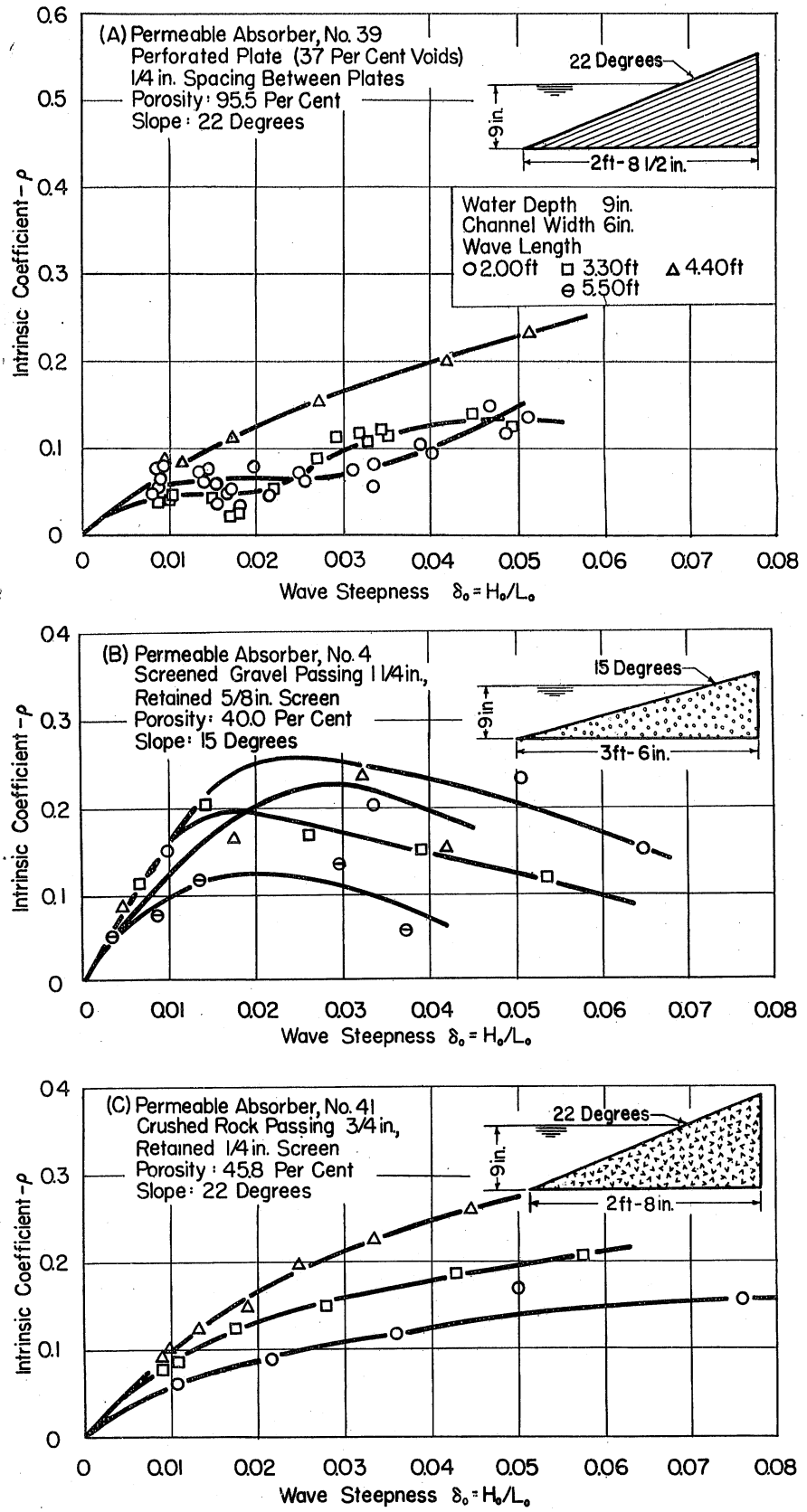

Fig 19 - Miche's Intrinsic Coefficient ρ for Various Absorbers

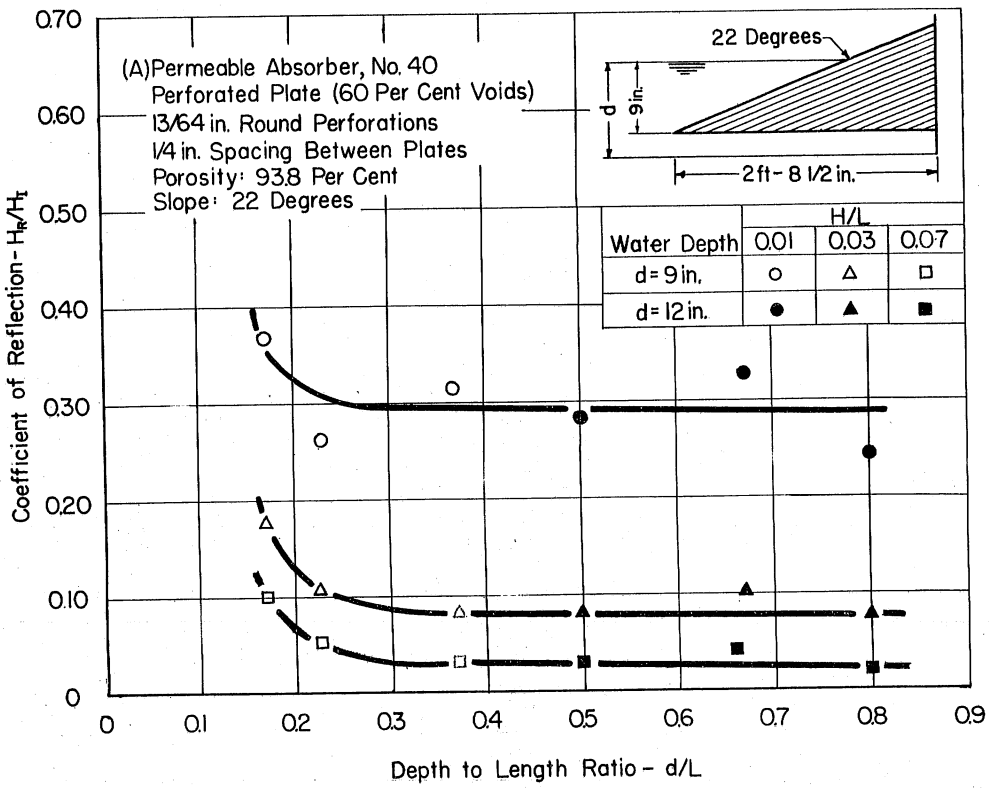

Fig. 20 - Effect of Depth-to-Length Ratio on Coefficient of Reflection

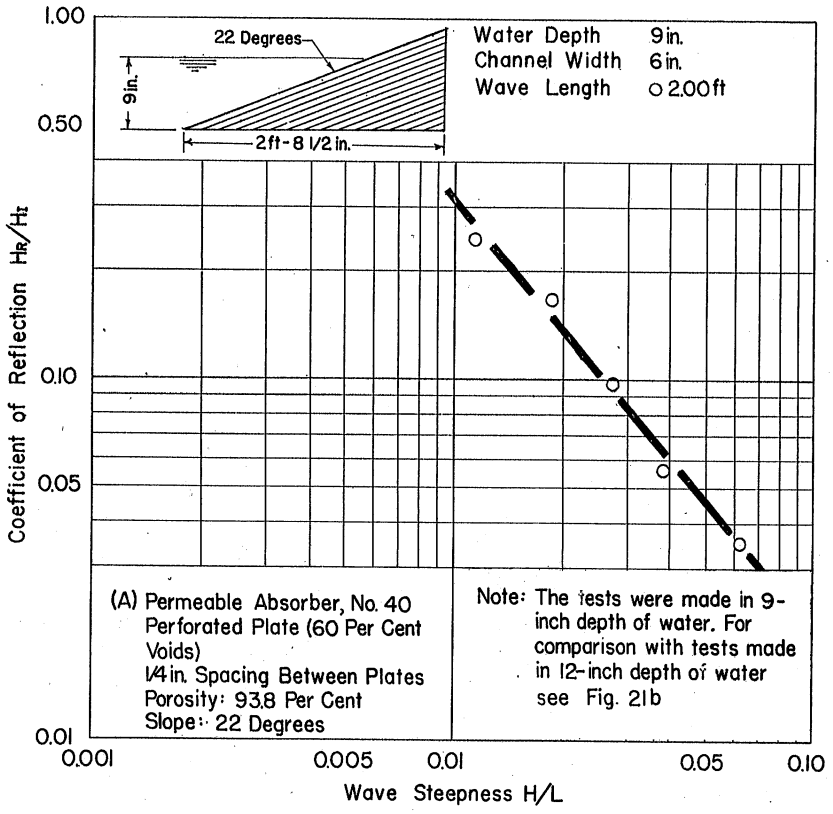

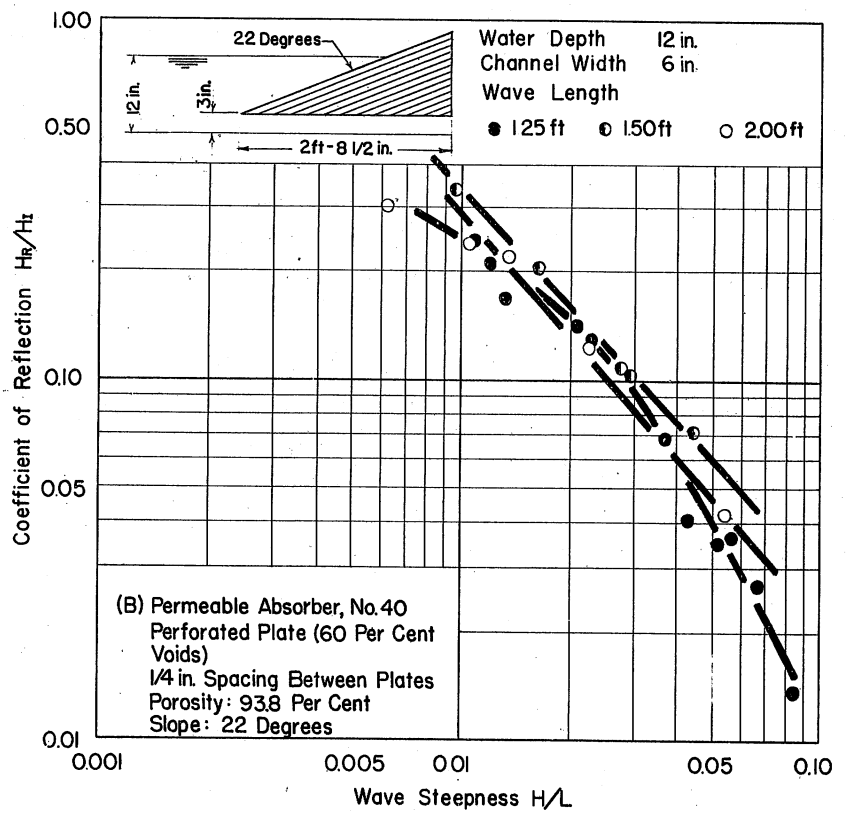

Fig. 21 - Effect of Depth of Water on Coefficient of Reflection

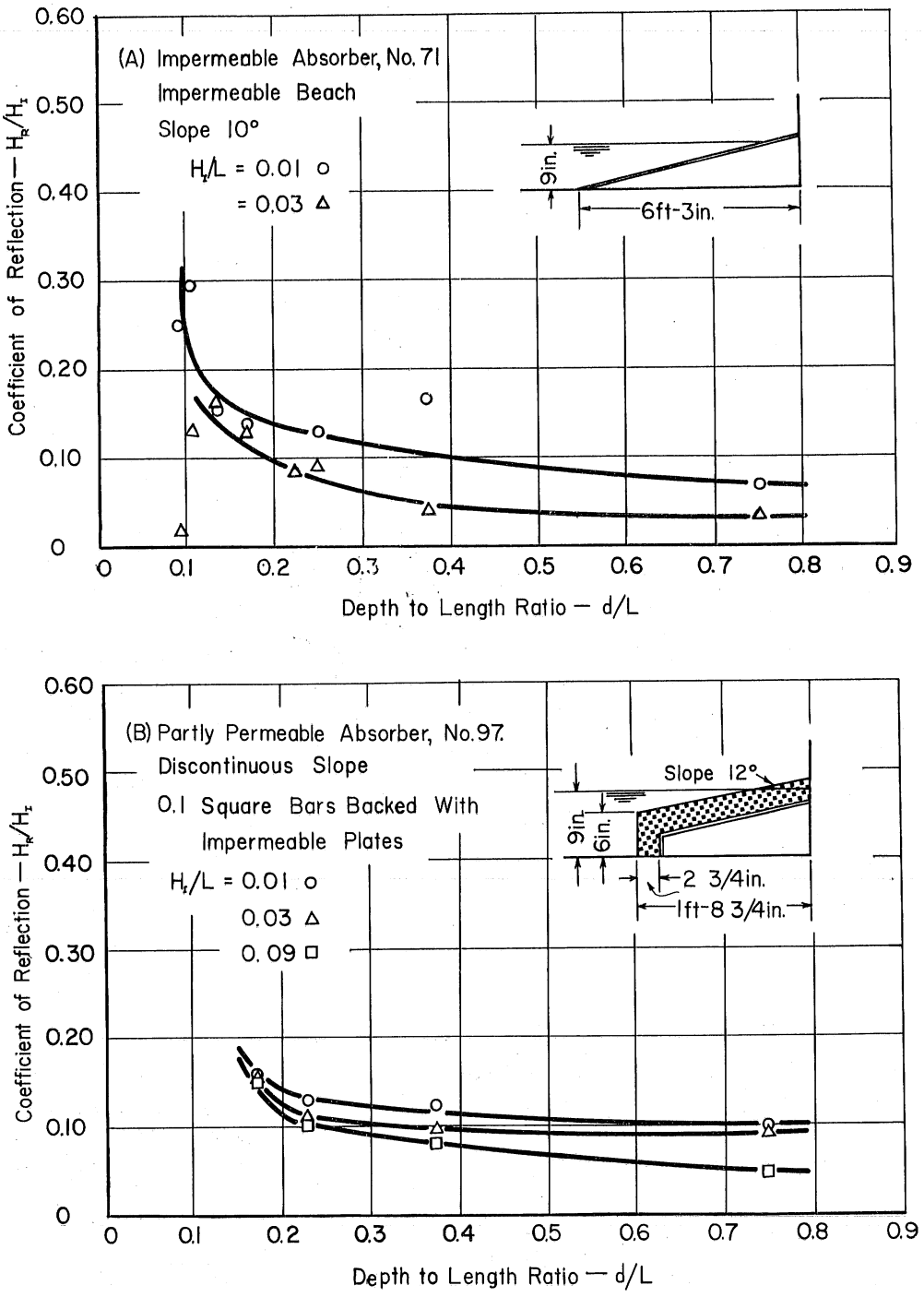

Fig. 22 - Effect of Depth-to-Length Ratio on Coefficient of Reflection

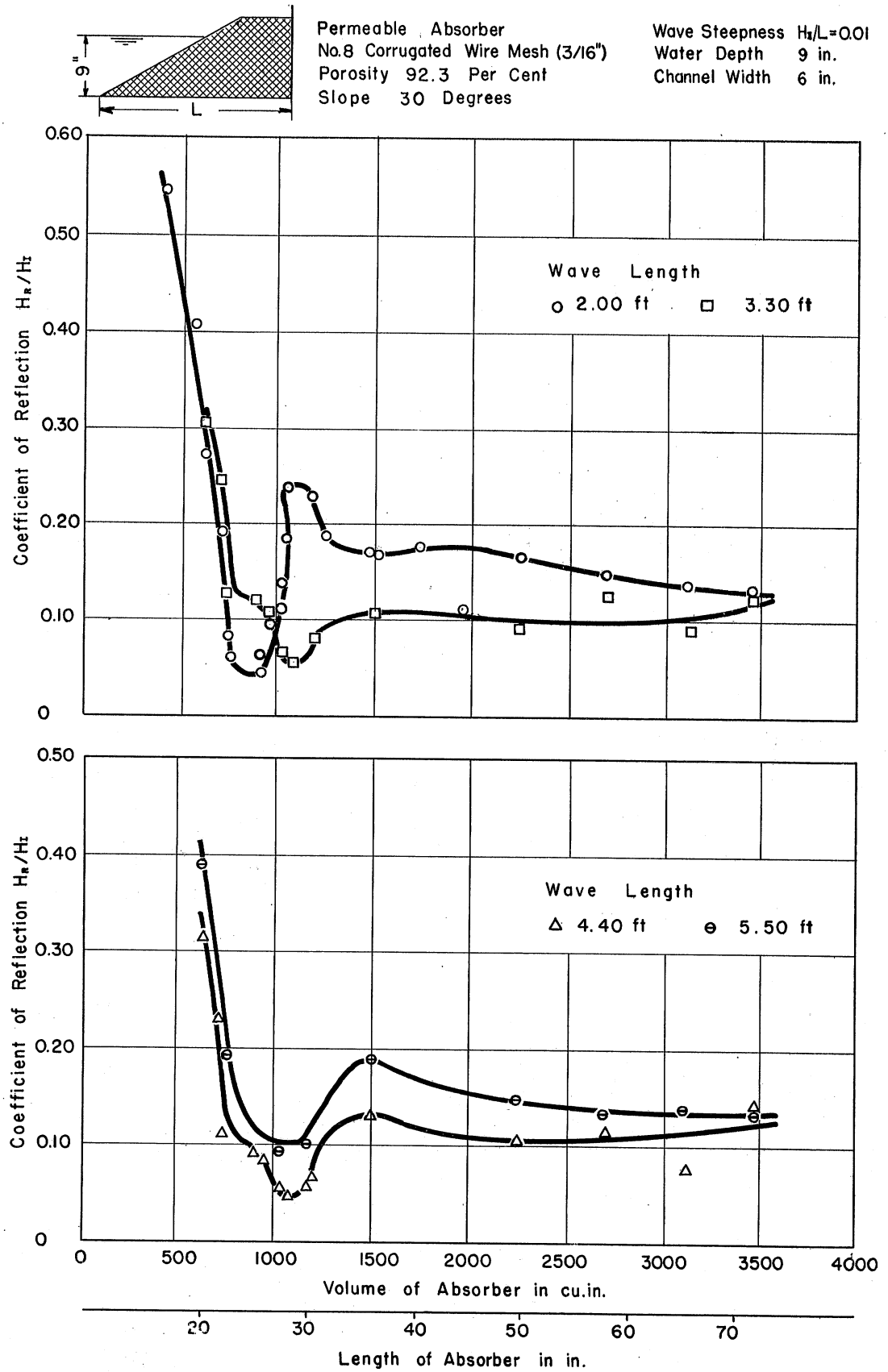

Fig. 23 - Effect of Volume on Coefficient of Reflection for a Wire-Mesh Absorber. Wave Steepness = 0.01

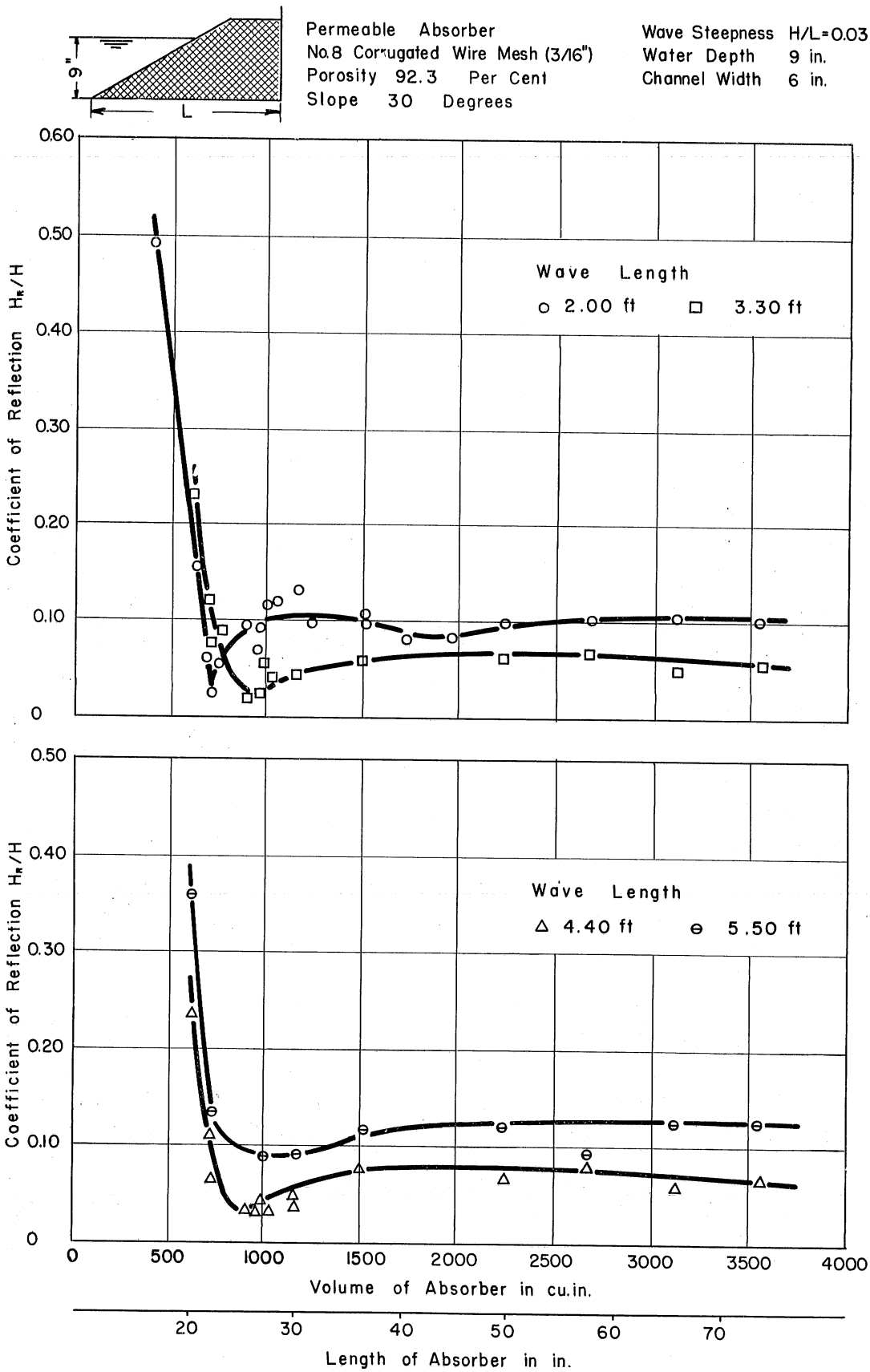

Fig. 24 - Effect of Volume on Coefficient of Reflection for a Wire-Mesh Absorber. Wave Steepness = 0.03

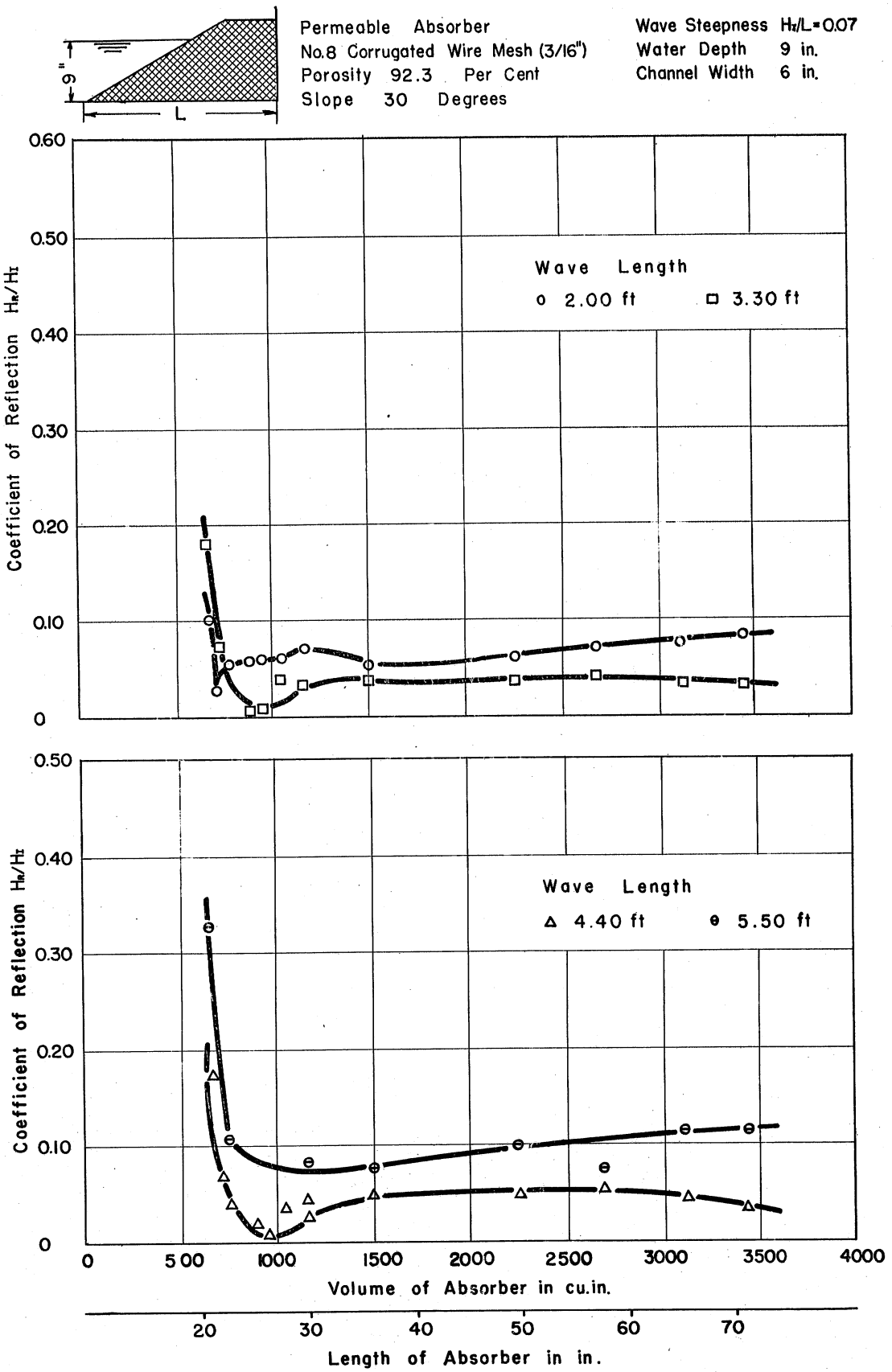

Fig. 25 – Effect of Volume on Coefficient of Reflection for a Wire-Mesh Absorber. Wave Steepness = 0.07

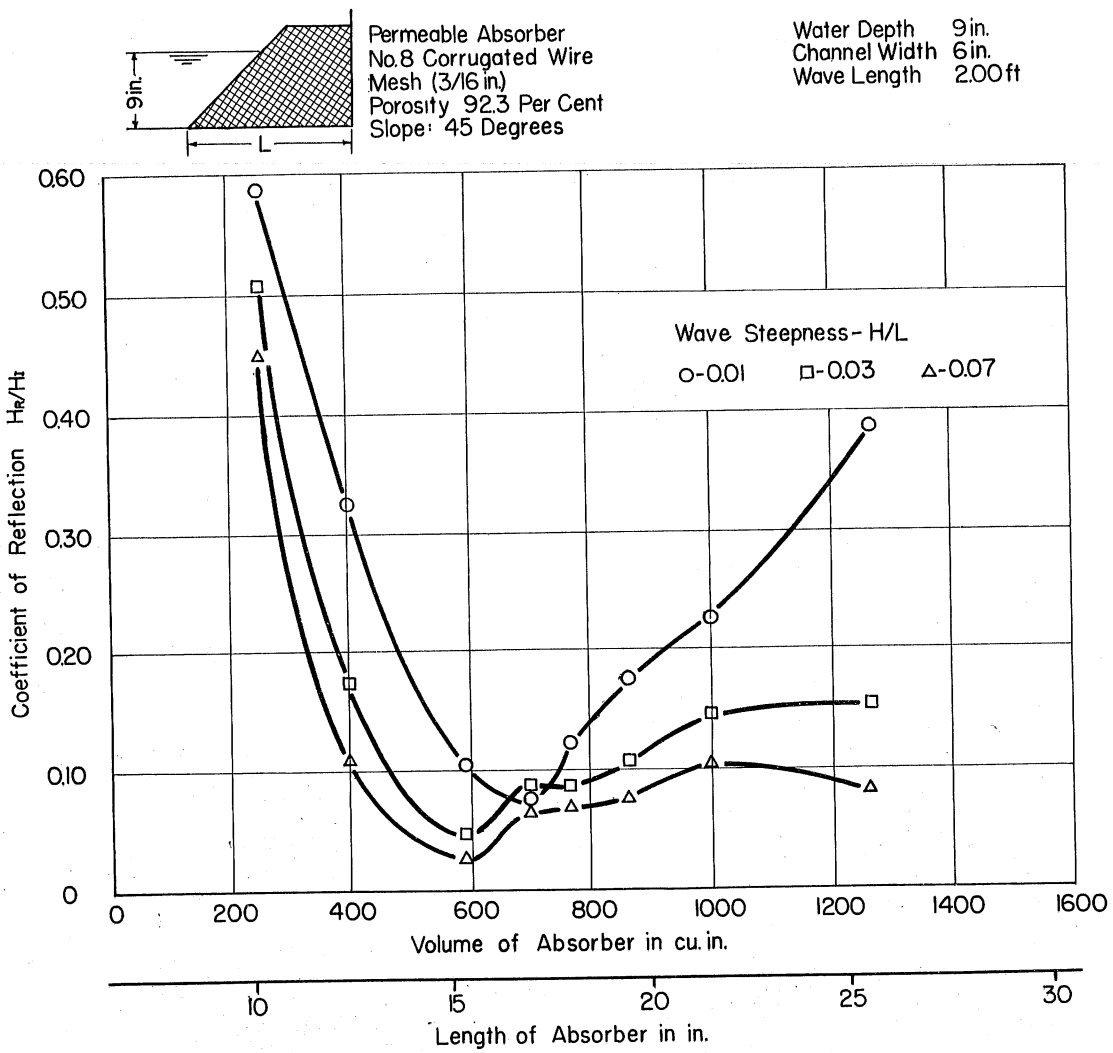

Fig. 26 - Effect of Volume on Coefficient of Reflection for a Wire-Mesh Absorber. Slope 45 degrees

Fig. 27 - A View of a Permeable Absorber Constructed of No. 8 Wire Mesh. Surface Slope 15 degrees, Porosity 92.3 per cent

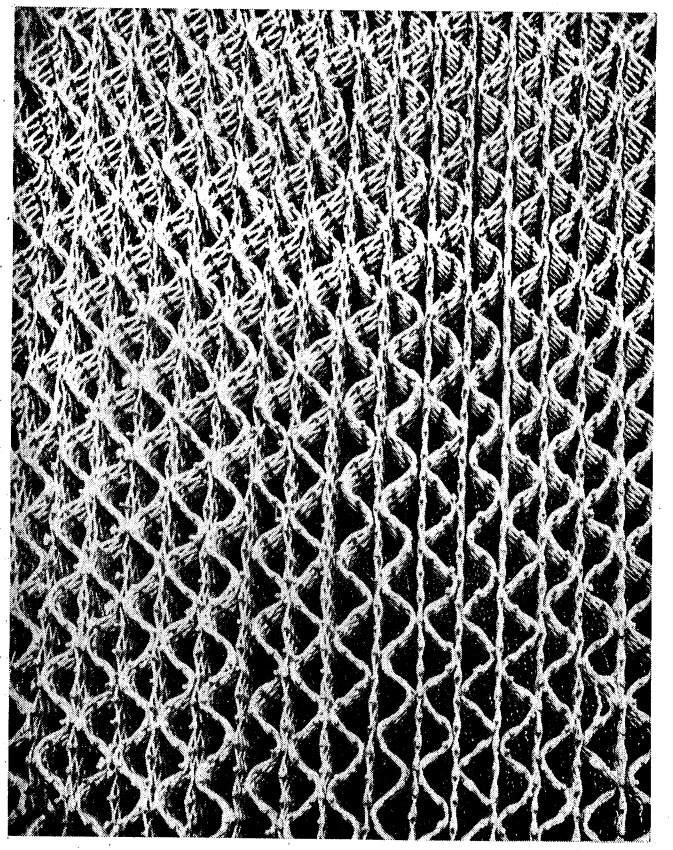

Fig. 28 - Detail View Showing Construction of a Wire-Mesh Absorber. (No. 8 wire mesh with corrugations 3/16 in. deep and 7/16 in. long were used. Corrugated wire mesh separated with flat sheets of wire mesh.)

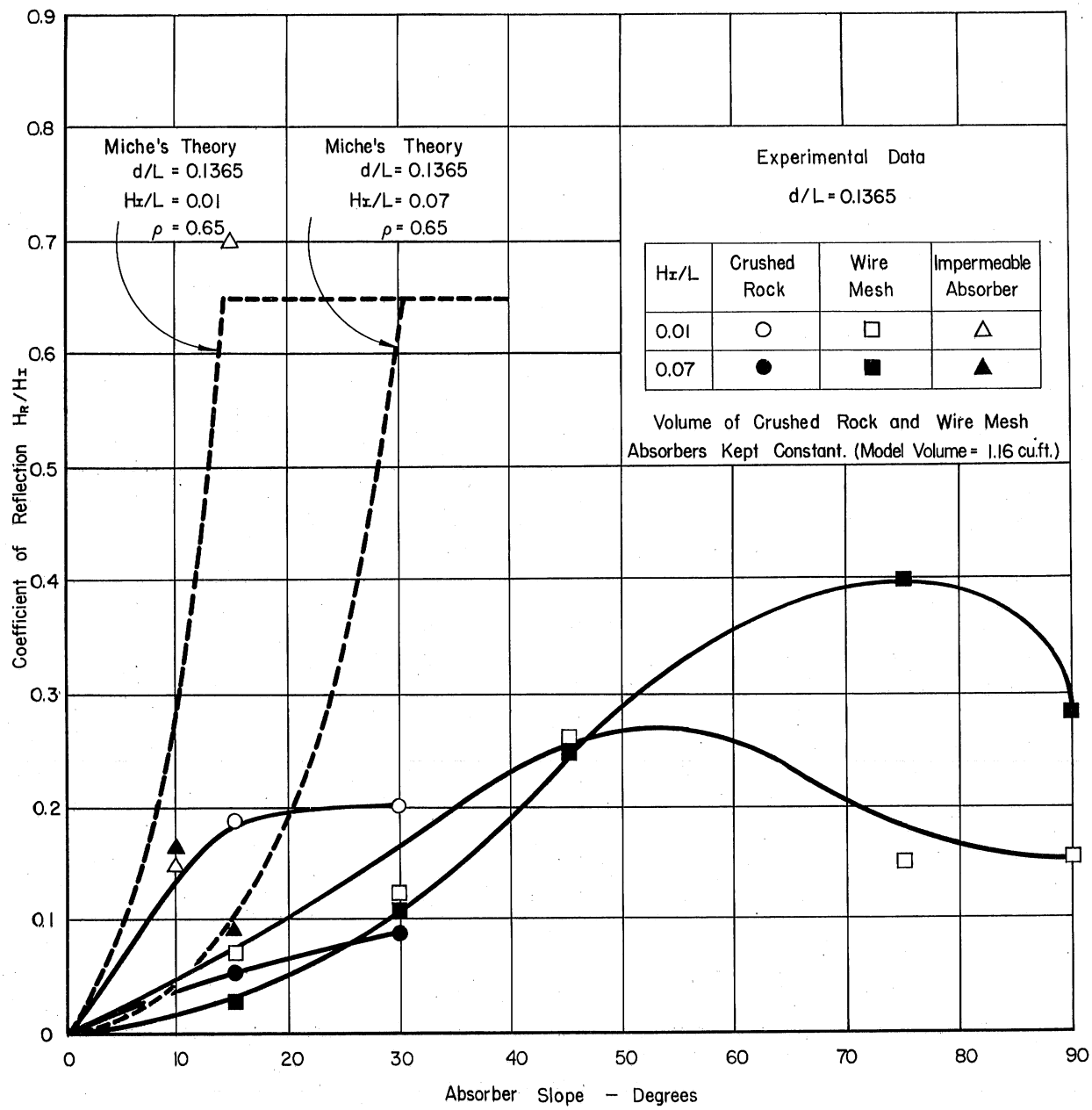

Fig. 29 – Effect of Slope of Permeable and Impermeable Absorbers on Coefficient of Reflection. d/L = 0.1365

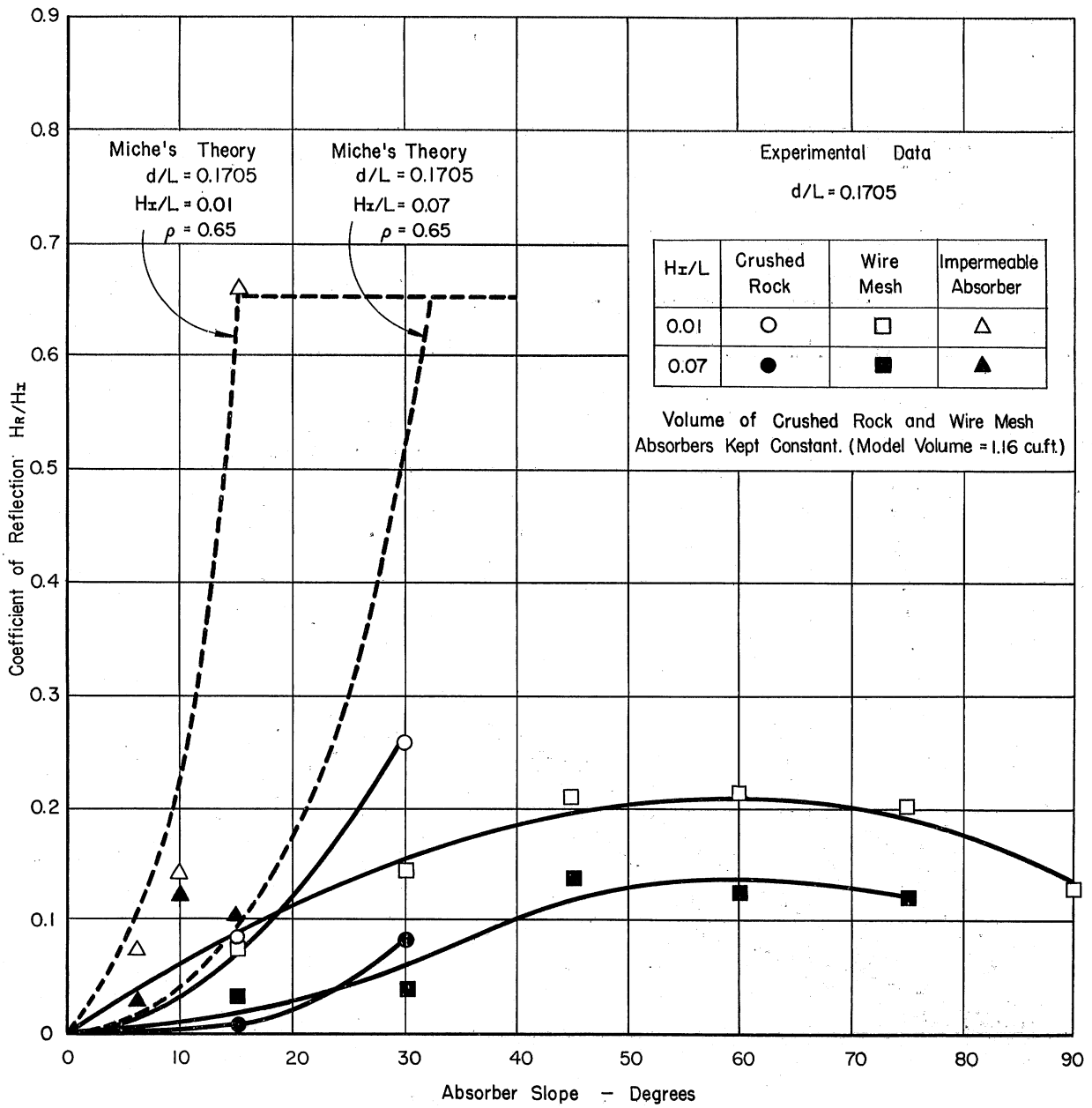

Fig. 30 – Effect of Slope of Permeable and Impermeable Absorbers on Coefficient of Reflection. d/L = 0.1705

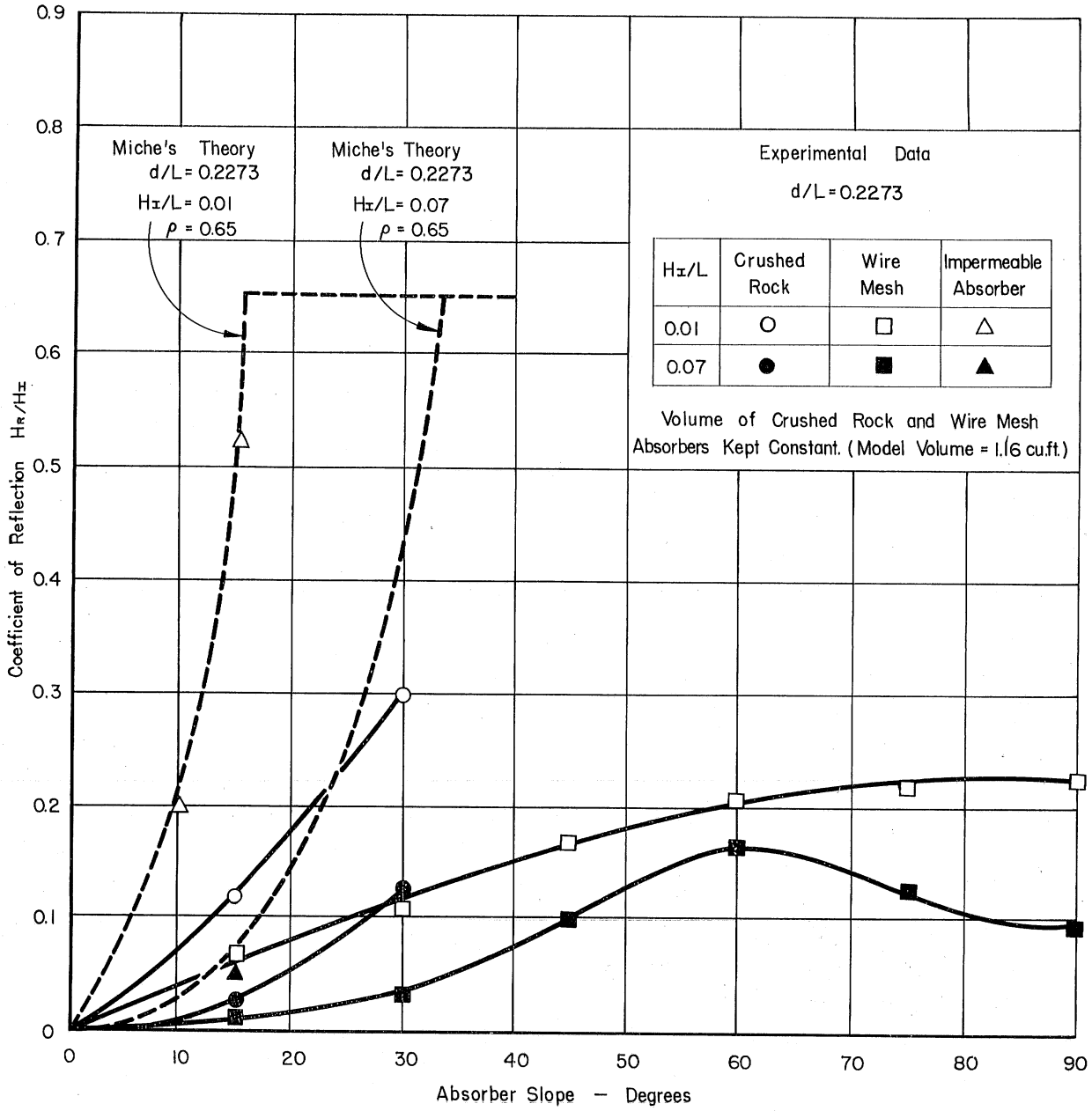

Fig. 31 - Effect of Slope of Permeable and Impermeable Absorbers on Coefficient of Reflection. d/L = 0.2273

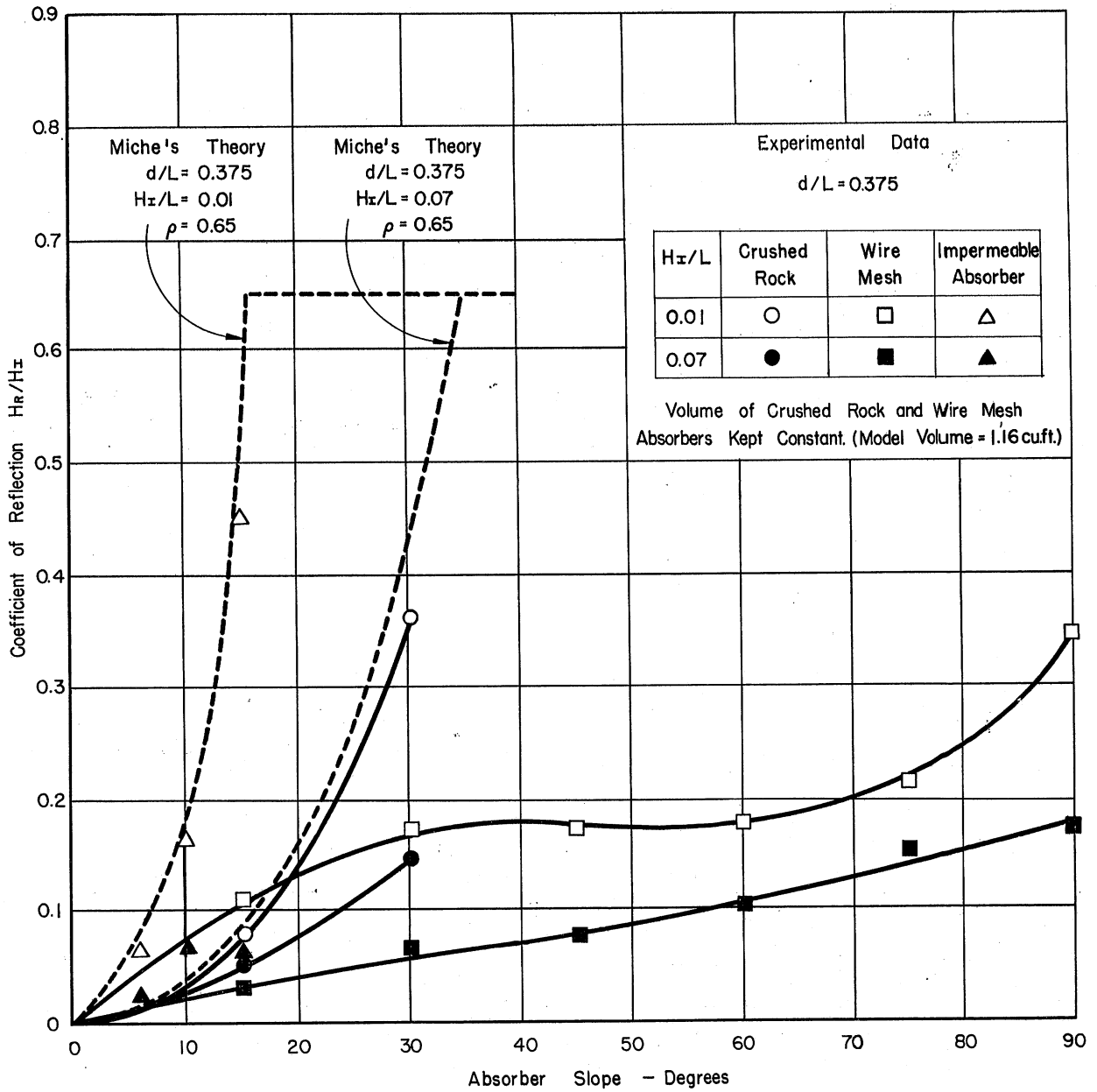

Fig. 32 – Effect of Slope of Permeable and Impermeable Absorbers on Coefficient of Reflection. d/L = 0.375

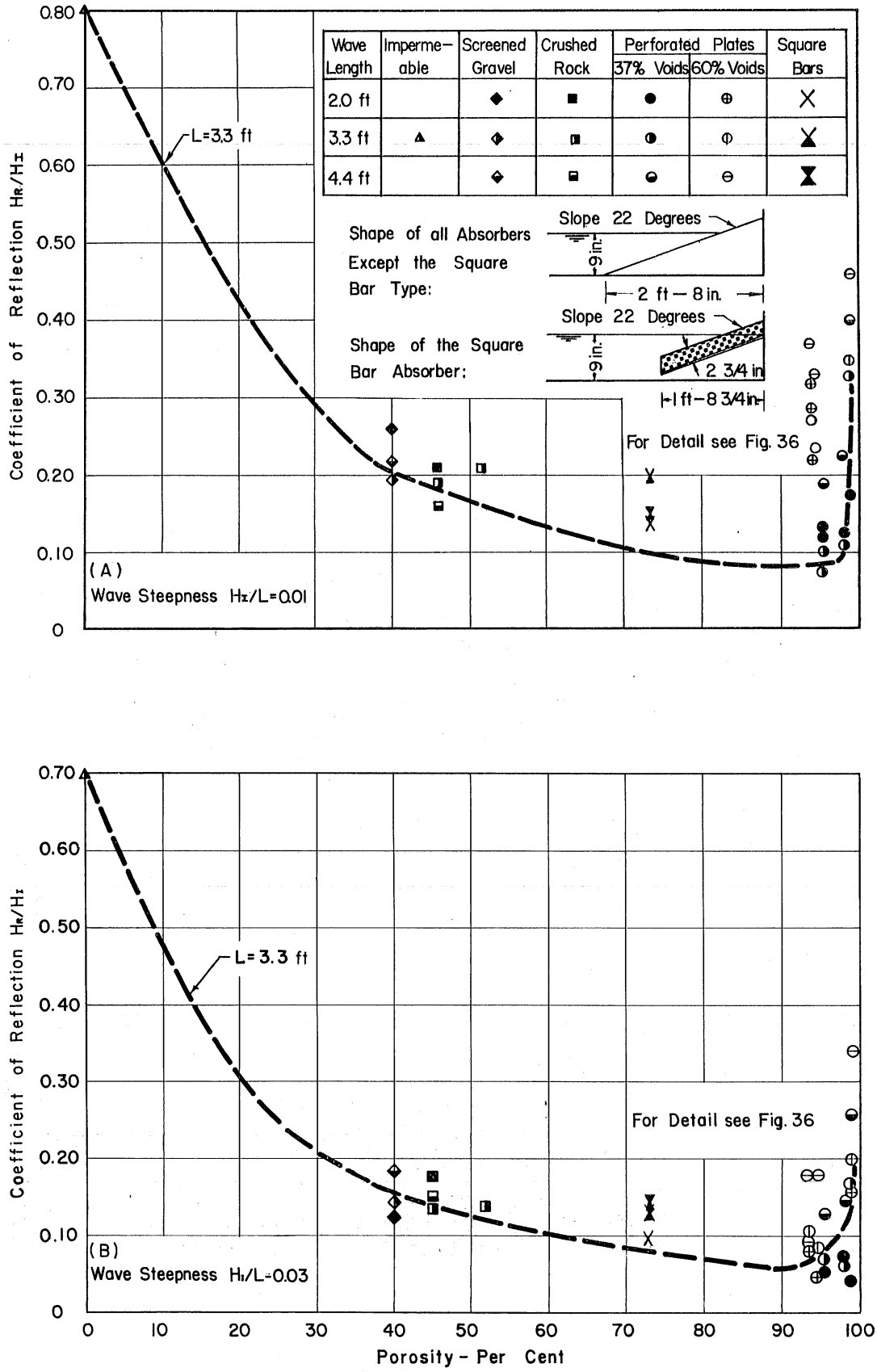

Fig. 33 - Effect of Porosity on Coefficient of Reflection for Various Absorbers. H_1/L = 0.01 and 0.03

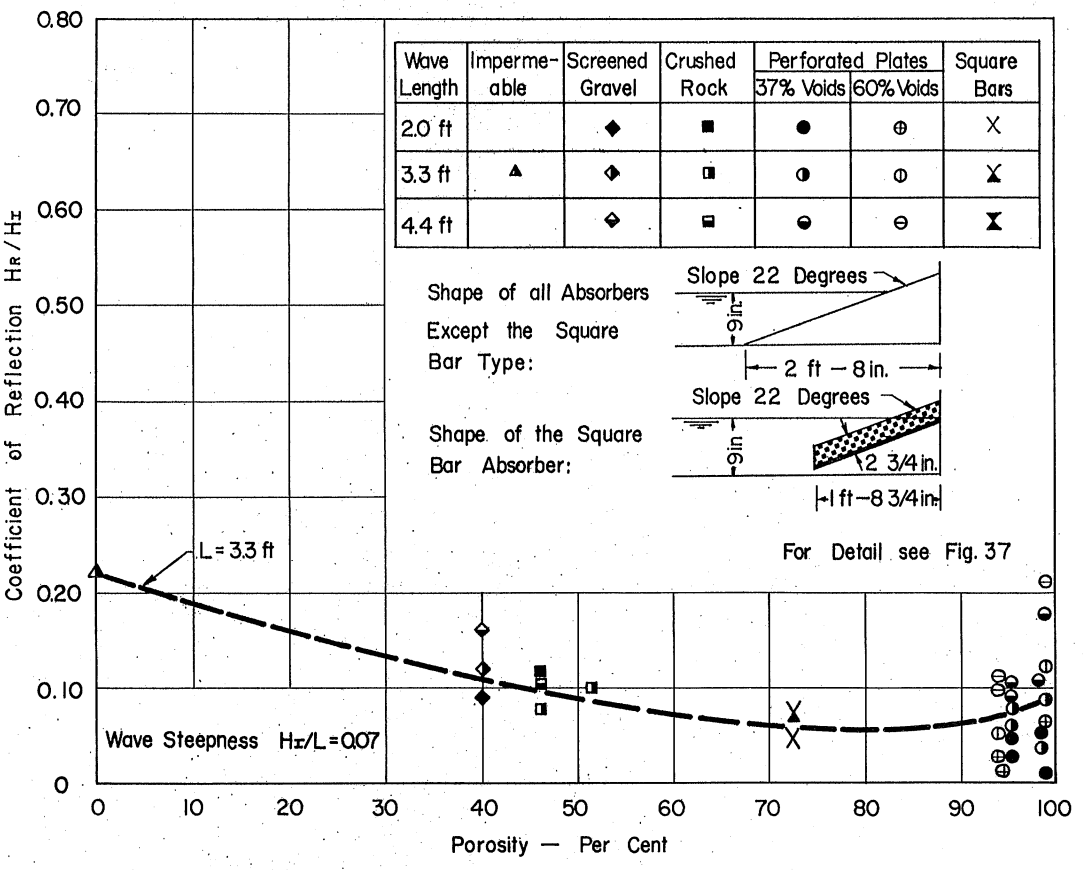

Fig. 34 - Effect of Porosity on Coefficient of Reflection for Various Absorbers. $H_I/L = 0.07$

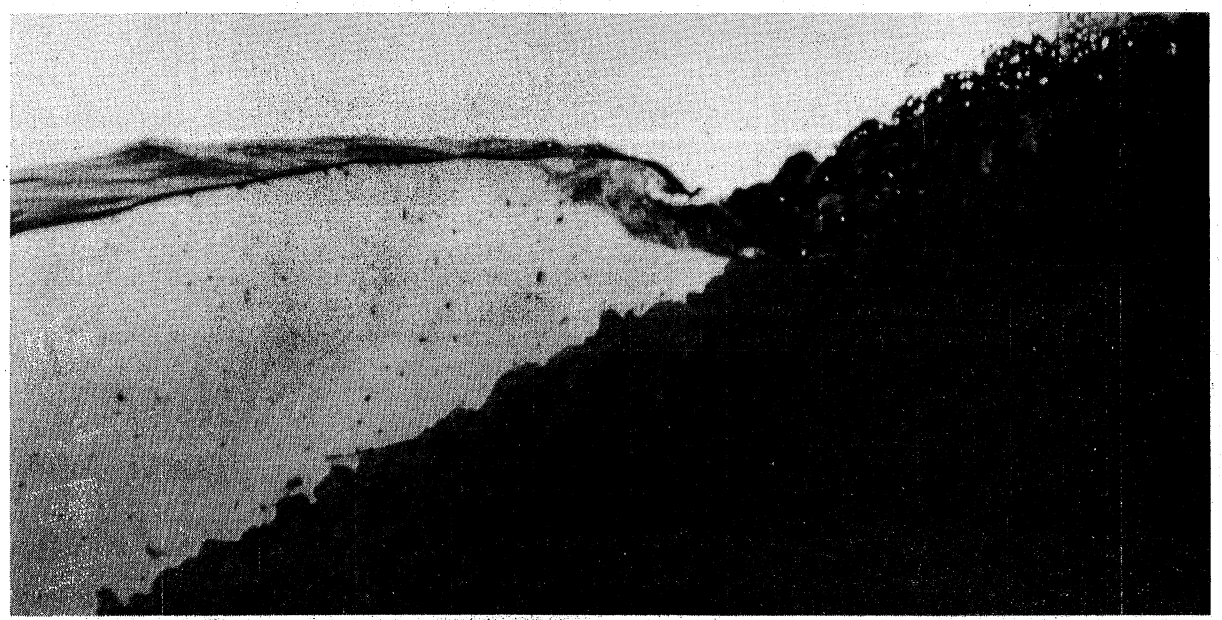

Fig. 35 - A View of a Permeable Absorber Constructed of Crushed Rock. Crushed Rock Passing 3/4-in. Screen and Retained on 1/4-in Screen. Porosity 46 per cent and Surface Slope 22 degrees

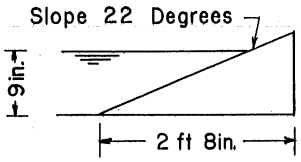

Wave Length	Wire Mesh	Perforated Plates	
		37% Voids	60% Voids
1.25 ft		⊖	⊘
1.50 ft		◐	⊘
2.00 ft	●	●	⊕
3.30 ft	◑	◑	◑
4.40 ft		⊖	⊖

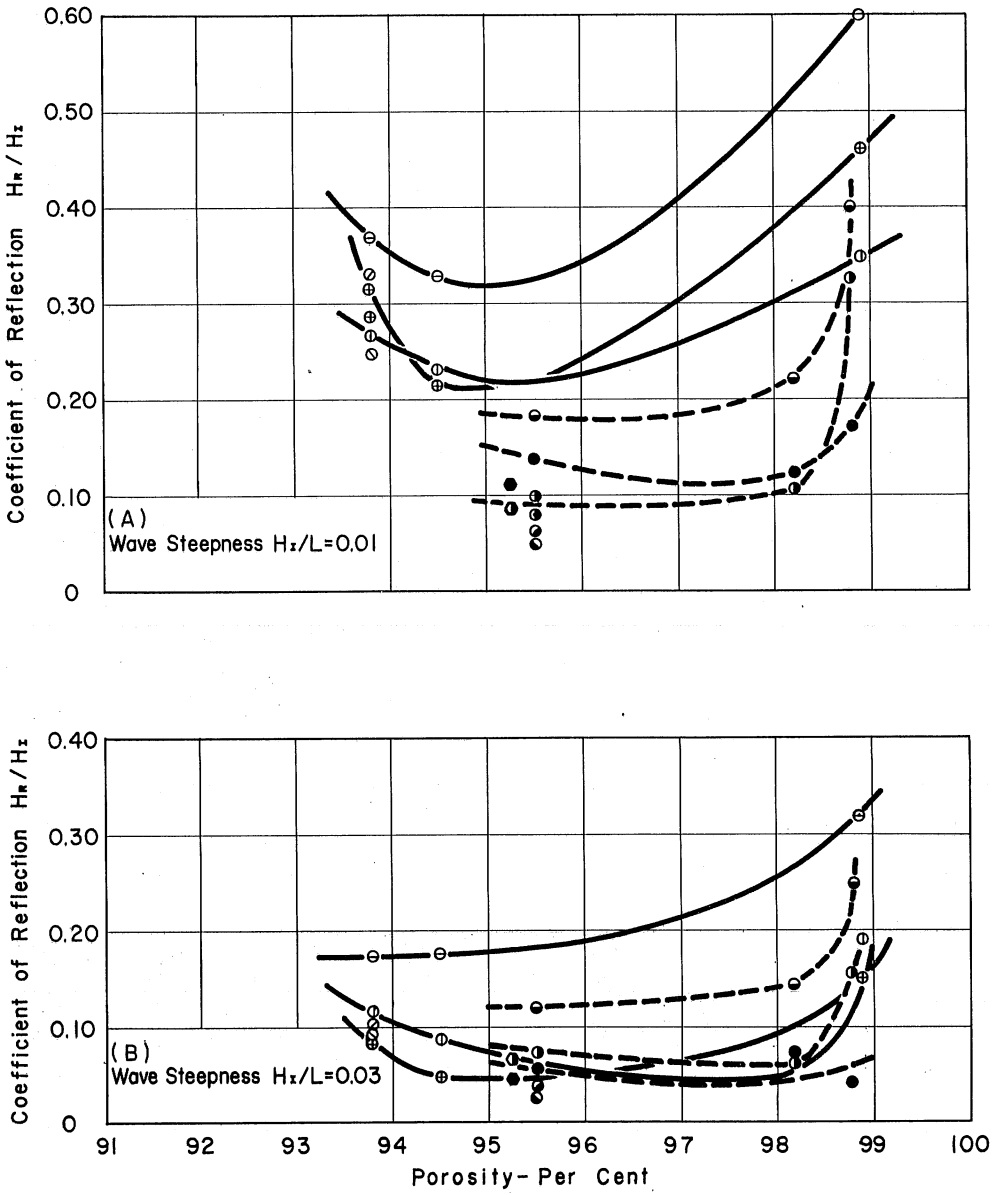

Fig. 36 - Effect of Porosity on Coefficient of Reflection for Perforated-Plate Absorbers. H_I/L = 0.01 and 0.03

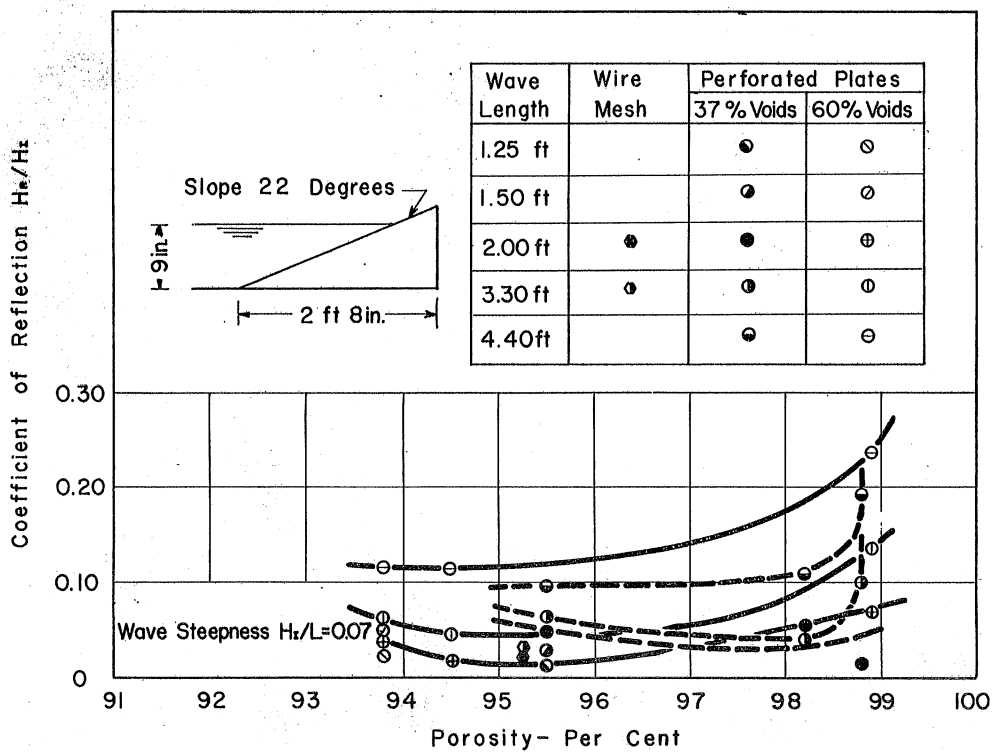

Fig. 37 - Effect of Porosity on Coefficient of Reflection for Perforated-Plate Absorbers. $H_I/L = 0.07$

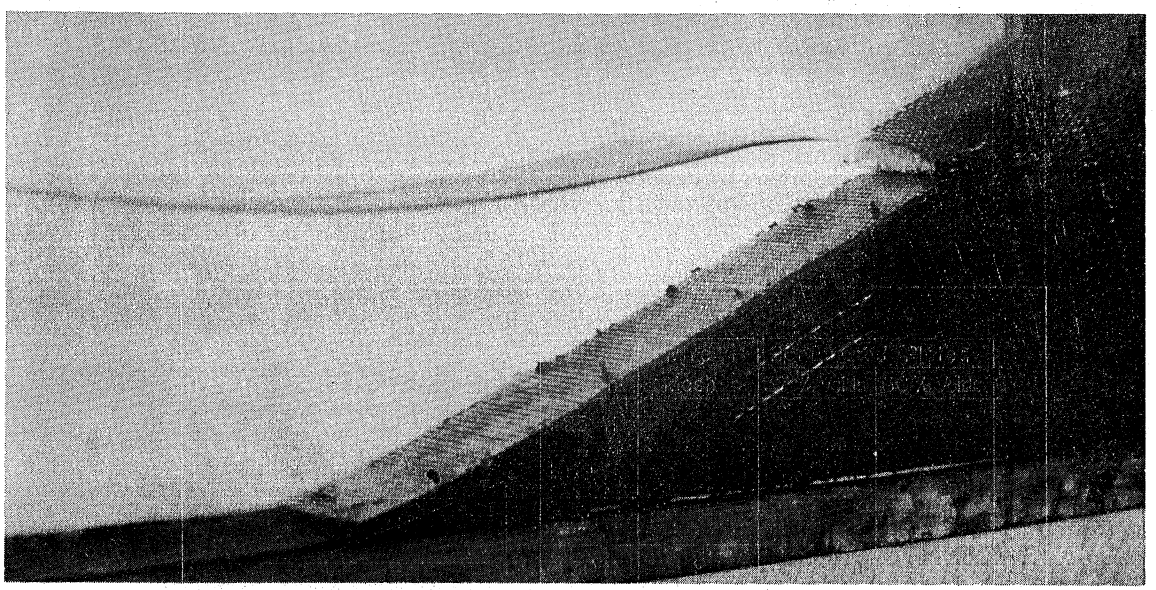

Fig. 38 - A View of Permeable Absorber Constructed of Perforated Plates. (Perforated plates 37 per cent voids, round perforations; spacing between plates 1/4 in.; porosity of absorber 95.5 per cent; slope of absorber 22 degrees.)

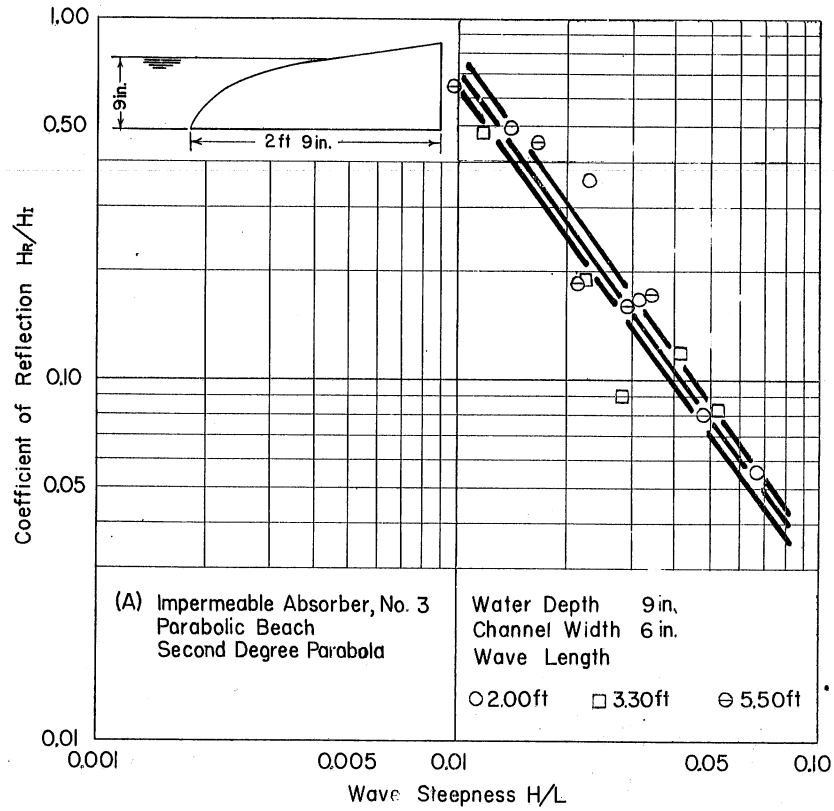

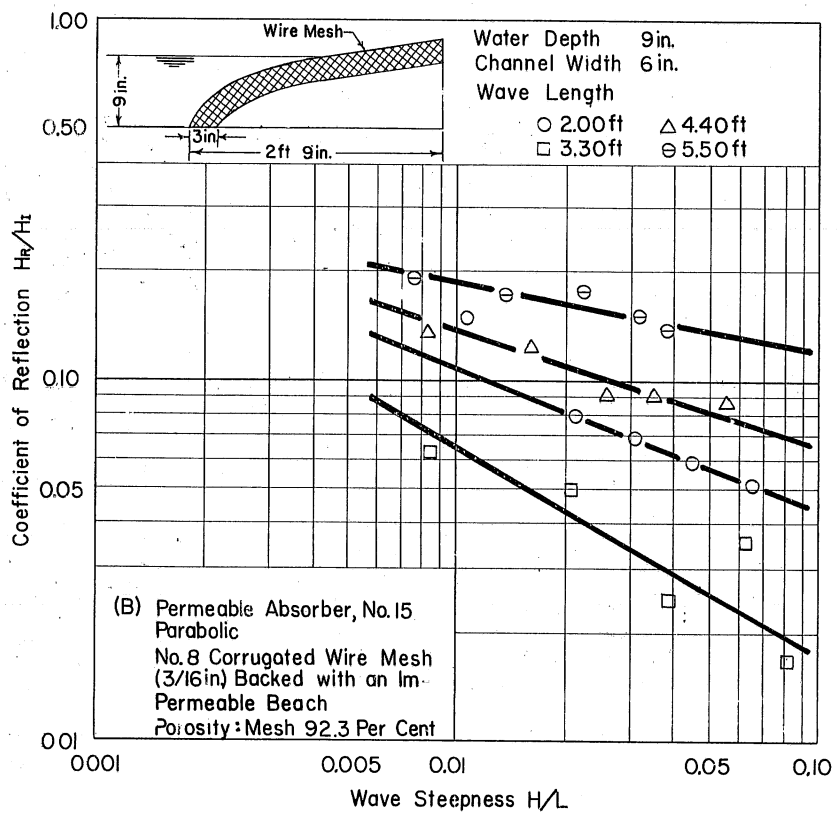

Fig. 39 – Coefficient of Reflection for Parabolic-Type Absorbers

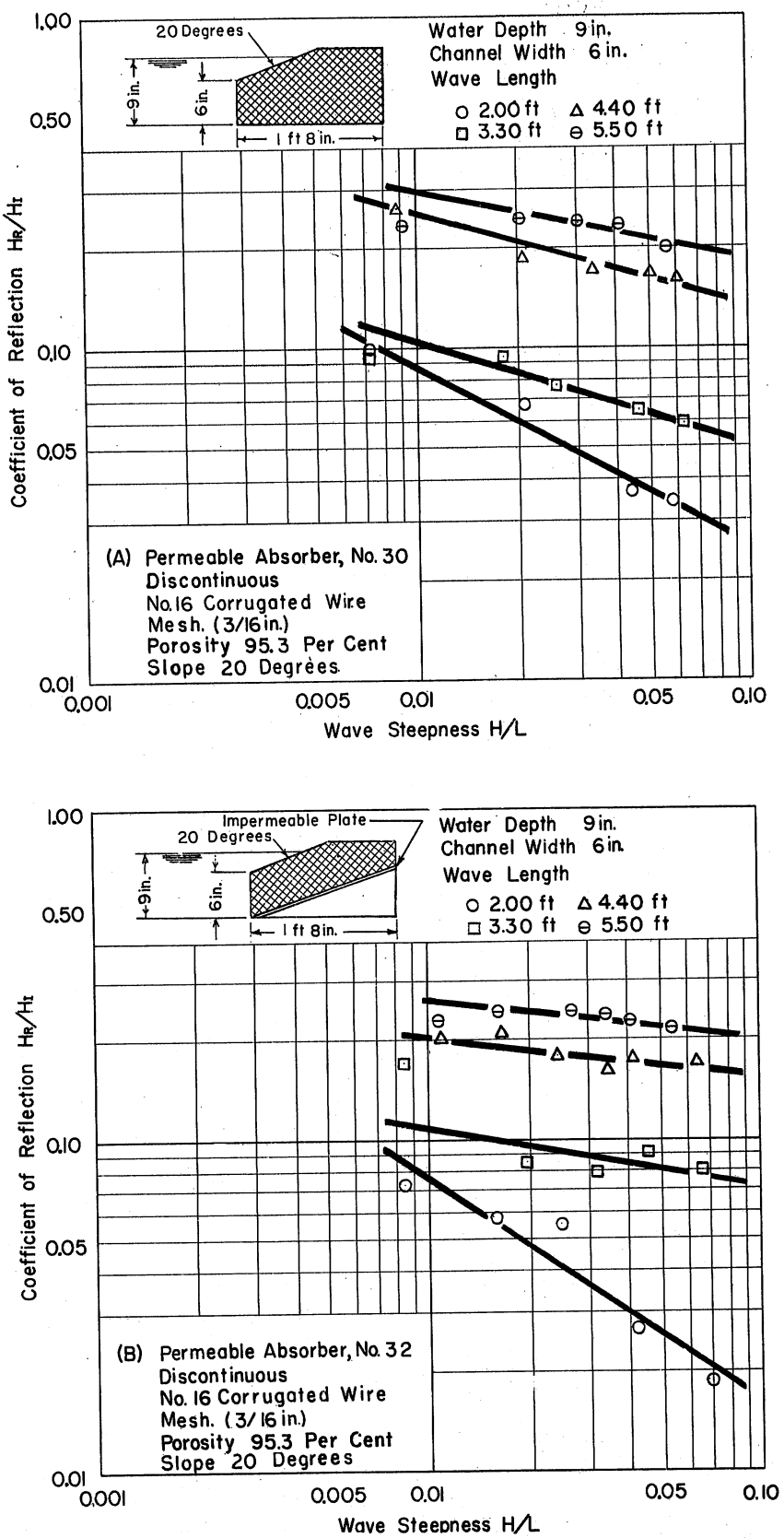

Fig. 40 - Coefficient of Reflection for Permeable Wire-Mesh Absorbers with a Discontinuous Slope

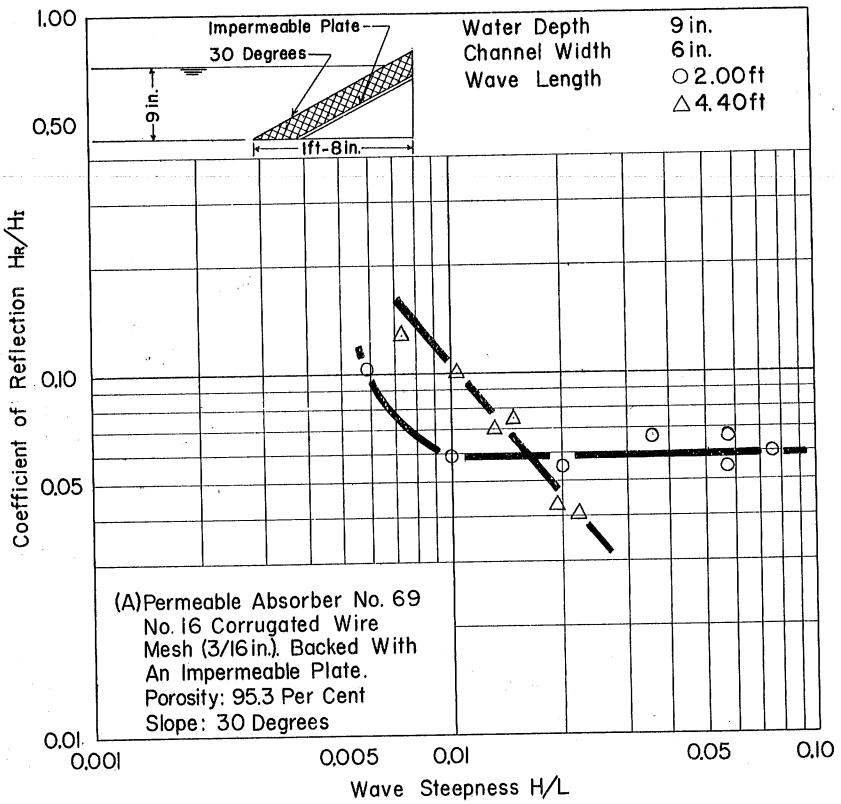

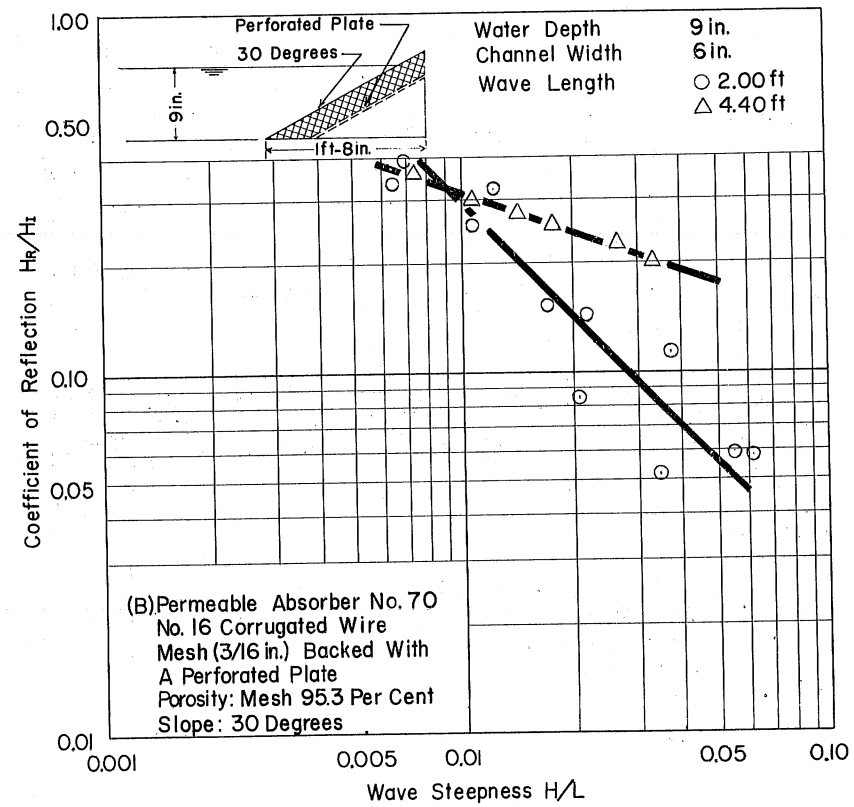

Fig. 41 - Coefficient of Reflection for Permeable Absorbers Backed with a Perforated or Impermeable Plate

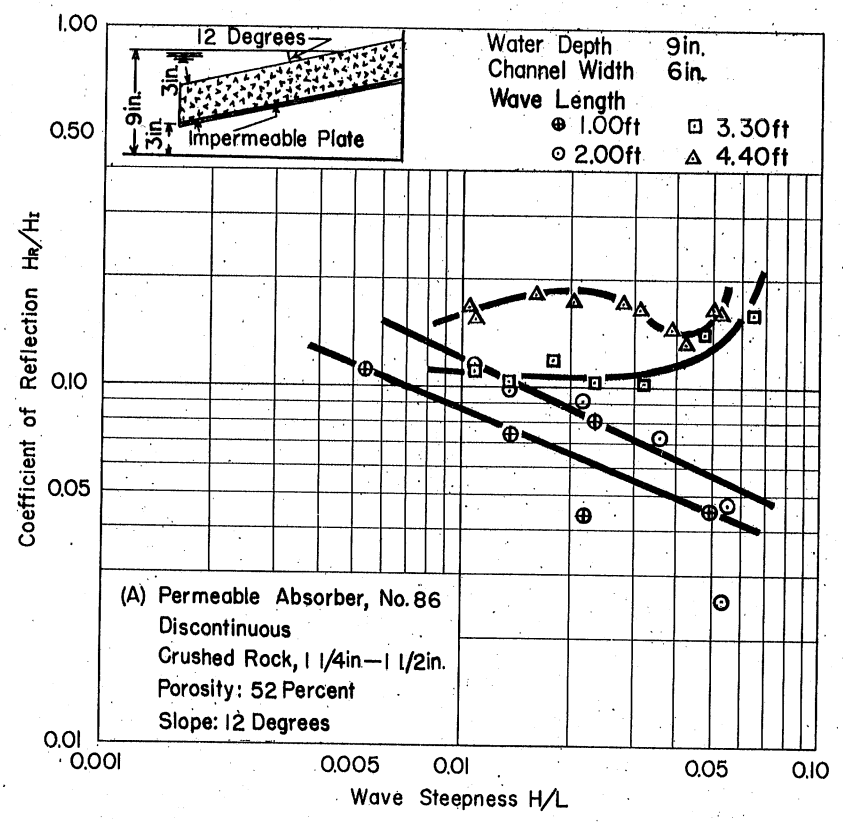

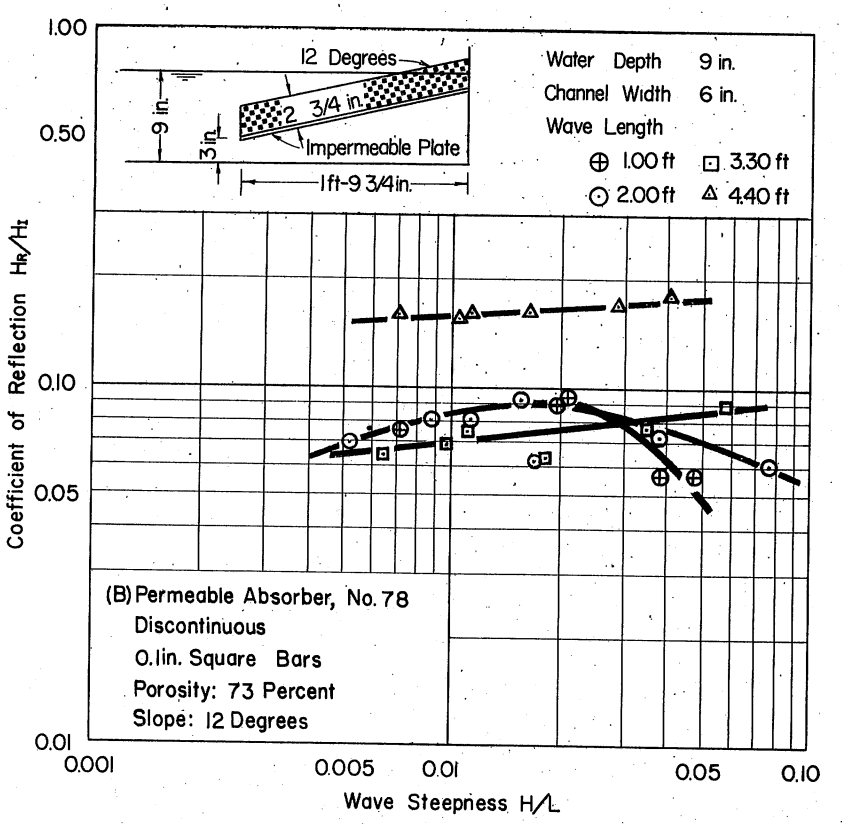

Fig. 42 - Coefficient of Reflection for Crushed-Rock and Square-Bar Absorbers of Discontinuous Type

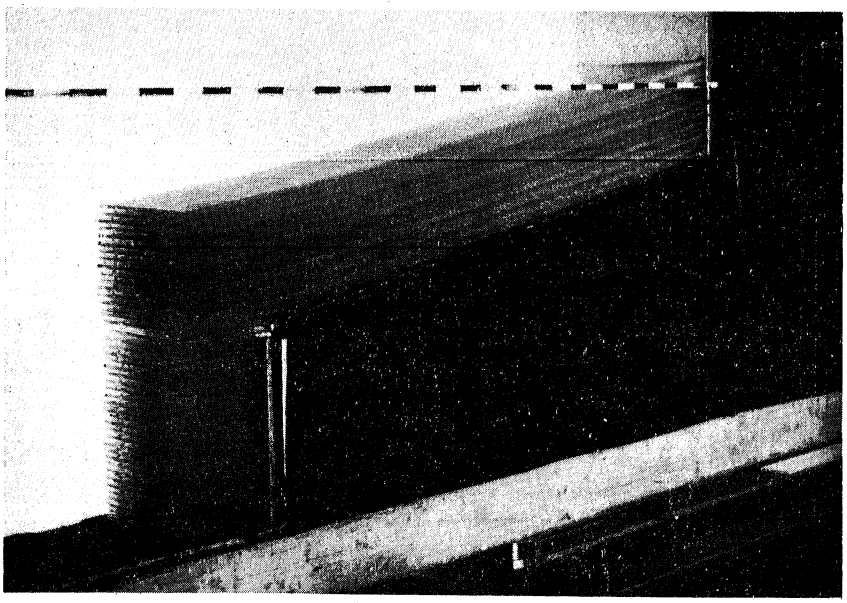

Fig. 43 - A View of a Permeable Absorber Constructed of 0.1-in. Square Bars Spaced 0.09 and 0.08 in. in Horizontal and Vertical Planes, Respectively. (Thickness of permeable layer 3-in., surface slope 12 degrees, porosity 73 per cent.)

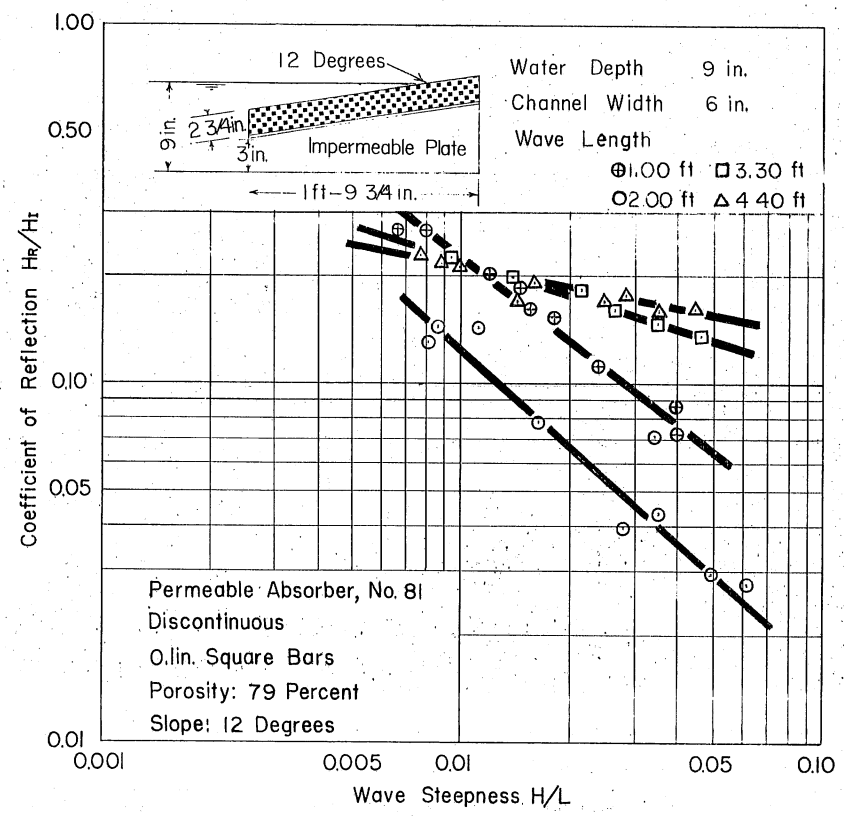

Fig. 44 - Coefficient of Reflection for a Square-Bar Absorber

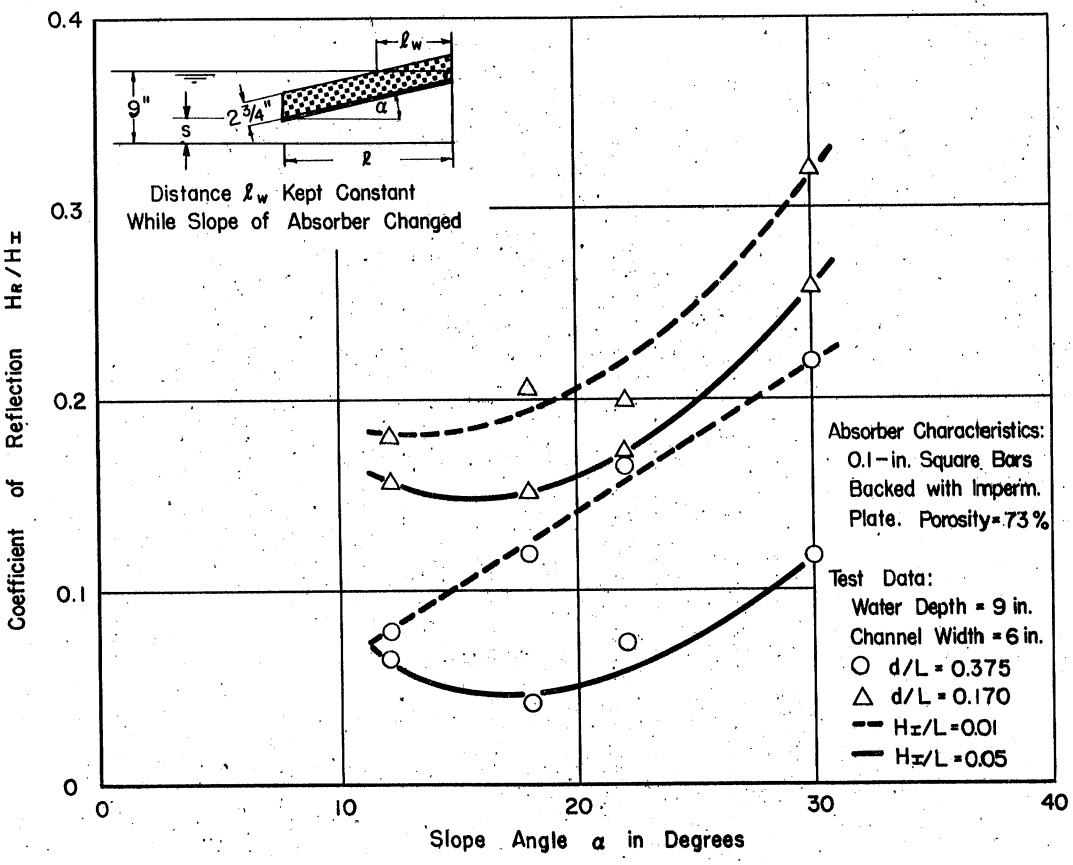

Fig. 45 - Effect of Surface Slope of a Discontinuous Permeable Absorber on Reflection Coefficient

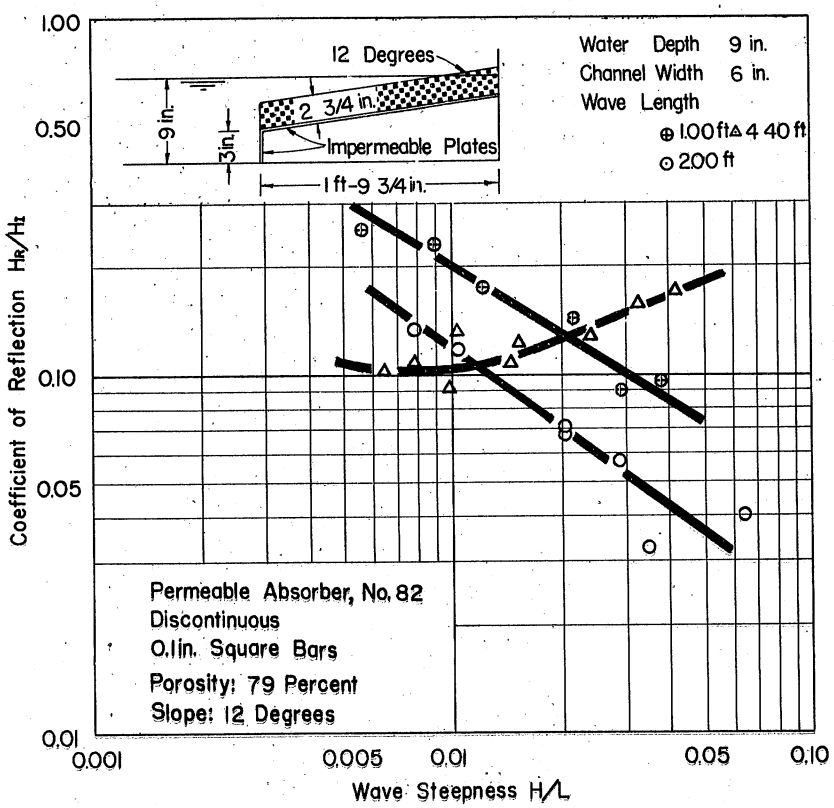

Fig. 46 - Coefficient of Reflection for a Discontinuous Square-Bar Absorber with an Impermeable Plate Placed in Front

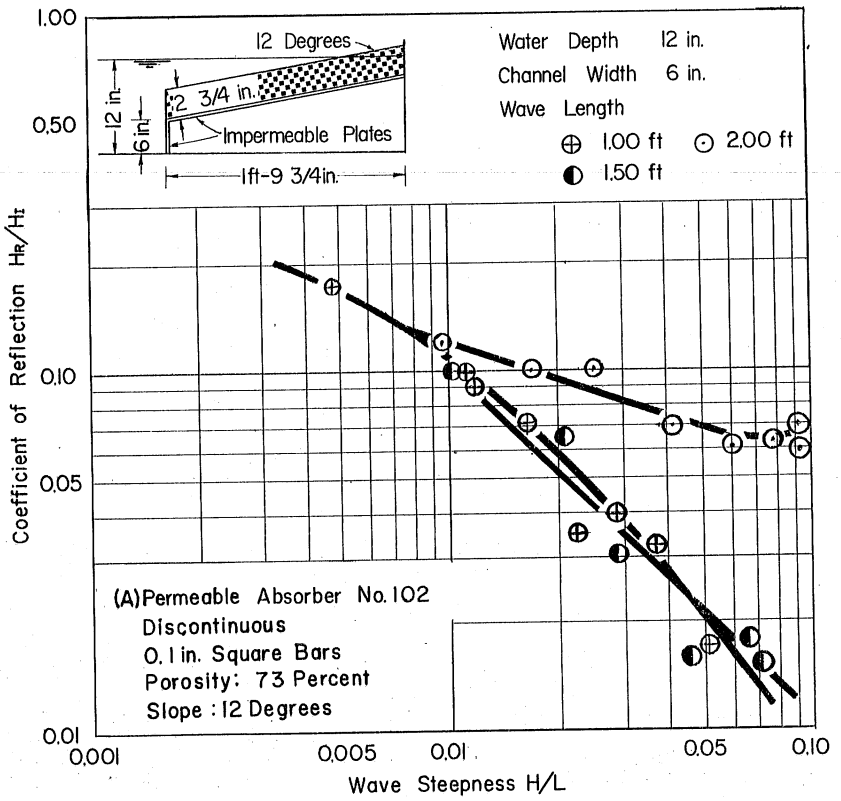

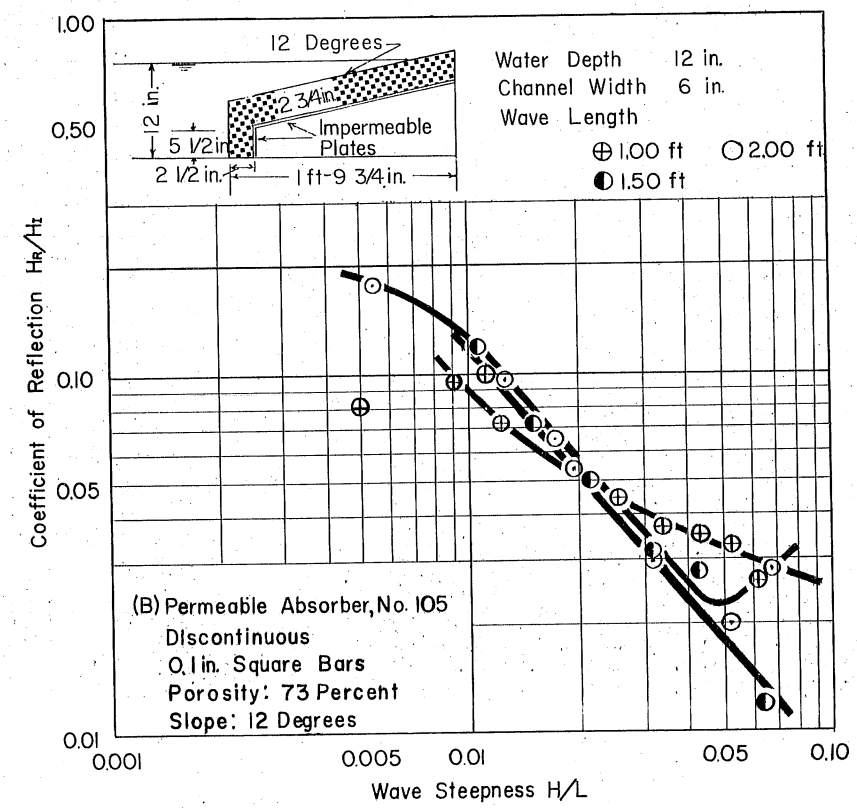

Fig. 47 – Effect of Permeable Material Placed in Front of the Absorber on Coefficient of Reflection

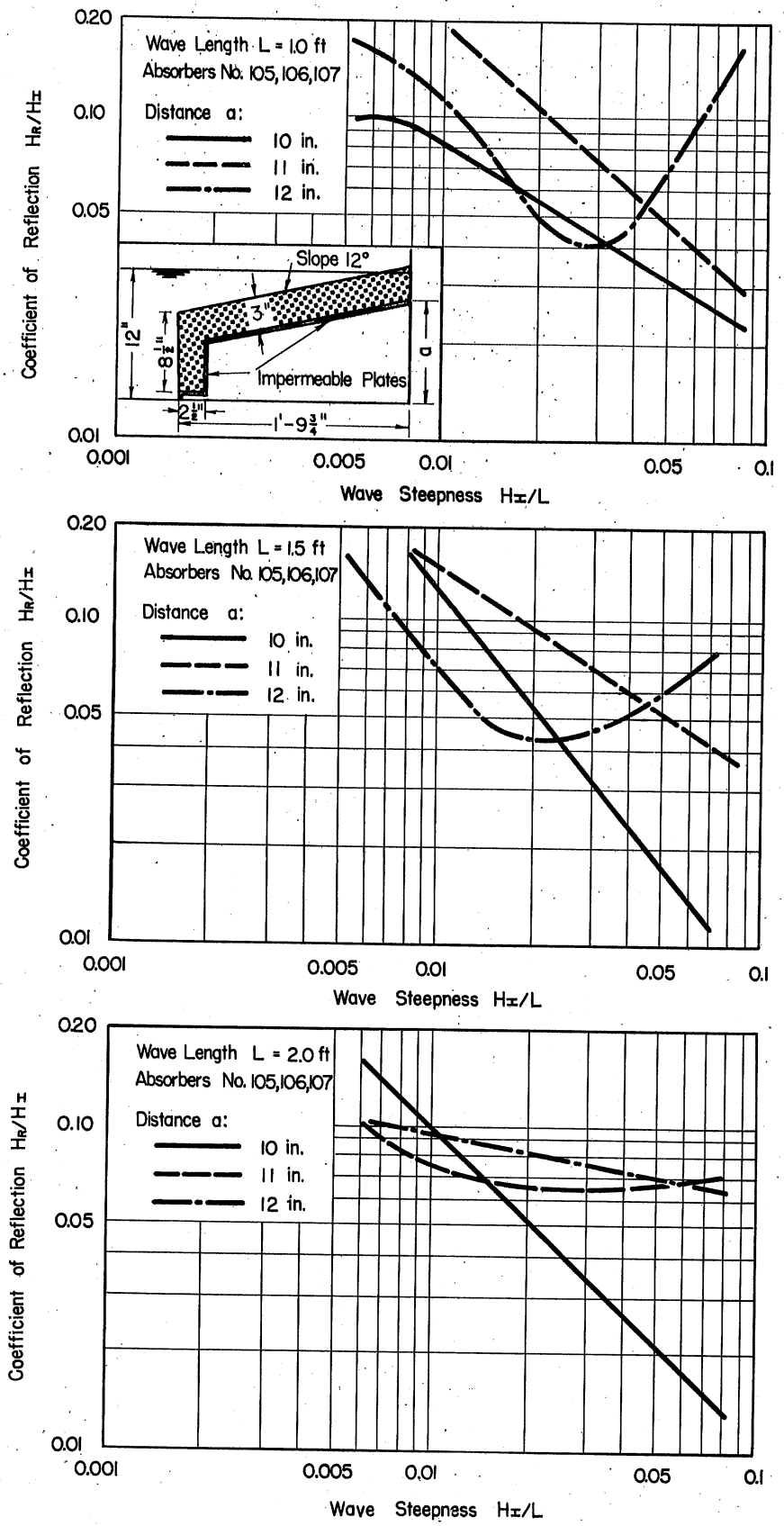

Fig. 48 – Effect of Location of the Impermeable Plate Backing the Permeable Part of the Absorber

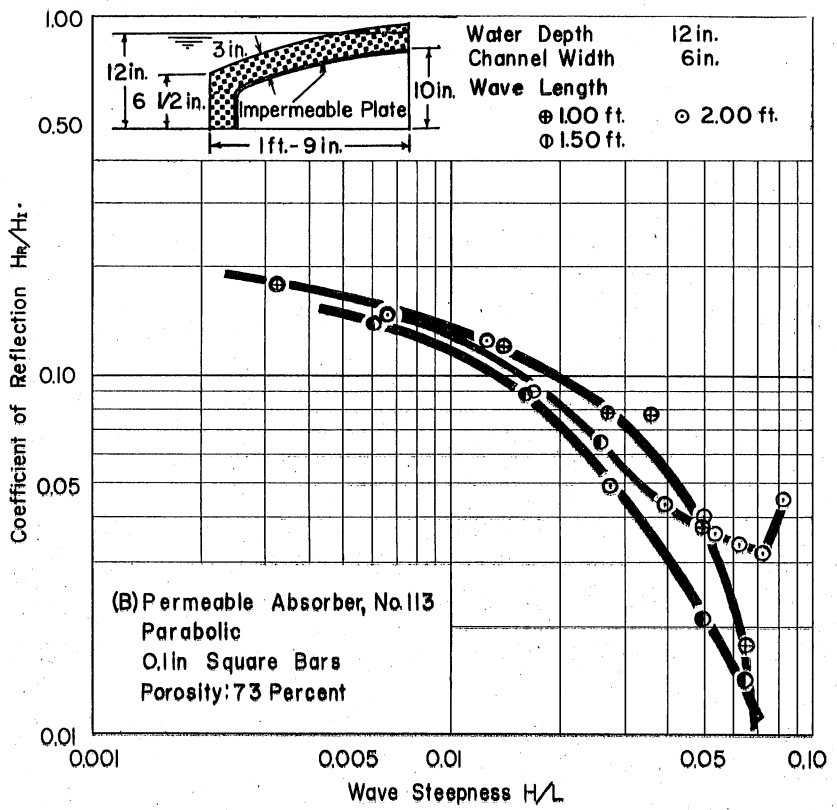

Fig. 49 - Coefficient of Reflection for a Permeable Discontinuous Parabolic Absorber

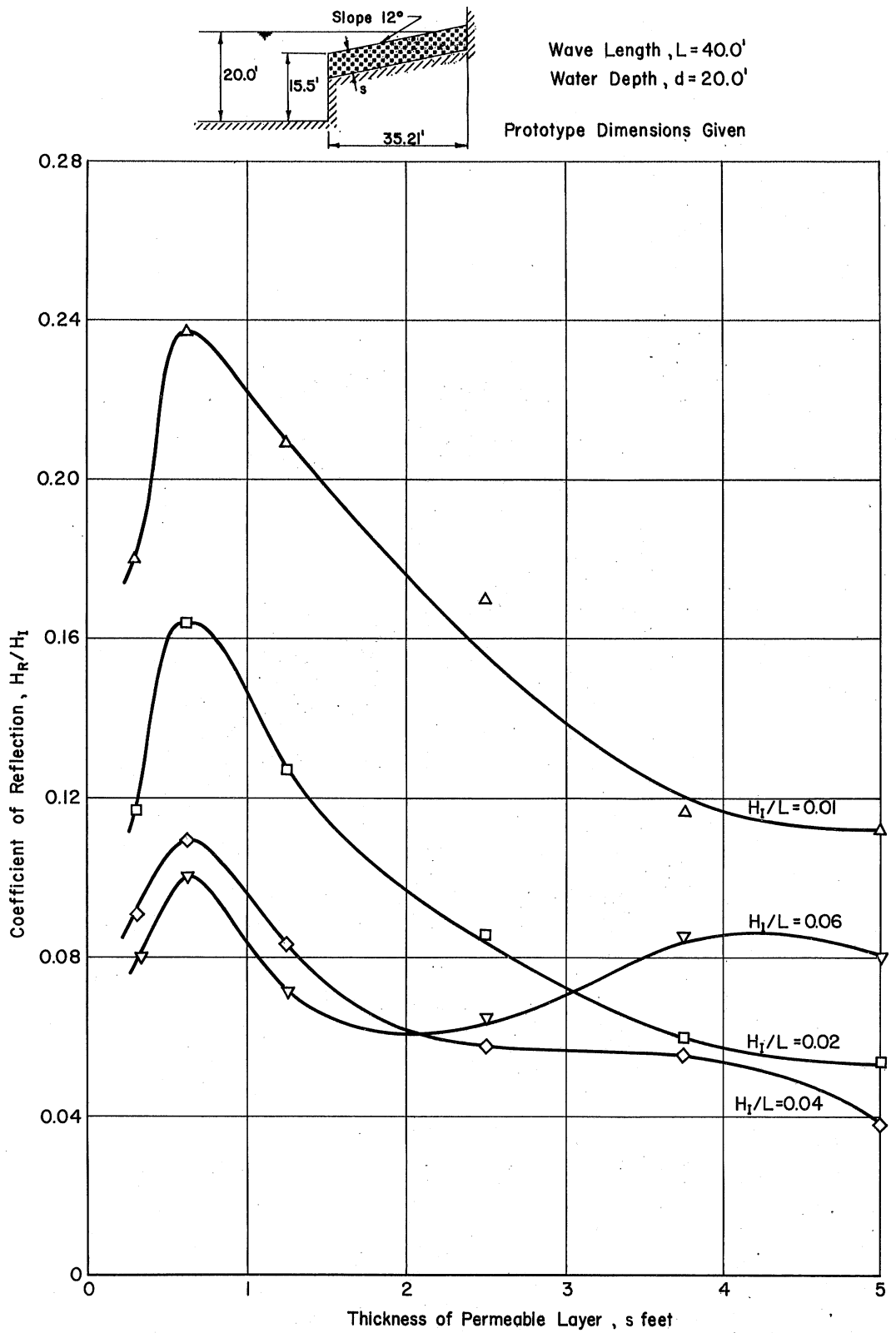

Fig. 50 – Coefficient of Reflection as a Function of Thickness of Permeable Layer. L_p = 40.0 ft

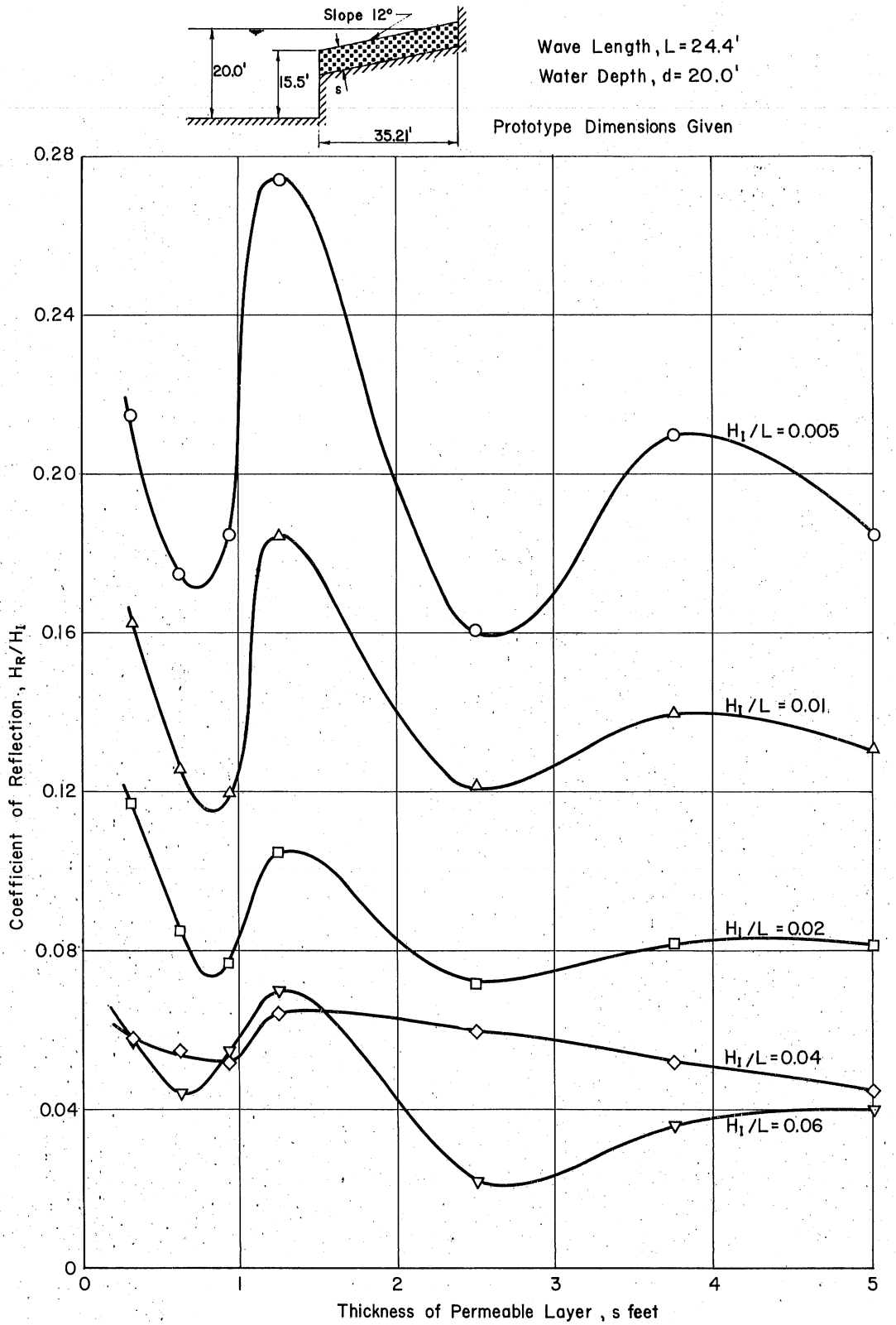

Fig. 51 - Coefficient of Reflection as a Function of Thickness of Permeable Layer. $L_p = 24.4$

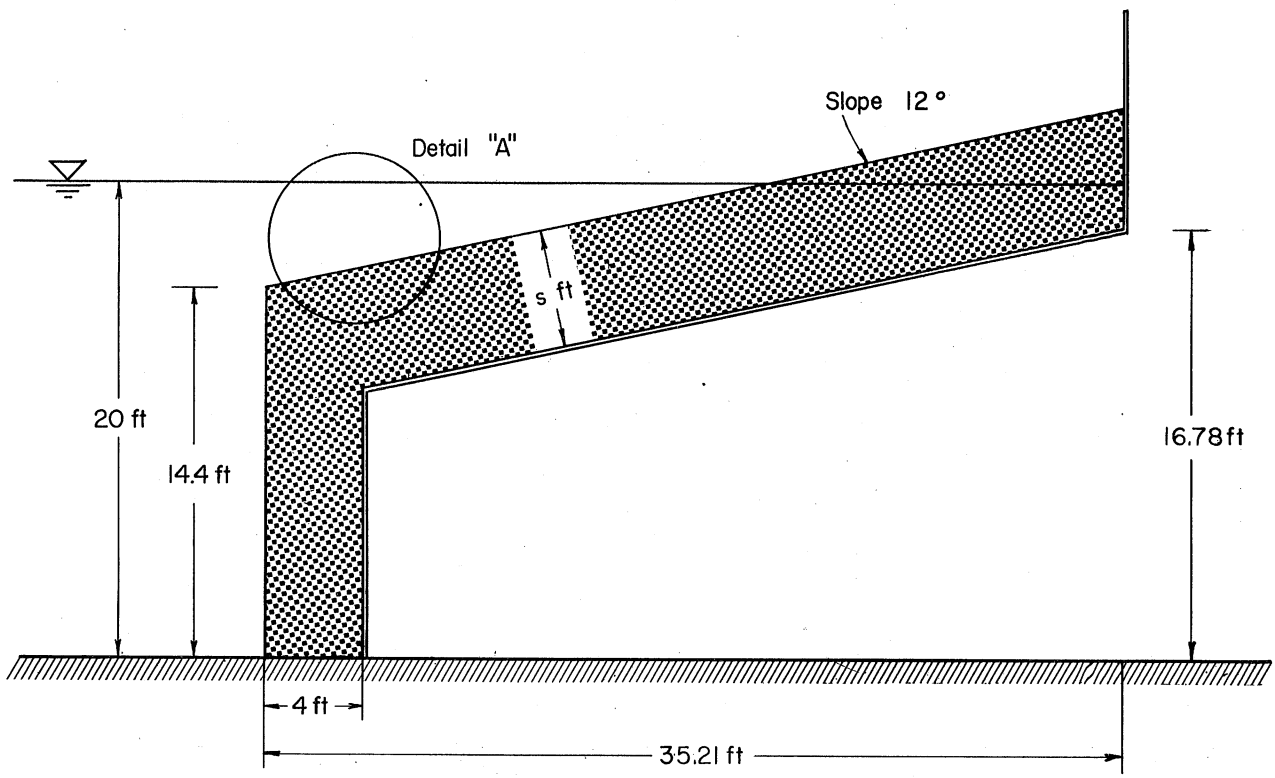

Fig. 52 - Sketch Showing Preliminary Design of Prototype Absorber. (Thickness s and the necessity of permeable material in front of absorber to be determined by large-scale data.)

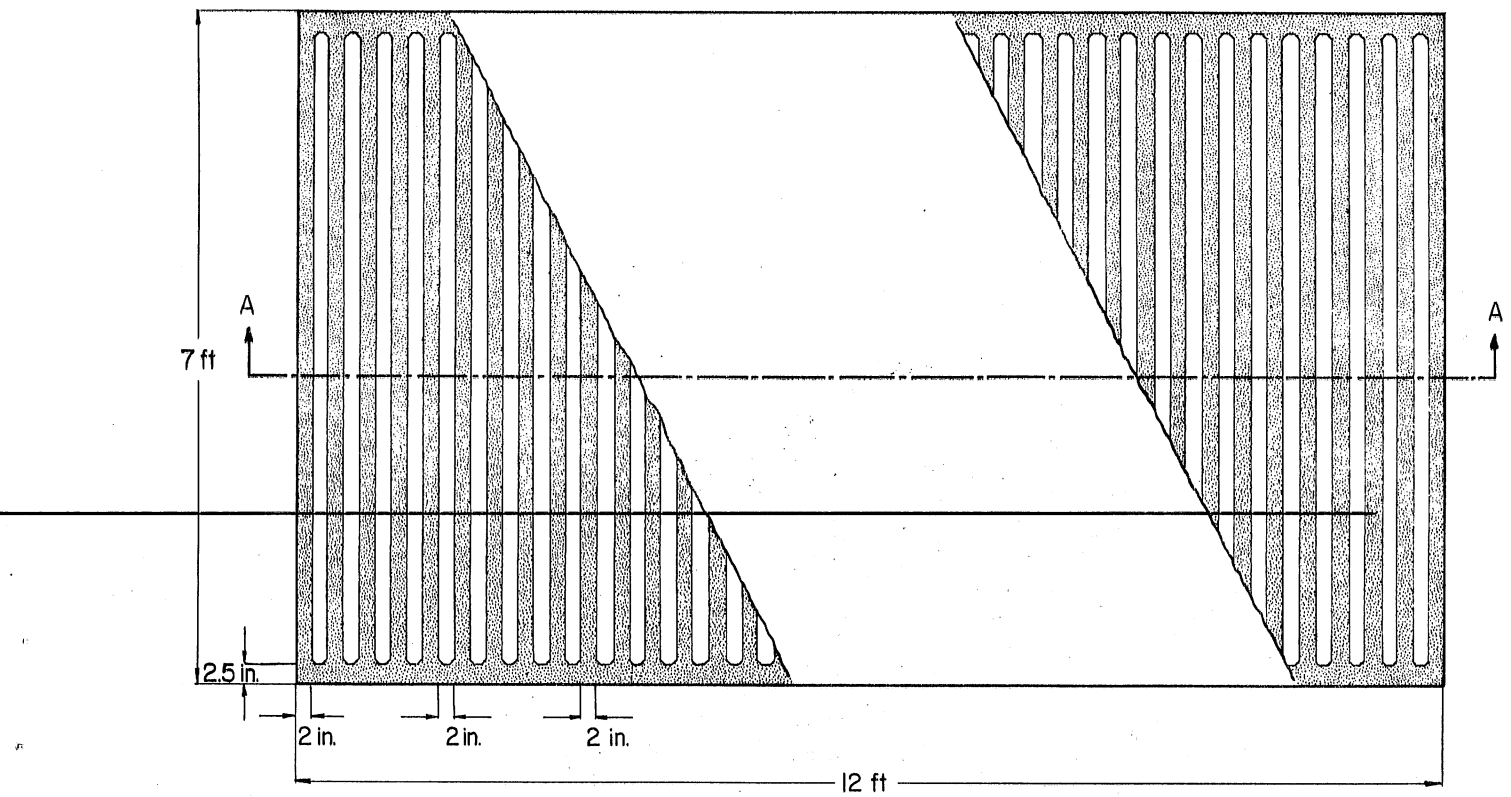

Plan View

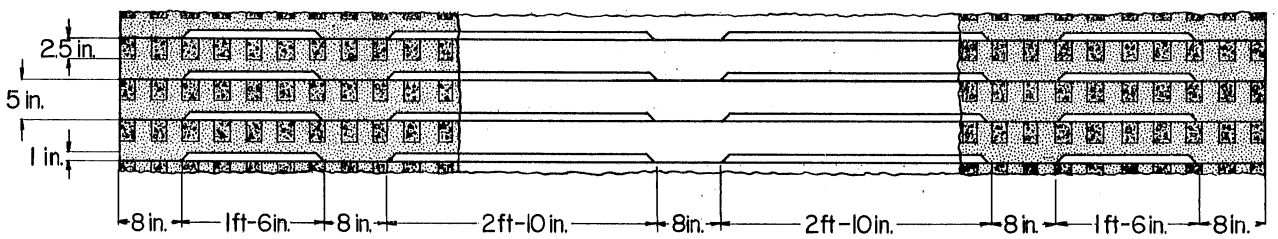

Cross Section A-A

Detail "A"

Fig. 53 - Details of the Precast, Concrete Panels Forming the Permeable Part of the Proposed Absorber

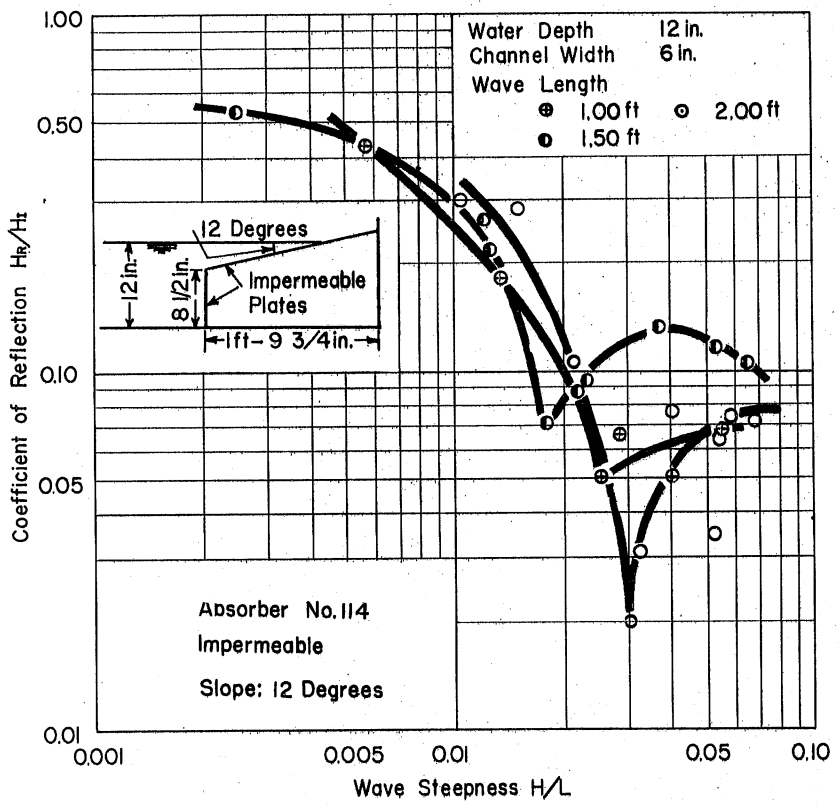

Fig. 54 - Coefficient of Reflection for a Discontinuous Impermeable Absorber

BIBLIOGRAPHY

[1] Beach Erosion Board. Reflection of Solitary Waves. Technical Report No. 11, November 1949. 35 pages.

[2] Biésel, F. "Équations de l'écoulement non lent en milieu perméable." La Houille Blanche, No. 2, pp. 157-160. March-April, 1950.

[3] Biésel, F. and Suquet, F. Laboratory Wave-Generating Apparatus ("Les appareils générateurs de houle en laboratoire.") Translated by M. Pilch. University of Minnesota, St. Anthony Falls Hydraulic Laboratory Project Report No. 39, November 1953.

[4] Costello, R. D. "Damping of Water Waves by Vertical Circular Cylinders." Transactions of the American Geophysical Union, pp. 513-519. Aug. 1952. Vol 33, No. 4.

[5] Healy, J. J. "Wave Damping Effect of Beaches." Proceedings of the Minnesota International Hydraulics Convention, Minneapolis, Minnesota. September 1953. pp. 213-220.

[6] Iribarren, R. and Nogales, C. "The Critical Slope Between Incipient Breaking and Reflecting of Waves." Revista de Obras Publicas, Madrid, February 1950. (Translation No. 50-2 by the Waterways Experiment Station.)

[7] Killen, J. M. A Capacitive Wave Profile Recorder. University of Minnesota, St. Anthony Falls Hydraulic Laboratory Technical Paper No. 11, Series B. October 1952. 16 pages.

[8] Laurent, J. and Devimeux, W. "Étude Expérimental de la Réflexion de la Houle sur des Obstacles accores." Reprint from Revue Générale de L'Hydraulique, No. 65. September-October 1951.

[9] Meyer, H. C., Jr. "Wave Generating Apparatus and Its Model Application." Unpublished M.S. Thesis, Louisiana State University, August 1950.

[10] Miche, M. "Mouvements ondulatoires de la mer en profondeur constante ou décroissante; forme limite de la houle lors de son déferlement. Application aux digues maritimes." Annales des Ponts et Chaussées, pp. 25-78, 131-164, 270-292, and 369-406. 1944.

[11] Miche, M. "Pouvoir réfléchissant des ouvrages maritimes exposés à l'action de la houle." Annales des Ponts et Chaussées, pp. 285-319. May-June 1951.

[12] O'Brien, M. P. and Chaffin, A. D., Jr. "The Effect of Wall-Friction on Gravity Waves." Transactions of the American Geophysical Union, Part I, pp. 84-87. August 1942.

[13] Ross, J. and Bowers, C. E. Laboratory Surface Wave Equipment. University of Minnesota, St. Anthony Falls Hydraulic Laboratory Project Report No. 38, November 1953. 124 pages.

[14] Schoemaker, H. J. and Thijsse, J. Th. "Investigations of Reflections of Waves," Proceedings of the Third Meeting of the International Association for Hydraulic Structures Research, Part I, pp. 2-7, Grenoble. September 1949.

[15] Straub, Lorenz G. and Hudson, Robert Y. Hydraulic Model Tests Establish Optimum Design for Indiana Harbour Development. Paper presented at Regional Technical Meeting, American Iron and Steel Institute, Chicago, October 8, 1953. 30 pages.

APPENDIX A

"ARTIFICIAL VISCOSITY" THEORETICAL DEVELOPMENT FOR WAVE FILTERS

The development describes the wave-damping rate due to a filter having vertical boundaries. The difference in entrant and exit wave-energy rate is equated to the rate of energy dissipation as computed from the dissipation function. The dissipation function is developed from the Navier-Stokes equation for two-dimensional viscous flow. From this the damping rate may be expressed as a function of known wave characteristics and an unknown "artificial viscosity," ν'.

Consider a filter of length Δx in which the wave amplitude is changed by an amount Δa. Invicid fluid is assumed and a shallow-water wave is considered here.

The rate at which energy crosses a vertical plane perpendicular to the direction of the wave is

$$1/2\ g\ \rho_f a^2 C_g$$

where

$$C_g = \frac{C}{2}\left[1 + \frac{2md}{\sinh 2md}\right]$$

Hence, for a unit width

$$\text{Rate of influx of energy} = \frac{1}{4}\ g\ \rho_f a^2 C\left[1 + \frac{2md}{\sinh 2md}\right]$$

$$\text{Rate of efflux of energy} = \frac{1}{4}\ g\ \rho_f (a + \Delta a)^2\ C\left[1 + \frac{2md}{\sinh 2md}\right] \quad (1)$$

$$\text{or, net rate of energy inflow} = -\frac{1}{2}\ g\ \rho_f a \Delta a\ C\left[1 + \frac{2md}{\sinh 2md}\right]$$

The rate of energy dissipation for a filter is

$$w_i = \mu 2\left[\left(\frac{\partial u}{\partial x}\right)^2 + 2\left(\frac{\partial v}{\partial y}\right)^2 + \left(\frac{\partial v}{\partial x} + \frac{\partial u}{\partial y}\right)^2\right]$$

and the complex potential is given by

$$w = aC\left[\cos\,(mx - \sigma t)\,\coth md - i\,\sin\,(mx - \sigma t)\right]$$

or

$$w = aC\Big\{\Big[\,(\cos mx\,\cosh my - i\,\sin mx\,\sinh my)\,\cos\,\sigma t + (\sin mx\,\cosh my + i\,\cos mx\,\sinh my)\,\sin\,\sigma t\,\Big]\,\coth md - i\,\Big[(\sin mx\,\cosh my + i\,\cos mx\,\sinh my)\,\cos\,\sigma t - (\cos mx\,\cosh my - i\,\sin mx\,\sinh my)\,\sin\,\sigma t\Big]\Big\}$$

Therefore, the real part of complex potential

$$\phi = aC\left[\cos mx\,\cosh my\,\coth md\,\cos\,\sigma t + \sin mx\,\cosh my\,\coth md\,\sin\,\sigma t + \cos mx\,\sinh my\,\cos\,\sigma t + \cos mx\,\cosh my\,\sin\,\sigma t\right]$$

Now

$$u = -\frac{\partial\phi}{\partial x} \text{ and } v = -\frac{\partial\phi}{\partial y}$$

and it follows that

$$\frac{\partial u}{\partial x} = aCm^2\left[\cosh my\,\coth md + \sinh my\right]\cos\,(mx - \sigma t)$$

and

$$\frac{\partial v}{\partial y} = -\,aCm^2\left[\cosh my\,\coth md + \sinh my\right]\cos\,(mx - \sigma t)$$

Therefore, by squaring and adding, the rate of energy dissipation is obtained

$$w_i = 4a^2C^2m^4\mu\Big\{\Big[\cosh my\,\coth md + \sinh my\Big]^2\cos^2\,(mx - \sigma t) + \Big[\sinh my\,\coth md + \cosh my\Big]^2\sin^2\,(mx - \sigma t)\Big\}$$

and the total rate of energy dissipation

$$W_i = \iint w_i \, da = \int_0^{\Delta x} \int_{-d}^{0} w_i \, dy \, dx$$

$$W_i = 4a^2C^2m^4\mu \left\{ \left[\frac{\sinh 2md}{4m} (\coth^2 md + 1) + \frac{2 \coth md}{4m} (1 - \cosh 2md) \right] + \frac{d}{4m} \left[(\sin (2m\Delta x - 2\sigma t) + \sin 2\sigma t) \operatorname{csch}^2 md \right] \right\} \Delta x$$

And the average value of dissipation is equal to

$$W_{iA} = a^2C^2m^3\mu \left[\sinh 2md (\coth^2 md + 1) - 4 \coth md \sinh^2 md \right] \Delta x$$

or

$$W_{iA} = 2a^2C^2m^3\mu (\coth md) \, \Delta x \qquad (2)$$

Equating (1) and (2) gives

$$-g\rho \, da \left[1 + \frac{2md}{\sinh 2md} \right] = 4\mu \, m^3 Ca \coth md \, dx$$

or

$$-\frac{da}{a} = \frac{4 \nu' \, m^3 C}{g} \frac{\coth md}{\left[1 + \frac{2md}{\sinh 2md} \right]} dx$$

Integrating gives

$$\log_e a = -\frac{4 \nu' \, m^3 C \coth md}{g \left[1 + \frac{2md}{\sinh 2md} \right]} x + \text{constant}$$

Letting $a = a_o$ when $x = 0$, and substituting $C = \sqrt{\frac{g}{m} \tanh md}$ for celerity we have

$$\log_e a = -\frac{4 \nu' \, m^2}{C \left[1 + \frac{2md}{\sinh 2md} \right]} x + \log_e A_o$$

or

$$\log_e \frac{a_o}{a} = \frac{4 \nu' \, m^2 x}{C \left[1 + \frac{2md}{\sinh 2md} \right]}$$

or

$$\frac{a}{a_o} = \text{exponential}\left\{ - \frac{4\,\nu'\,m^2\,x}{C\left[1 + \frac{2md}{\sinh 2md}\right]} \right\} \qquad (3)$$

and the ν' the artificial viscosity

$$\nu' = \log_e \frac{a_o}{a}\ \frac{1}{2K}\ \frac{L}{\ell} \qquad (4)$$

where

$$K = \frac{8\,\pi^2}{C\,L\left[1 + \frac{2md}{\sinh 2md}\right]}$$

Hence, value of ν' can be determined for a given wave filter from Eq. (4). Therefore, upon once determining a value of ν' for the filter, use of any particular wave characteristic will yield the corresponding amplitude change for that filter and that wave (Eq. 3).

APPENDIX B

EXPERIMENTAL APPARATUS

All the tests described in this report were carried out in a glass wall channel 6 in. wide, 16 in. deep, and 40 ft long. Figure B-1 shows the experimental channel with wave generator at the left, two measuring probes in the center, and wave-profile recorder in the background.

The wave generator was of the pendulum type. The bottom section was oscillated horizontally by a connecting rod attached to the drive wheel. Two vertical arms supported the lower unit. By shifting the upper pivot points of the arms, the lower unit was tilted back and forth during each stroke resulting in motion similar to the orbital motion of the water. The stroke could be varied readily. The generator was powered by a 1/2 hp, 1724 rpm a-c electric motor and was capable of producing waves up to 10 ft long and with a maximum height of 4 inches. Generator speed or wave period was readily adjustable through a hydraulic transmission between the motor and the wave generator.

A capacitive-type wave profile recorder was used for measurement of wave characteristics [7]. Wave heights were measured electrically with a recording oscillograph; the deflections corresponded to the depths of submergence of an insulated wire in the water. The wire acted as a small capacitor whose capacity varied directly with the wetted area of the wire. Permanent records were obtained with an ink-writing oscillograph on millimeter paper.

The majority of the tests were conducted at a water depth of 9 in., although some tests were run at a depth of 12 in. in order to determine the effect of d/L ratio and scale ratio on the coefficient of reflection.

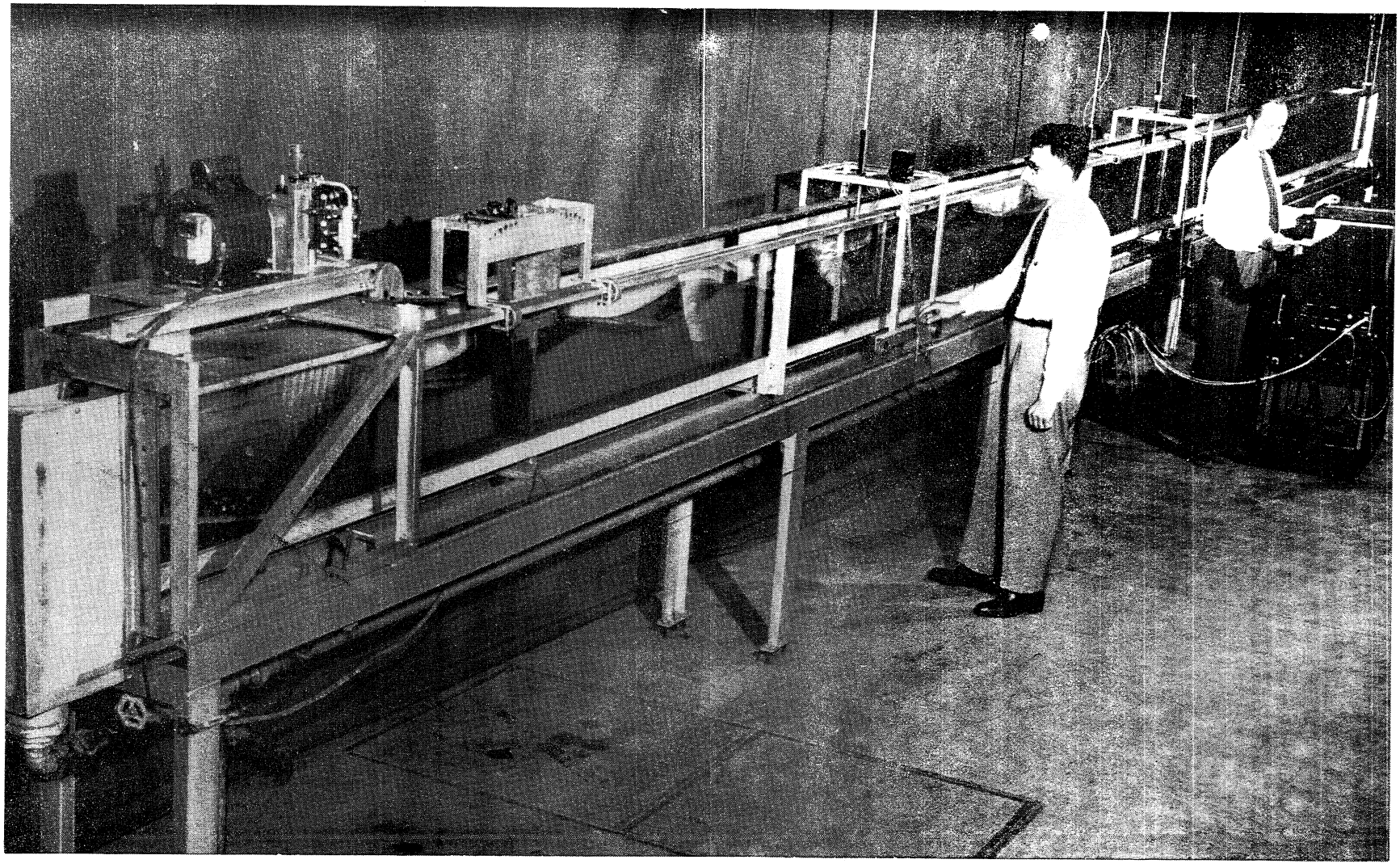

Fig. B-1 - View of 6-in. Wide, 16-in. Deep, and 40-ft Long Wave Channel and Equipment Used in Generation and Measurement of Waves

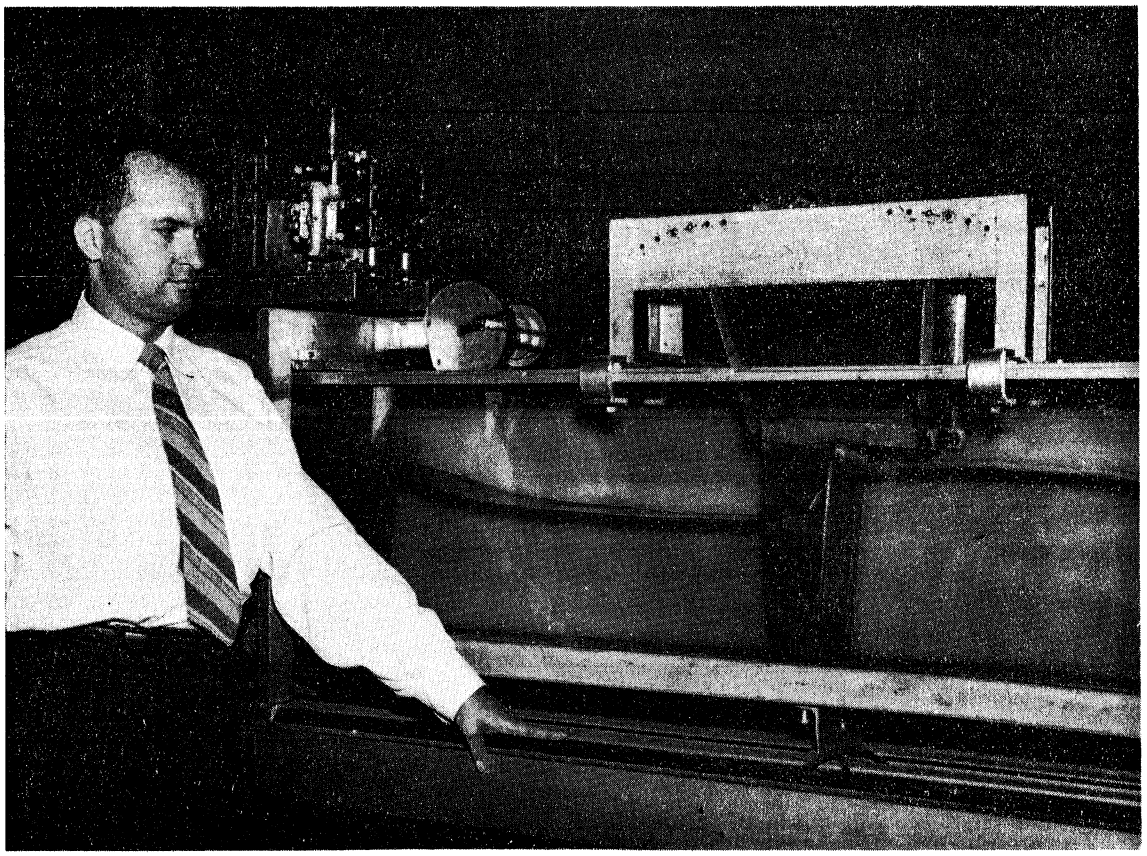

Fig. B-2 - View of the Pendulum-Type Wave Generator Installed in 6-in. Channel

APPENDIX C

TESTING TECHNIQUE

A. Wave Filters

The test procedure consisted essentially of taking measurements of wave height at various points upstream and downstream of the filter. The filters were installed 8 ft 6 in. from the wave generator. Two probes were employed in determining the wave height at 1-ft intervals upstream and downstream. Figure C-1 presents a typical example of experimental data showing the wave attenuation caused by a plate filter.

B. Wave Absorbers

Measurements of wave reflection were made with a continuous train of incident waves as opposed to the method involving intermittent generation of incident waves. The actual procedure consisted of measuring the envelope of the standing wave by moving the recording probe at uniform speed along the channel over a distance equal to at least one-half the wave length. The values of wave heights at the loop (maximum) and at the node (minimum) are then used to determine the coefficient of reflection by means of the following formula:

$$R = \frac{H_\ell - H_n}{H_\ell + H_n}$$

where H_ℓ is the wave height at the loop and H_n is the wave height at the node. The above formula was developed for sinusoidal waves and it is realized that for longer shallow-water waves, where the shape of the wave differs materially from a sine wave, the formula provides only an approximate value of reflection coefficient. However, as this method provides a rapid means of determining the magnitude of wave reflection, it was used throughout the study. The development of the formula for sinusoidal waves is given in Appendix D.

The measurements of reflection were generally made 2 ft from the toe of the absorber. This location was selected following a brief survey to determine the most suitable location. Continuous records were obtained on a paper tape recorder.

All the studies described herein have been conducted in a channel 6 in. wide, 16 in. deep, and 40 ft long.

The testing technique was critically examined early in the experimental study, as it was thought that the following factors could affect the measurement of the reflection coefficient:

(a) water temperature

(b) relative position of absorber with respect to generator

(c) location of wave filters with respect to the generator

(d) location of the point where reflections are measured

(e) ratio of length of the channel behind the wave generator to the length between absorber and generator

(f) method of varying incident wave height, i.e., by varying generator stroke or by inserting filters.

Of major interest was the possible influence of reflected waves on the incident wave. For example, the portion of the wave reflected by the absorber might in turn be reflected by the wave generator, becoming superimposed on the generated or incident wave. If the reflected wave were of sufficient height, serious distortion of the incident wave would result. When conditions of this type exist, standing waves or clapotis develop; and if the filters are not being used, the height of the clapotis is usually a maximum if the space between generator and absorber is an integral number of half-wave lengths. The magnitude of this effect can be determined by varying the distance between generator and absorber or by conducting tests in which a filter is employed to absorb the reflected wave and comparing it with a case when a filter is not used.

To study the effect of water temperature and viscosity, two tests were carried out, one with water at 3.5 degrees C and another with water at 20.5 degrees C. The experimental data are plotted in Fig. C-3. The results obtained indicate that temperature has little or no effect on the coefficient of reflection within the range of variables covered by the model studies.

To study the effect of location of the absorber in the channel, measurements of reflections were taken with the absorber at 5 ft and 4 ft 6 in. from the end of the channel. The results which are shown in Fig. C-4 indicate that the location of the absorber in the 6-in. channel has little or no effect on the coefficient of reflection.

Two tests were carried out to determine the effect of location of filters on the coefficient of reflection, one with a filter 18 ft from the

generator and another with a filter 4 ft from the generator. The experimental data which are plotted in Fig. C-5 indicate that the location of a filter has little or no influence on the coefficient of reflection.

In order to locate the point where reflections from an absorber should be measured, tests were made in which the reflection coefficient was measured at 1-ft intervals along the channel. The results which are plotted in Fig. C-6 indicate that the coefficient of reflection decreases slightly as the distance from the absorber increases.

Other tests were made to determine the effect of the ratio of length of channel behind the generator to the length between the absorber and the generator on the reflection coefficient. The results which are plotted in Fig. C-7 show that the reflection coefficient is not affected by this ratio.

Figure C-8 illustrates that it is unimportant whether the wave height is adjusted by varying the generator stroke or by inserting filters for the rather low reflections encountered in this study.

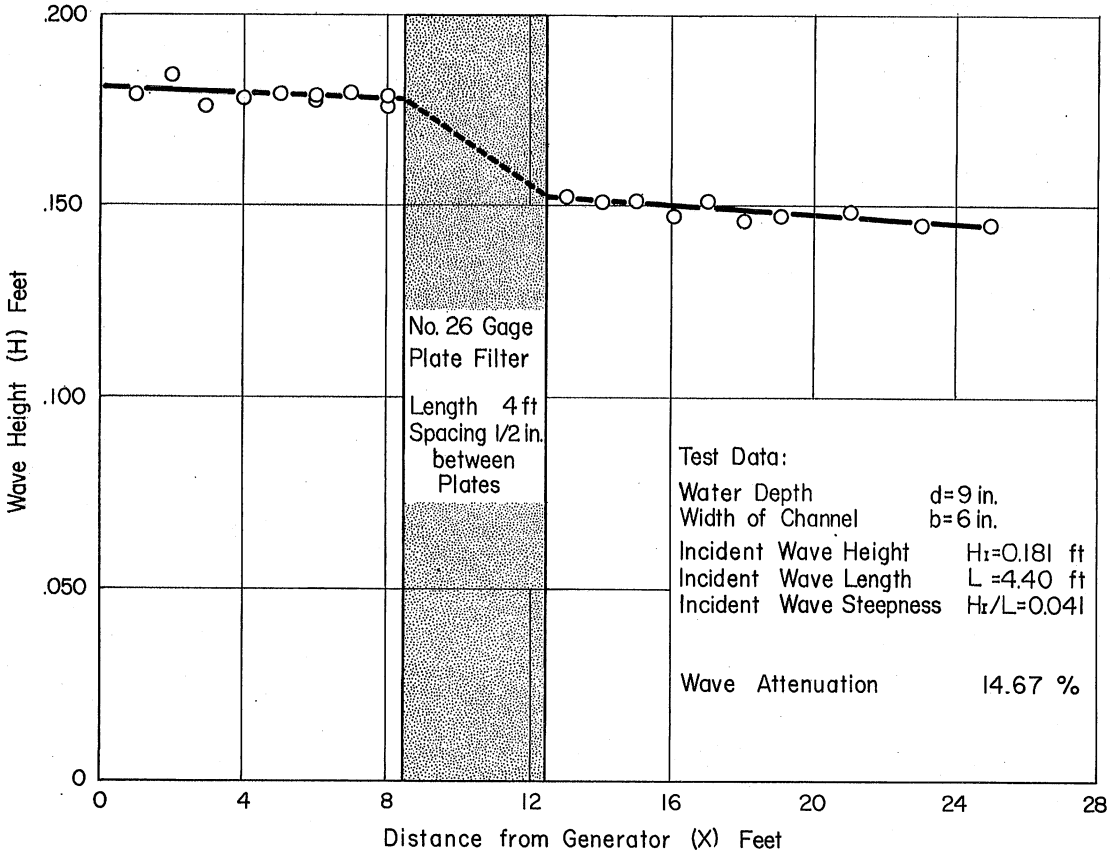

Fig. C-1 – Typical Example of Wave Attenuation Caused by a Plate Filter

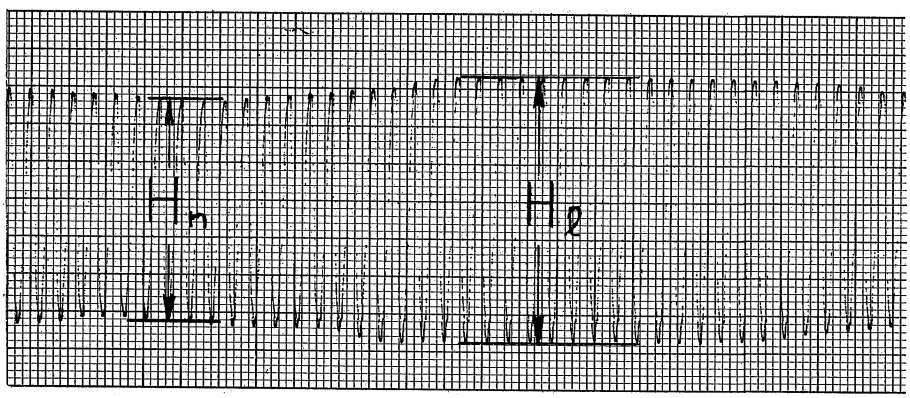

Fig. C-2 – Sample Record Showing Method of Measuring the Envelope of Wave. (Wave heights at the loop and at the node are indicated.)

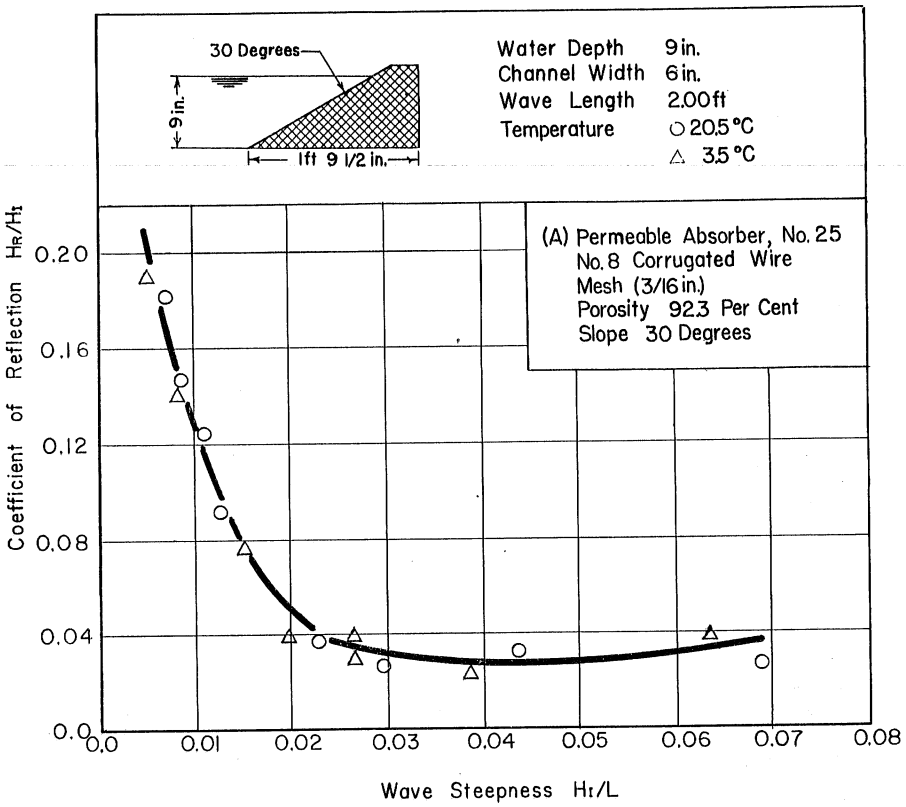

Fig. C-3 - Effect of Water Temperature on Coefficient of Reflection

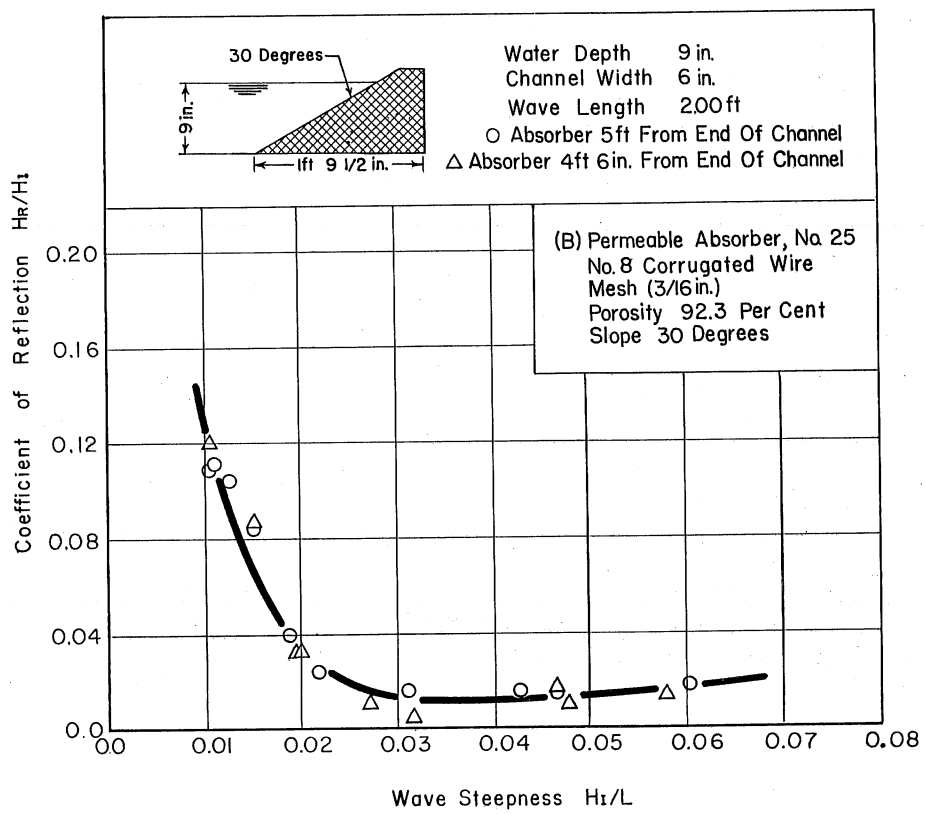

Fig. C-4 - Effect of Location of Absorber in the Channel

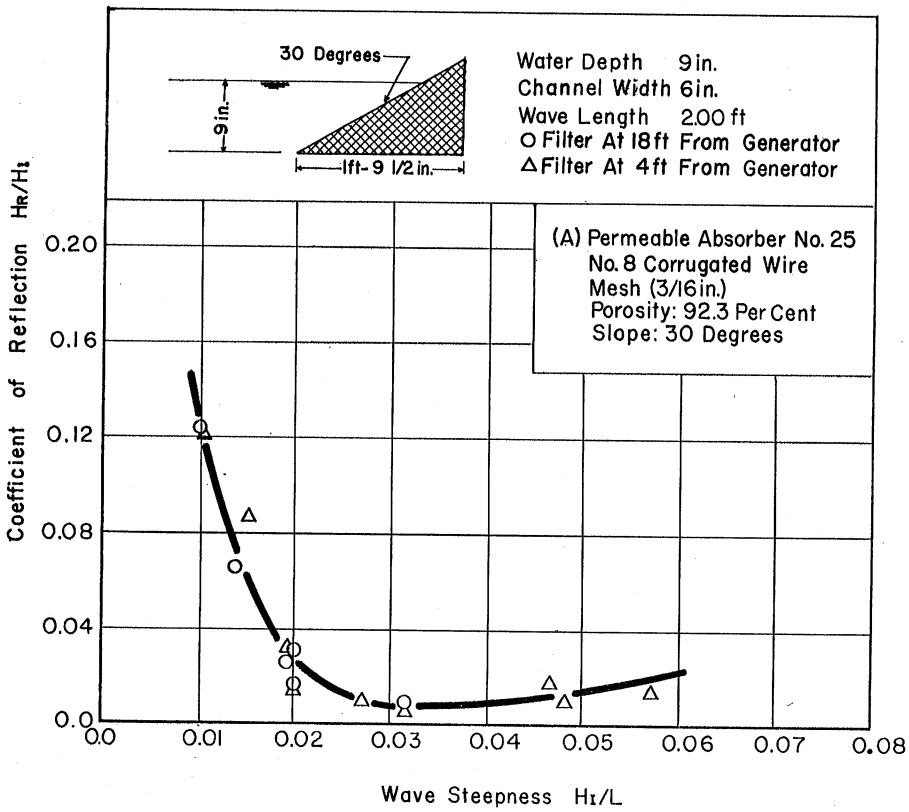

Fig. C-5 – Effect of Location of Filters in the Channel

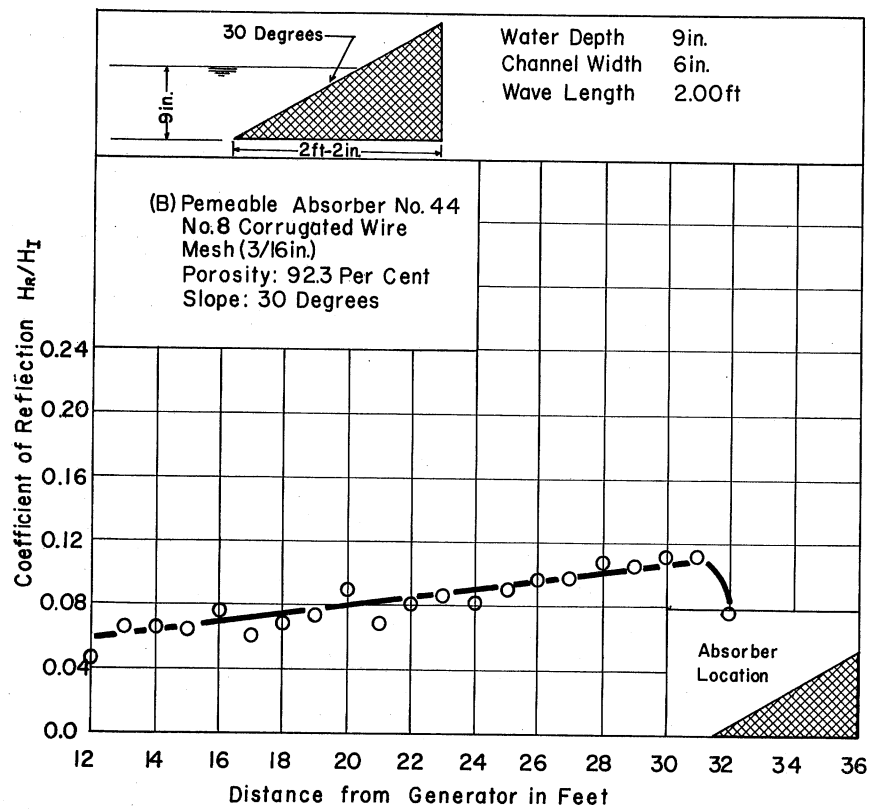

Fig. C-6 – Variation of Coefficient of Reflection Along the Channel

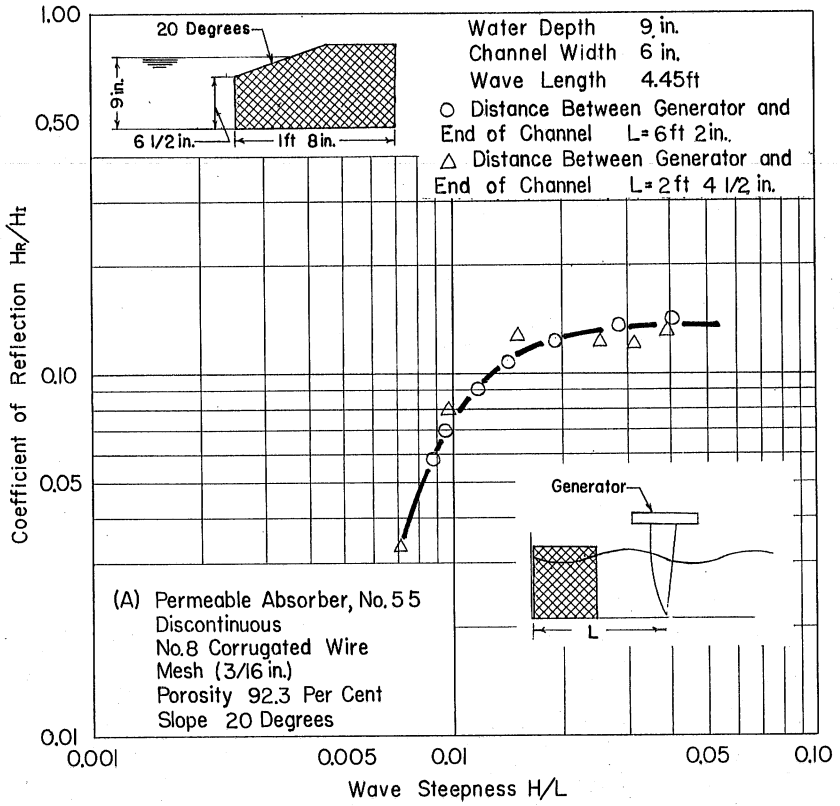

Fig. C-7 - Effect of Location of Generator in the Channel

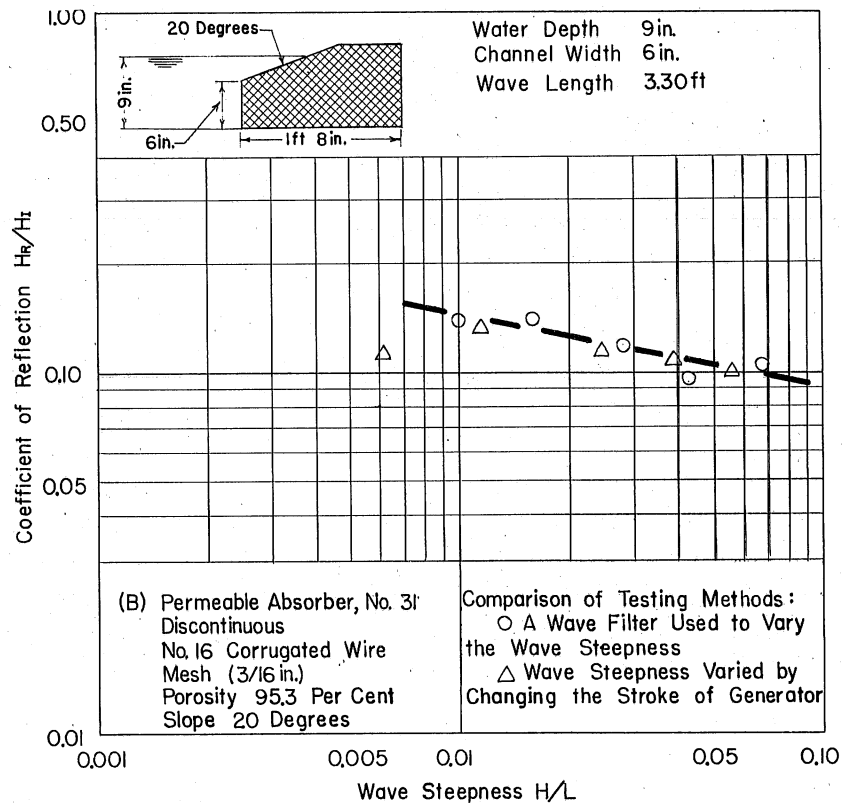

Fig. C-8 - Comparison of Two Methods of Varying Incident Wave Height

APPENDIX D

MEASUREMENT OF WAVE REFLECTION

The following development is for a sinusoidal wave.

Let the incident wave be

$$\eta_I = a \sin (mx - \sigma t)$$

and the reflected wave

$$\eta_R = b \sin (mx + \sigma t)$$

where η is the surface elevation, a and b the wave amplitudes, $m = 2\pi/L$, x is the distance along a horizontal axis, $\sigma = 2\pi/T$, and t is time.

For the clapotis we have

$$\eta = \eta_I + \eta_R$$

thus $\eta = (a + b) \sin mx \cos \sigma t - (a - b) \cos mx \sin \sigma t$ and we have a value at the nodes $x = 0, L/2, L$, etc.

$$\eta = (a - b) \sin \sigma t$$

and at the loops $x = L/4, 3L/4$, etc.

$$\eta = (a + b) \cos \sigma t$$

The envelope of the standing wave is developed as follows:

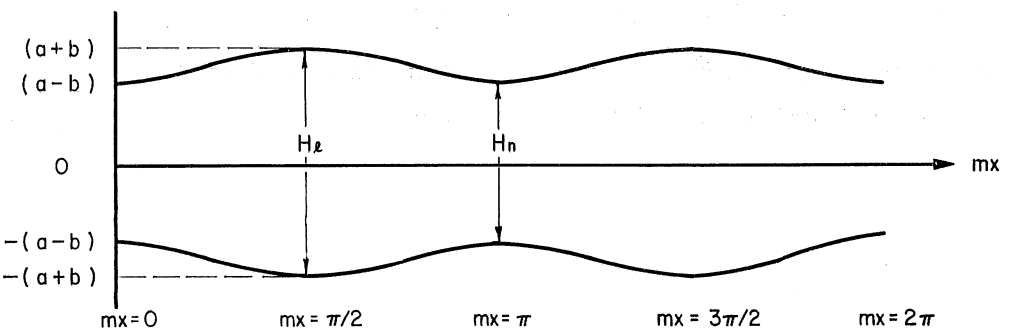

where H_ℓ is the envelope height at the loop and H_n is the envelope height at the node.

It follows from the diagram that

$$\left(H_\ell\right) = 2\ (a + b) \quad \text{and} \quad \left(H_n\right) = 2\ (a - b)$$

and

$$H_\ell - H_n = 4b$$

$$H_\ell + H_n = 4a$$

The coefficient of reflection is

$$\frac{b}{a} = \frac{H_\ell - H_n}{H_\ell + H_n} = \frac{H_r}{H_I} = R$$

where H_R is the height of the reflected wave and H_I is the height of the incident wave.

Also the incident wave height, or height of the wave as it enters the absorber, is

$$H_I = \frac{H_\ell + H_n}{2}$$

As indicated earlier this method of measuring the coefficient of reflection is true for a sinusoidal wave. Deep-water waves ($d/L > 0.5$) approximate the sinusoidal wave in shape while the shallow-water waves ($d/L < 0.5$) approach the trochoidal shape; thus this method would not be entirely correct in evaluating the coefficient of reflection for shallow-water waves. However, for the purpose of expedience in evaluating a large number of tests and the fact that the wave characteristics of most interest were deep-water waves, this method was used throughout the study.

APPENDIX E

A COMPARISON OF WAVE ENERGY DISSIPATION BY IMPERMEABLE AND PERMEABLE ABSORBERS

A photographic record of wave-breaking on various types of absorbers is given in Figs. E-1 and E-4. The time interval between each picture is 1/16 sec except for the perforated-plate absorber for which the time interval is 1/10 sec. It can be seen that a 2.0-ft long wave is breaking on an impermeable beach-type absorber (Fig. E-1), while there is no evidence of wave breaking on a wire-mesh absorber of 95.3 per cent porosity (Fig. E-2). There is a partial breaking of wave on a crushed-rock absorber of 46 per cent porosity (Fig. E-3) and on a perforated-plate-type absorber of 95.5 per cent porosity (Fig. E-4).

It appears that for impermeable absorbers the wave energy is dissipated by breaking and friction, or both. The proportion of energy dissipated by each action would depend on wave steepness and beach slope. For permeable absorbers wave energy is dissipated by breaking, friction, and form drag. The proportion of energy dissipated by each action would depend on wave steepness, beach slope, nature of permeable medium and its porosity. In the case of wire mesh, perforated plates, crushed rock and bars, it is expected that form-drag loss will be predominant by far for low steepness waves and that both breaking action and form-drag losses will be responsible for high steepness waves, possibly with the exception of wire-mesh absorber of high porosity.

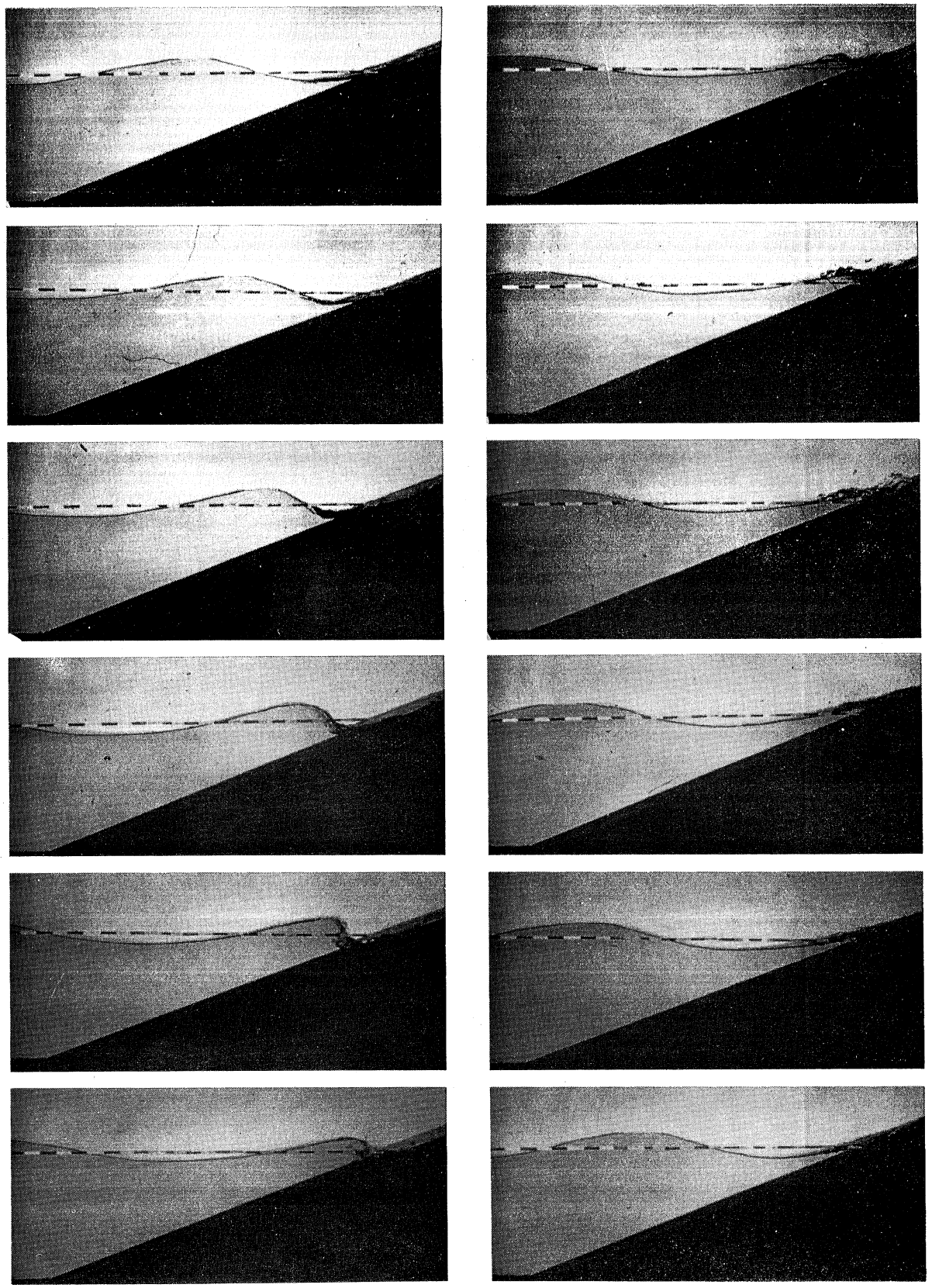

Fig. E-1 - A Sequence of Pictures Showing Wave Breaking on an Impermeable Beach-Type Absorber

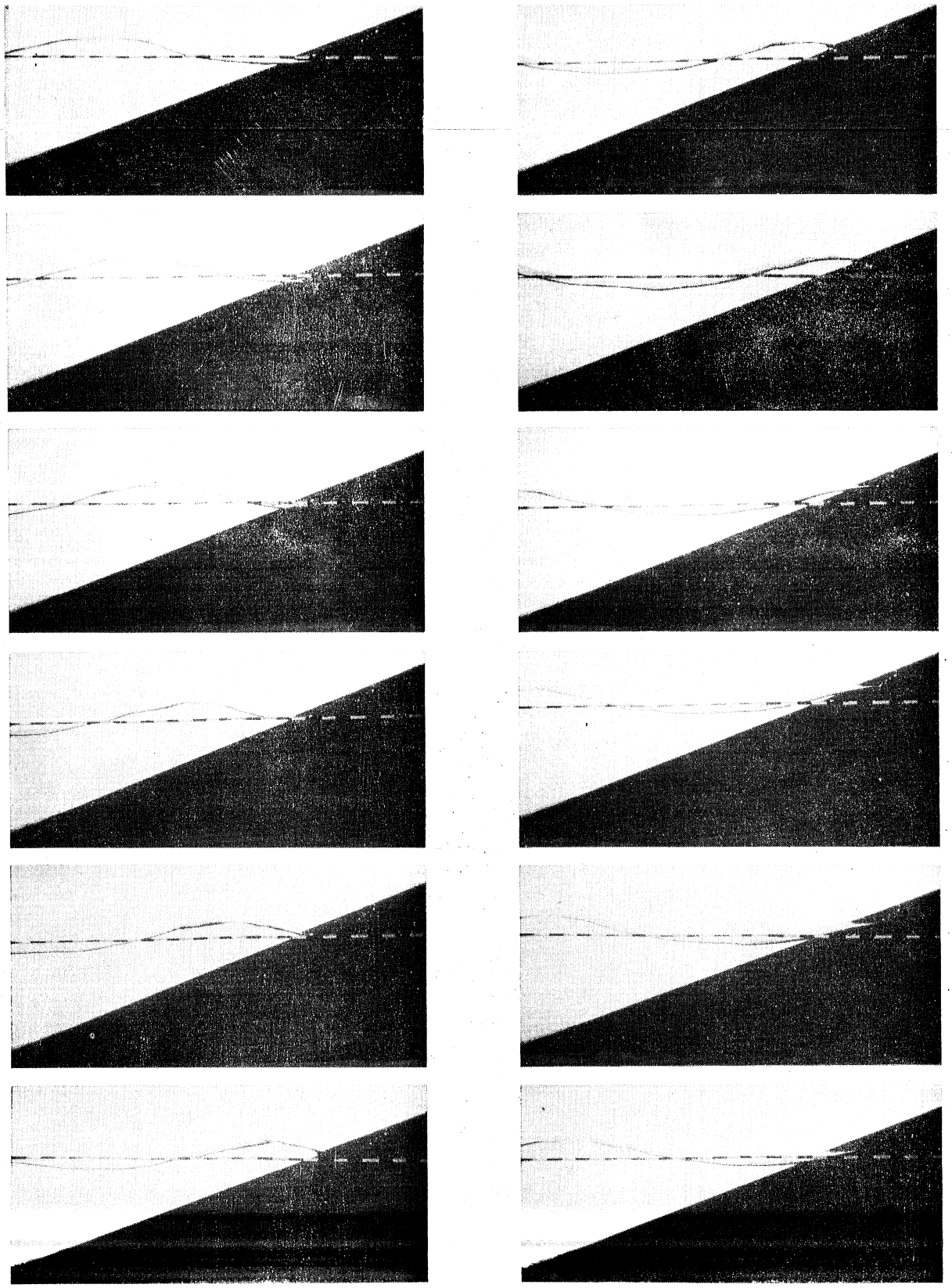

Fig. E-2 – A Sequence of Pictures Showing Wave Breaking on a Wire-Mesh-Type Absorber

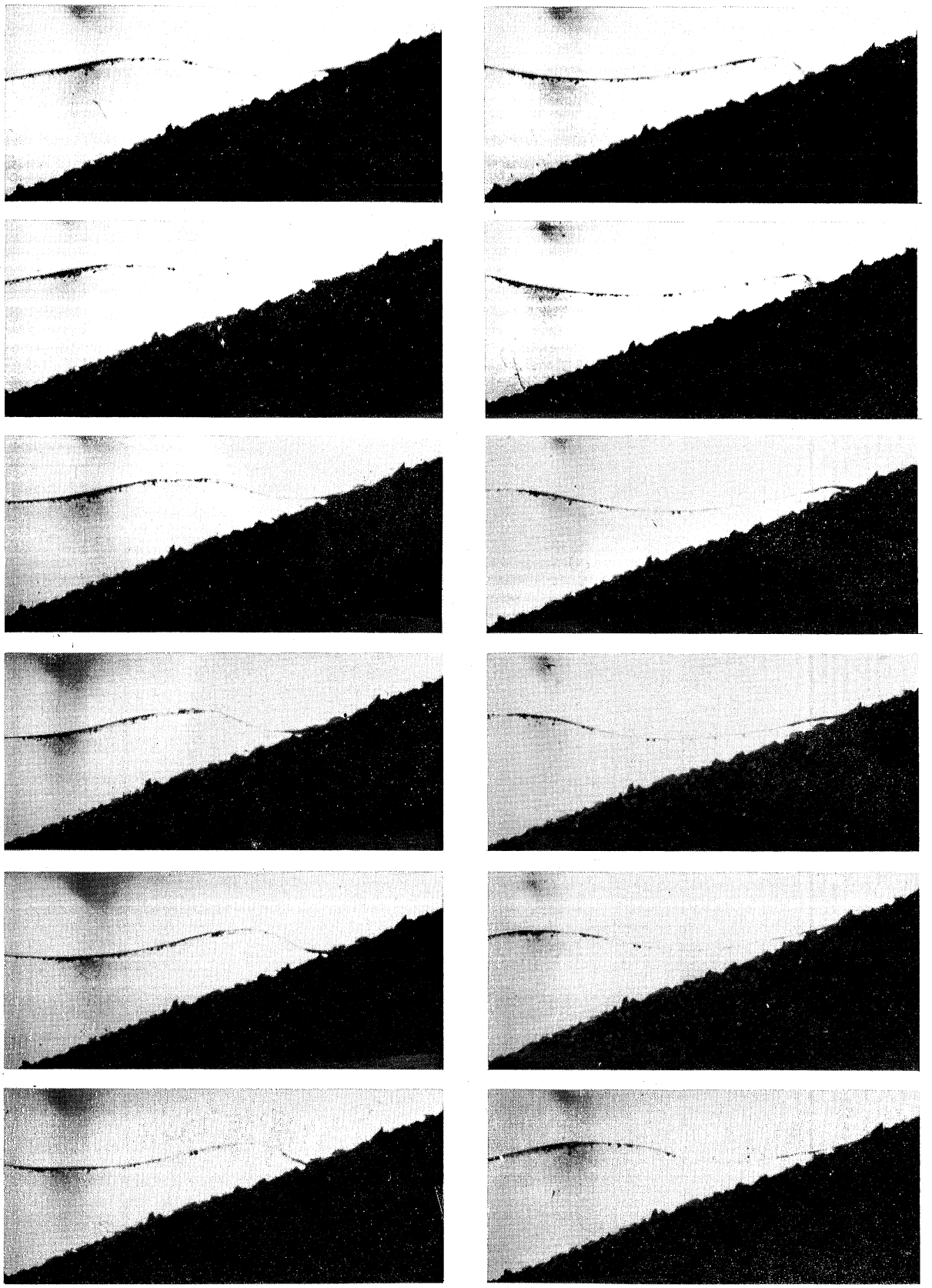

Fig. E-3 - A Sequence of Pictures Showing Wave Breaking on a Crushed-Rock-Type Absorber

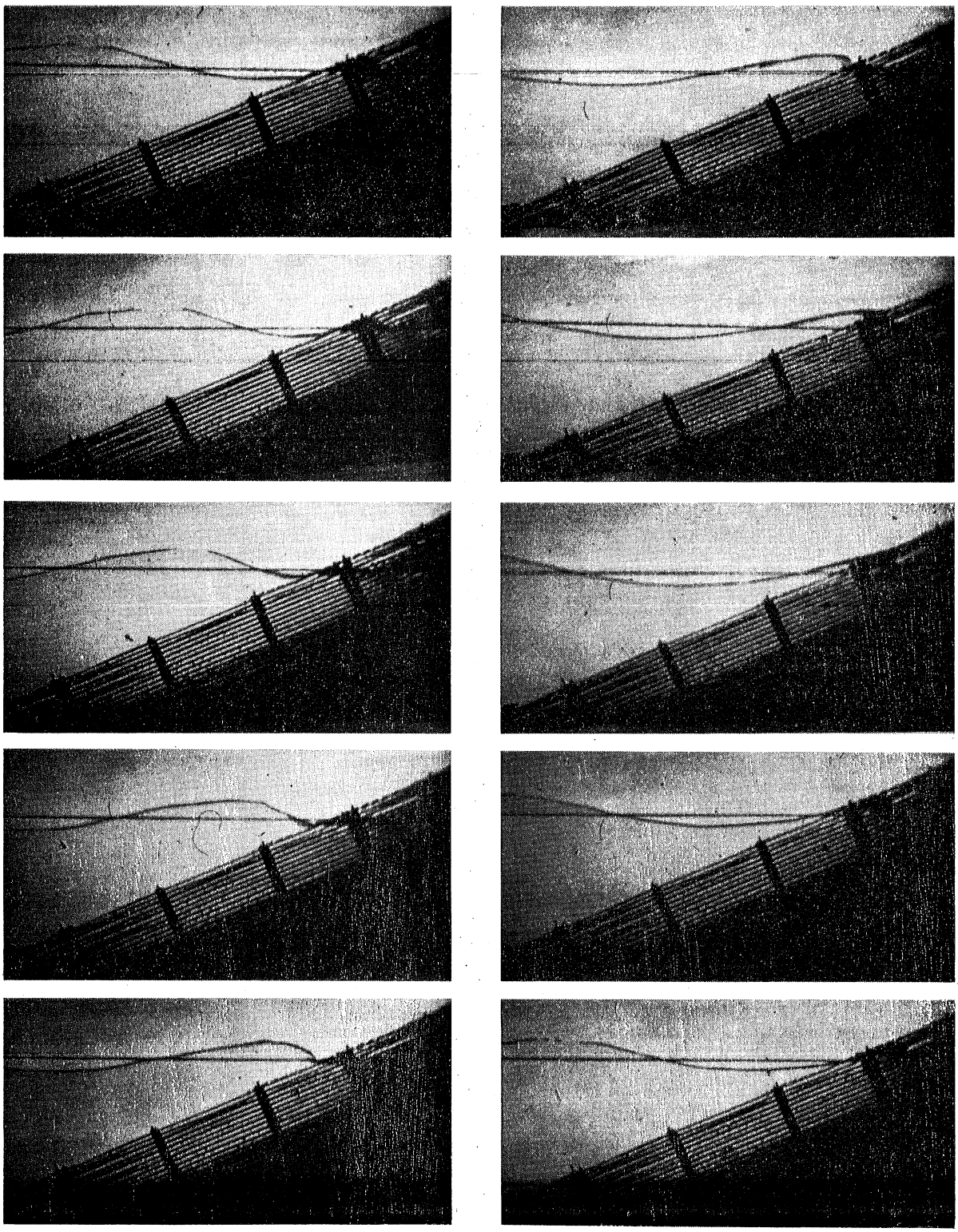

Fig. E-4 - A Sequence of Pictures Showing Wave Breaking on a Perforated Plate-Type Absorber

A P P E N D I X F

VARIOUS EXPERIMENTAL DATA

This Appendix includes various experimental investigations not described, or only referred to, in the main body of the report.

(1) Round Rods and Triangular-Wedge Absorbers

In accordance with a request of the Sponsor's representative, a limited number of tests was conducted on absorbers consisting of round rods and triangular-wedge bars placed on a 6-degree (approximately 1:10) slope. It was indicated that the information was desired for a special application in which it was possible to employ a long absorber with a flat slope.

The shape and spacing of the bars is shown in Figs. F-1, F-3, and F-4.

Tests were conducted in a 6-in. channel at a water depth of 9 inches. The reflection coefficient was measured for waves with a length of 2.0 ft and 4.4 ft and steepness ratios (H_I/L) varying from 0.01 to 0.07. Absorbers with surface slope of 6 degrees and 30 degrees were tested.

Test data for the 6-degree slope are shown in Figs. F-3(a) and F-4(a). For comparison reasons data for an impermeable beach absorber of the same slope are also indicated. The reflections from both the round and triangular bars, as well as the impermeable beach, are quite low, the round bars having a slight advantage.

Test data for the 30-degree slope are presented in Figs. F-3(b) and F-4(b). Here the triangular bars were superior to the round bars; the reflected wave height for the triangular bars was approximately 75 per cent of that for the round bars, depending on the incident wave steepness and length. For comparative purposes, the wire-mesh unit had a reflected wave height ranging from one-sixth to one-half of the triangular bars. It is possible that somewhat greater efficiencies could be achieved with the bar-type units by varying the bar size and spacing.

(2) "Sandwich" Type Absorbers

A number of absorbers were constructed where layers of crushed rock were separated by square-bar mats. It was thought that by doing so, it would

be easier to control the porosity of rock, and that the square-bar mats might have a beneficial effect. The tests (Figs. F-7 and F-8 indicated that there is no reduction in coefficient of reflection when a "sandwich" type was employed, but due to the difficulty of controlling the placement of rock and its porosity, the tests are considered inconclusive. In order to determine the comparative merits of the "sandwich" type construction, other materials of uniform porosity should be selected for the permeable part of the absorber.

Figure F-7 presents the results obtained for absorbers with permeable layers 3 in. deep and Fig. F-8 with permeable layers 4-1/2 in. deep.

(3) Combination-Type Absorber

In connection with study of discontinuous-slope absorbers, some tests were performed on absorbers constructed of crushed rock and perforated plates. Figure F-10(a) illustrates the data obtained for an absorber with one perforated plate over a 3-in. crushed-rock layer backed with an impermeable plate. The reflections are low for the 1.0- and 2.0-ft wave lengths, but an increase of wave lengths to 3.3 and 4.4 ft produced considerable reflections. The addition of two more perforated plates Fig. F-10(b) produced lower reflections for the 4.4-ft wave length. For comparison purposes, the data for a similar absorber, but without perforated plates, are presented in Fig. F-11. Figure F-13 indicates that an absorber backed with an impermeable beach was more efficient than that employing a perforated plate.

(4) Crushed-Rock Absorbers

In connection with choice of materials for the permeable part of the absorber, a great number of tests were performed on screened gravel and crushed-rock absorbers. The data for some of these tests are presented here.

(5) Perforated-Plate Absorbers

In the main body of the report (Chap. III on p. 28) studies were described on the effect of porosity of permeable medium on coefficient of reflection. Perforated-plate absorbers were chosen for porosity range above 93 per cent. In connection with this study, a brief test was performed on the effect of slope of perforated plates forming such an absorber. The tests showed that the absorber constructed of sloping plates was more efficient for a 3.3-ft wave, as compared with a similar absorber constructed of horizontal plates (Fig. F-18).

(6) Parabolic and Discontinuous-Slope Absorbers

In connection with the applied study of short length absorbers, a number of tests were performed on parabolic and discontinuous-slope-type absorbers. The experimental data obtained is presented in Fig. F-19.

(7) Square-Bar-Type Absorbers

In connection with the applied study (Chap. III, p. 31) a number of tests were performed on a short length square-bar absorber. The experimental data are presented in Fig. 20.

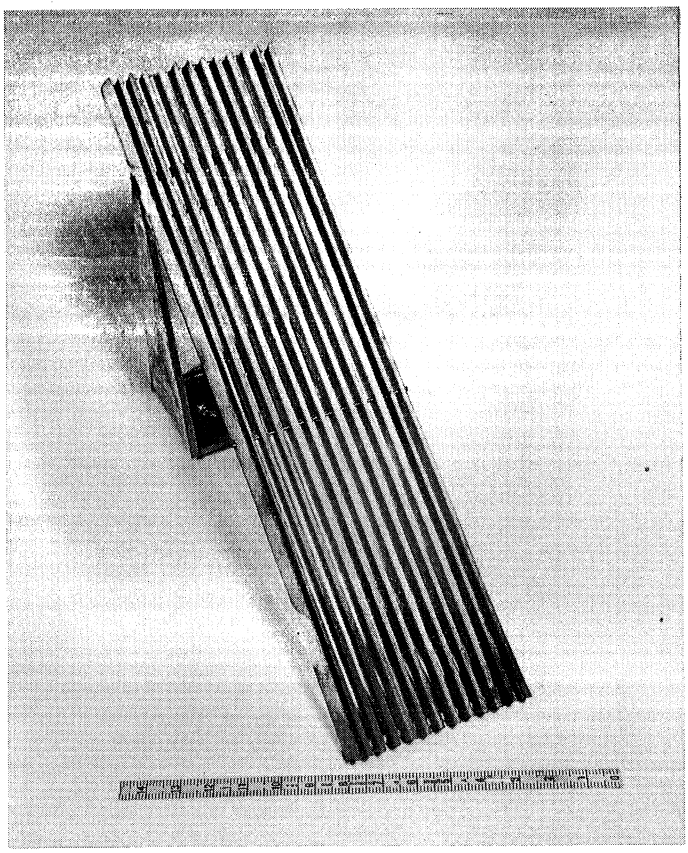

Fig. F-1 - A Close-Up View of a Triangular-Wedge Absorber

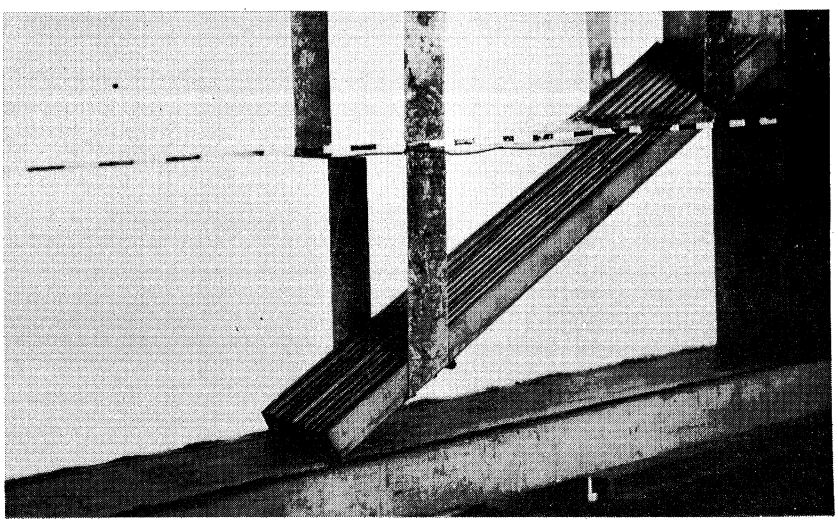

Fig. F-2 - View of a Triangular-Wedge Absorber Installed in a 6-in. Channel. Surface Slope 30 degrees

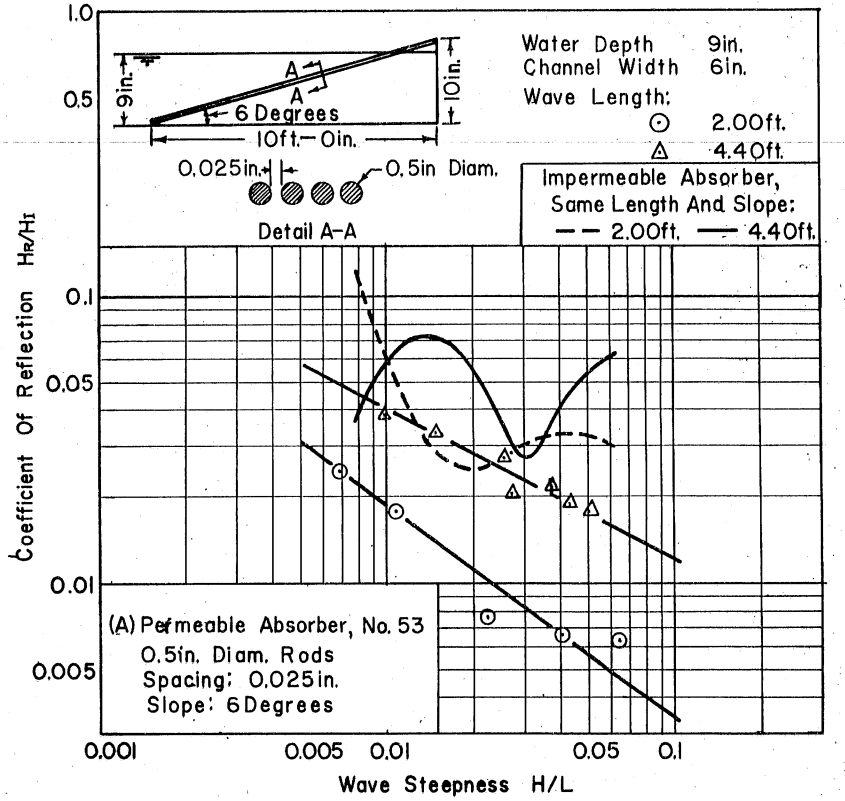

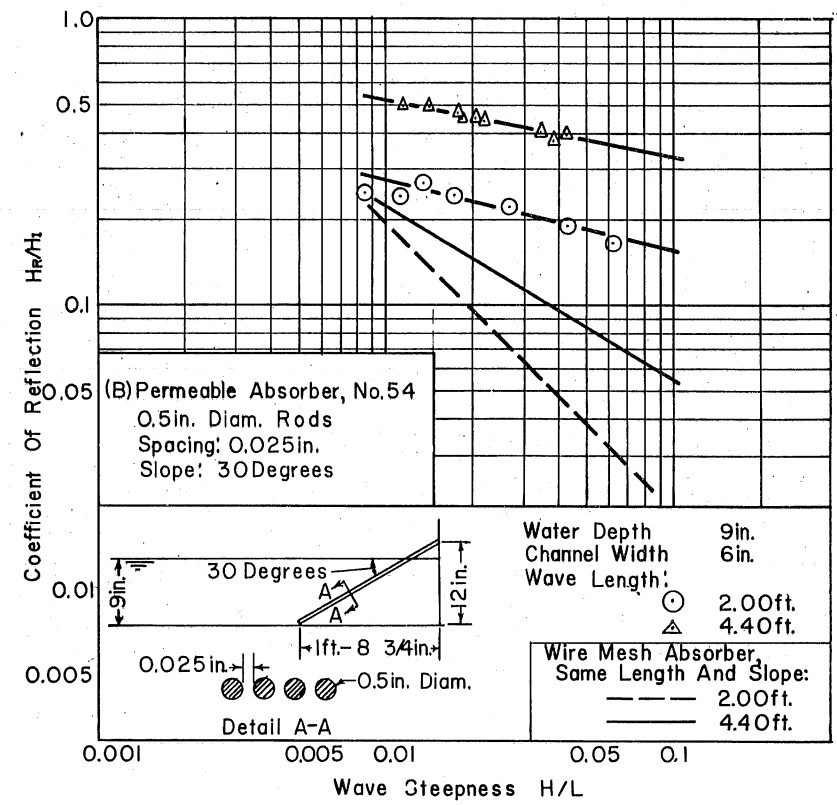

Fig. F-3 – Coefficient of Reflection for Round-Rod Absorbers

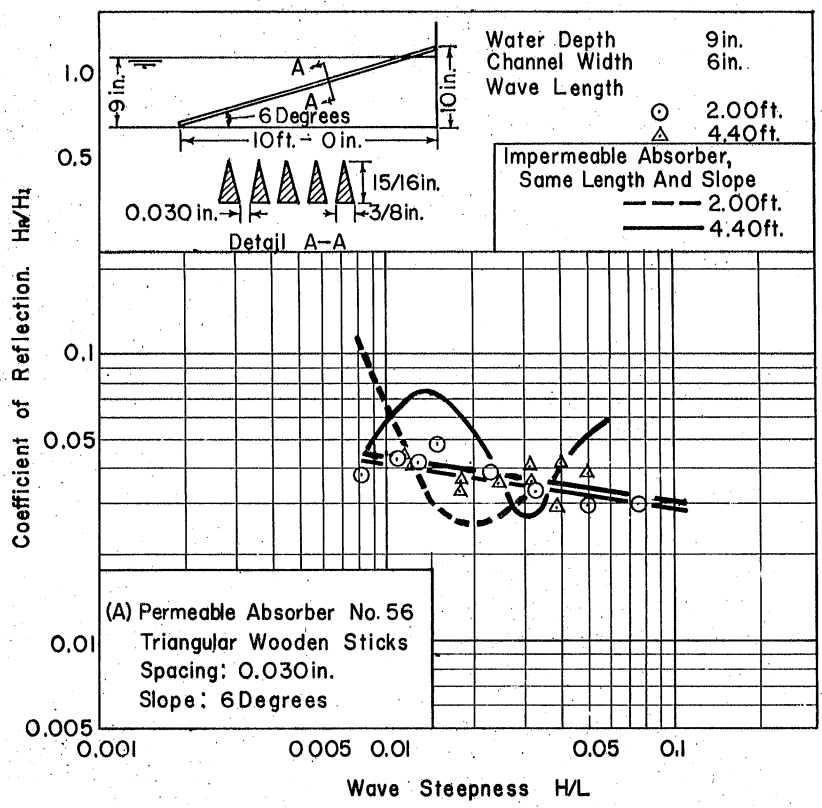

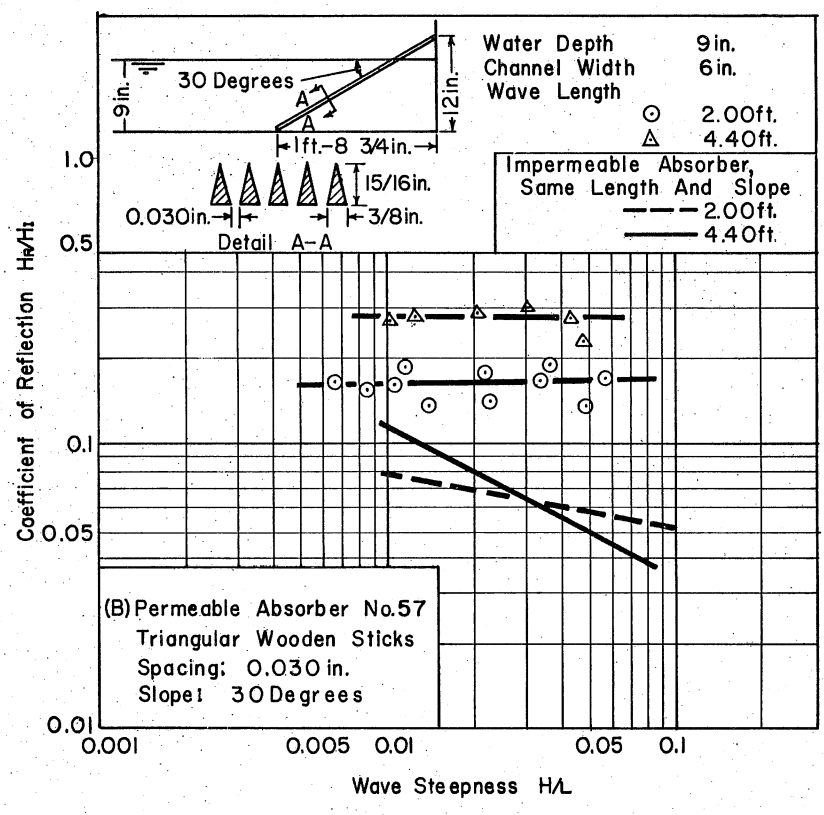

Fig. F-4 – Coefficient of Reflection for Triangular-Wedge Absorbers

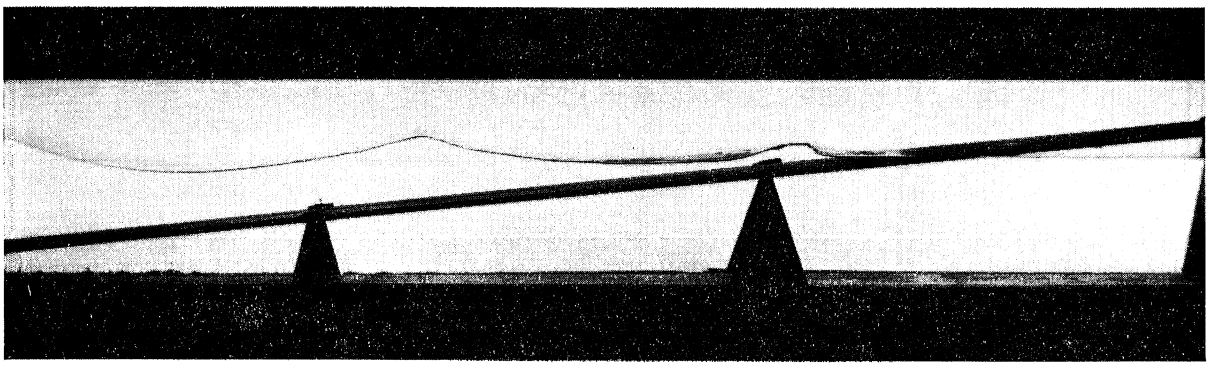

Fig. F-5 - View of Wave Action on a Round-Rod Absorber. (A 3-ft wave with H_I/L = 0.087 is shown approaching the absorber. Only a very low reflection was observed.)

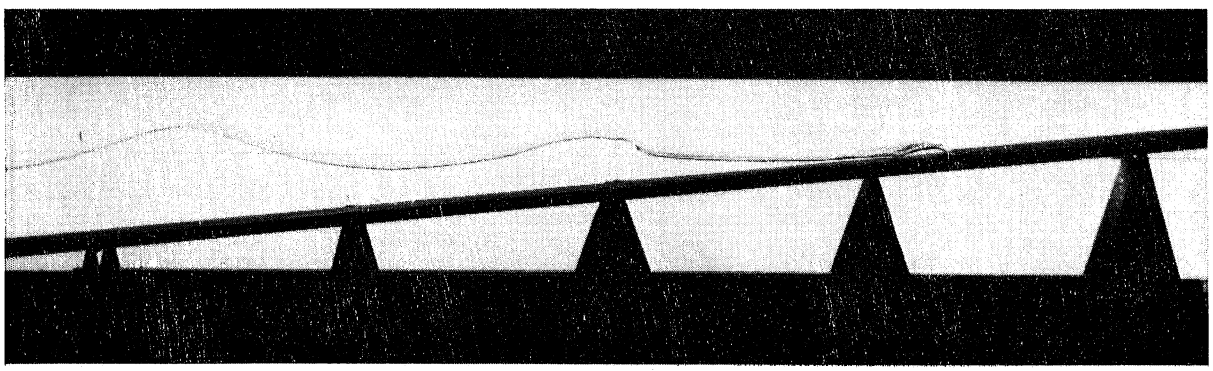

Fig. F-6 - View of Wave Action on a Triangular-Wedge Absorber. (A 3-ft wave with H_I/L = 0.073 is shown approaching the absorber. Only a very low reflection was observed.)

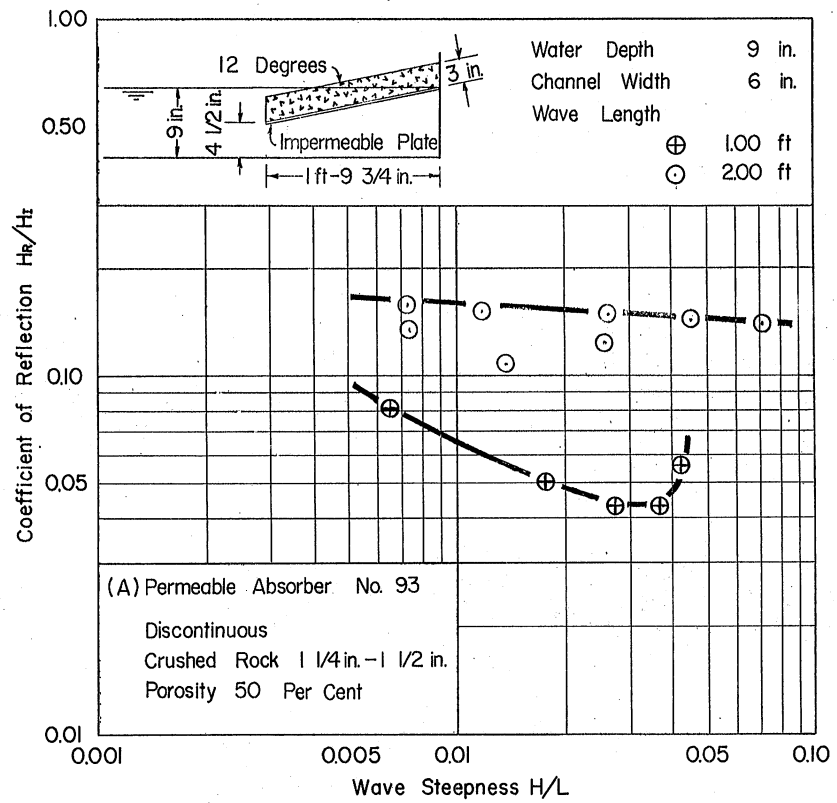

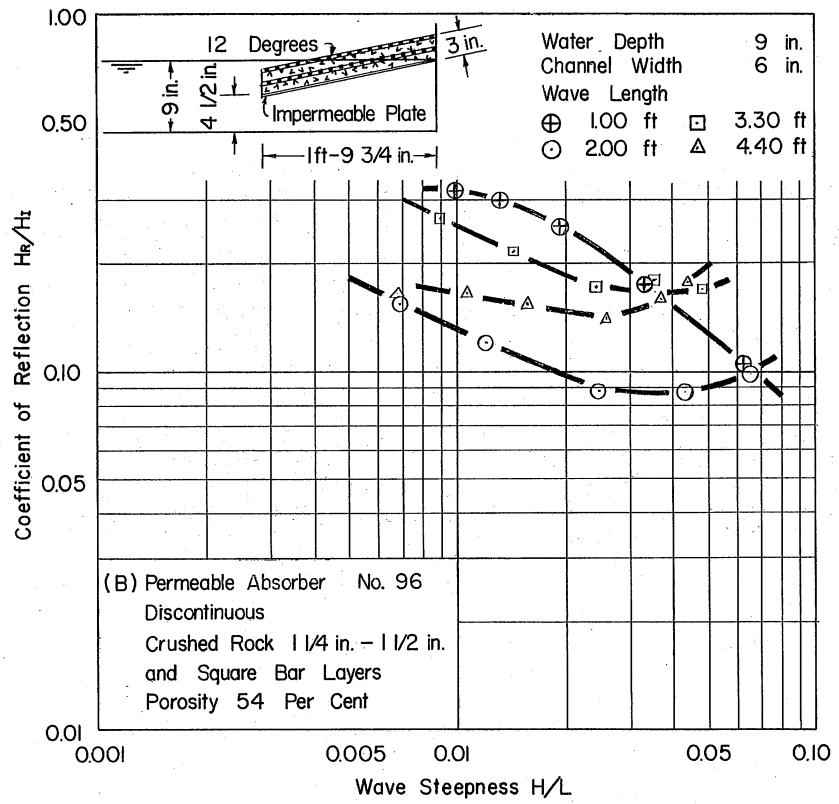

Fig. F-7 - Wave Reflection for a "Sandwich" Type Crushed-Rock Absorber

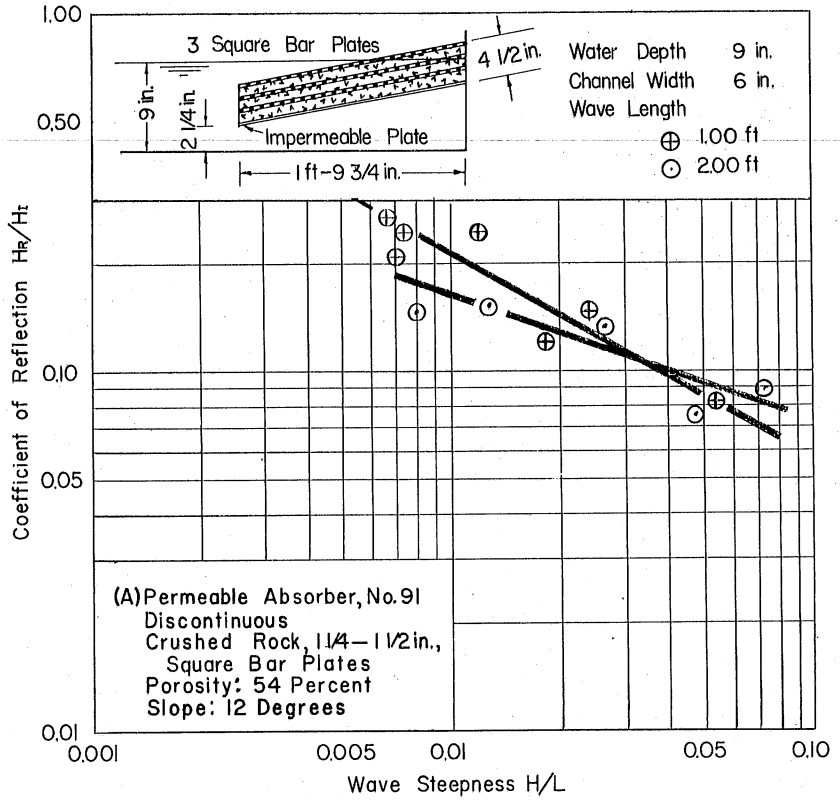

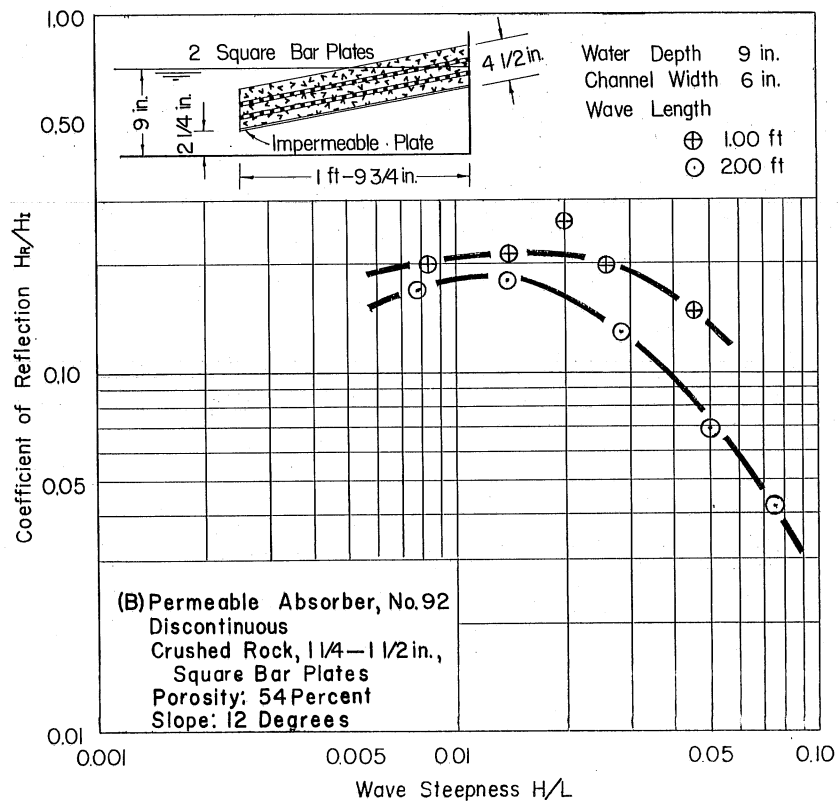

Fig. F-8 - Wave Reflection for a "Sandwich" Type Crushed-Rock Absorber

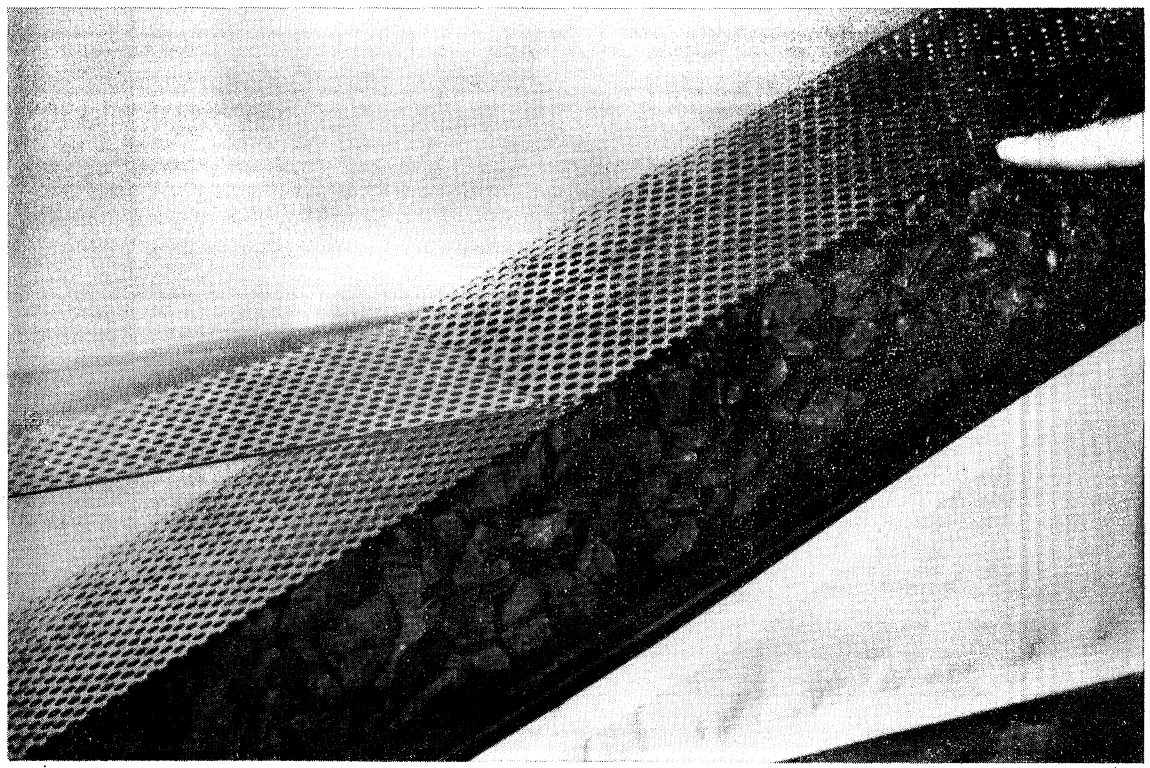

Fig. F-9 - A View of Permeable Absorber No. 65 Constructed of Crushed Rock and Perforated Plates. (Crushed rock passing a 2-in. screen and retained on 1-1/2-in. screen, perforated plate 37 per cent voids. Surface slope 22 degrees.)

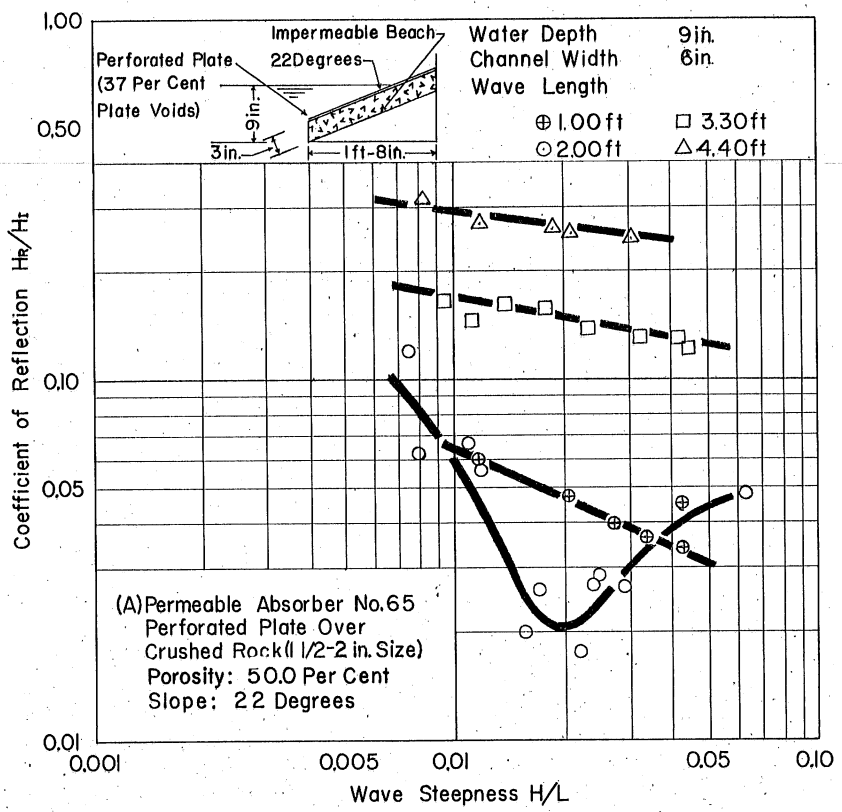

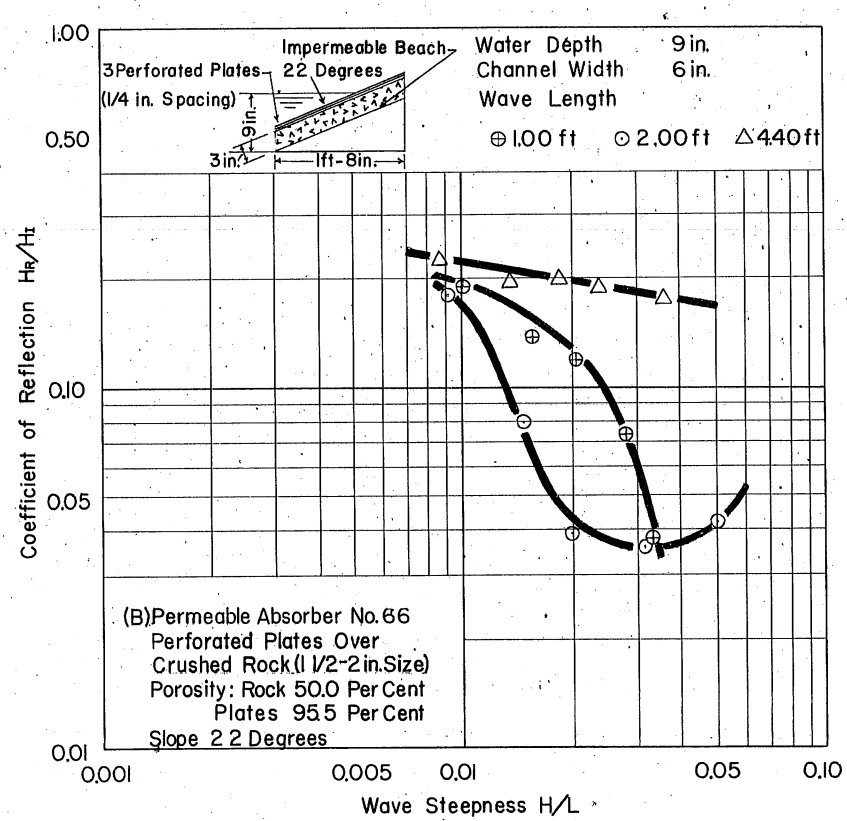

Fig. F-10 - Coefficient of Reflection for Perforated-Plate—Crushed-Rock Absorbers

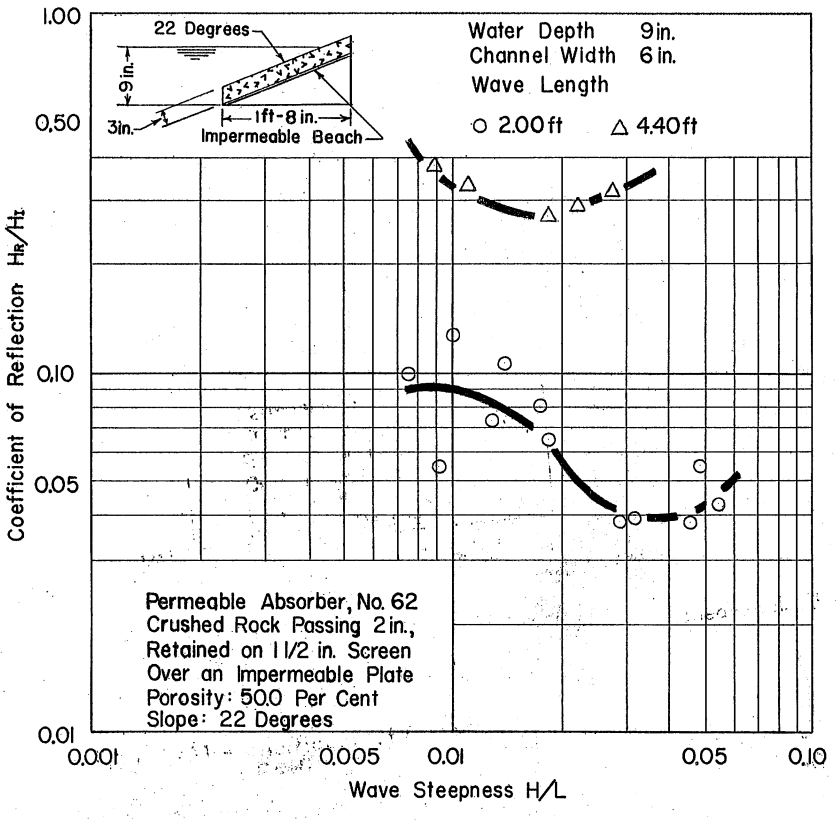

Fig. F-11 – Coefficient of Reflection for a Crushed-Rock Absorber

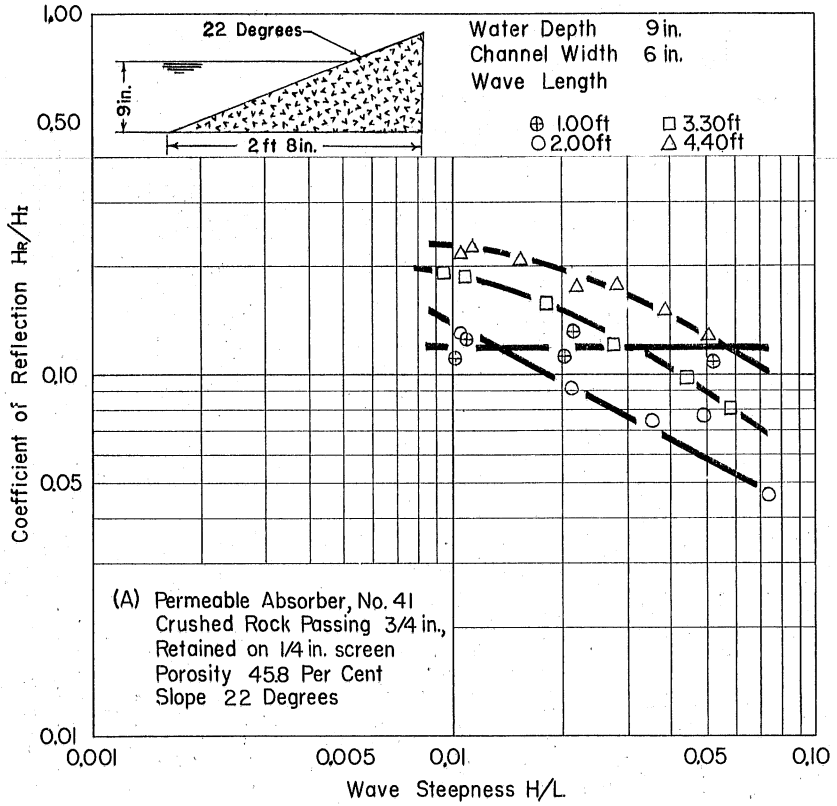

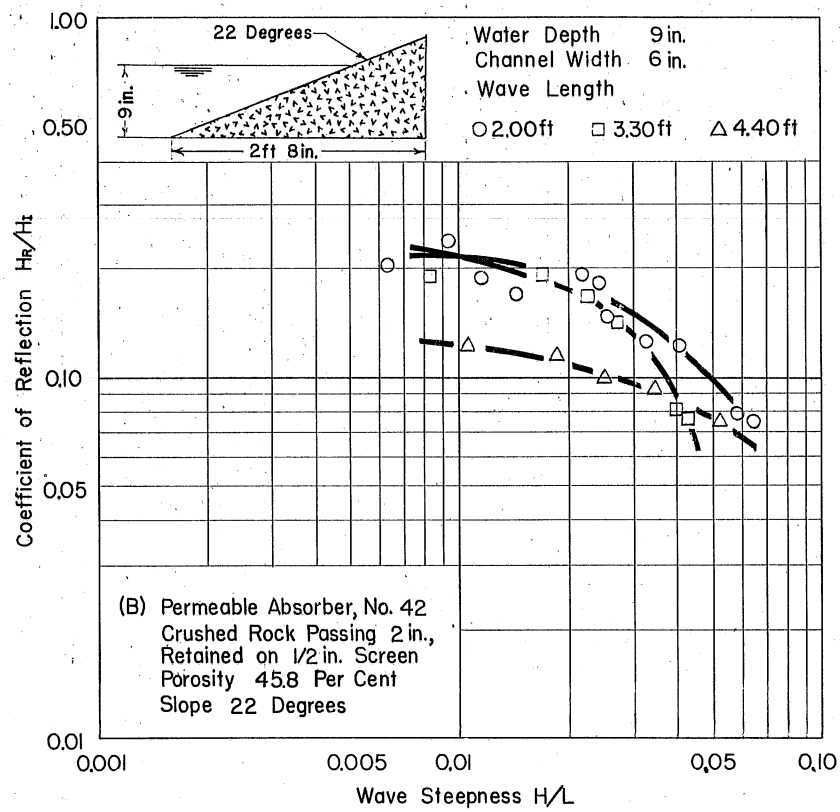

Fig. F-12 - Coefficient of Reflection for Crushed-Rock Absorbers--Surface Slope 22 degrees

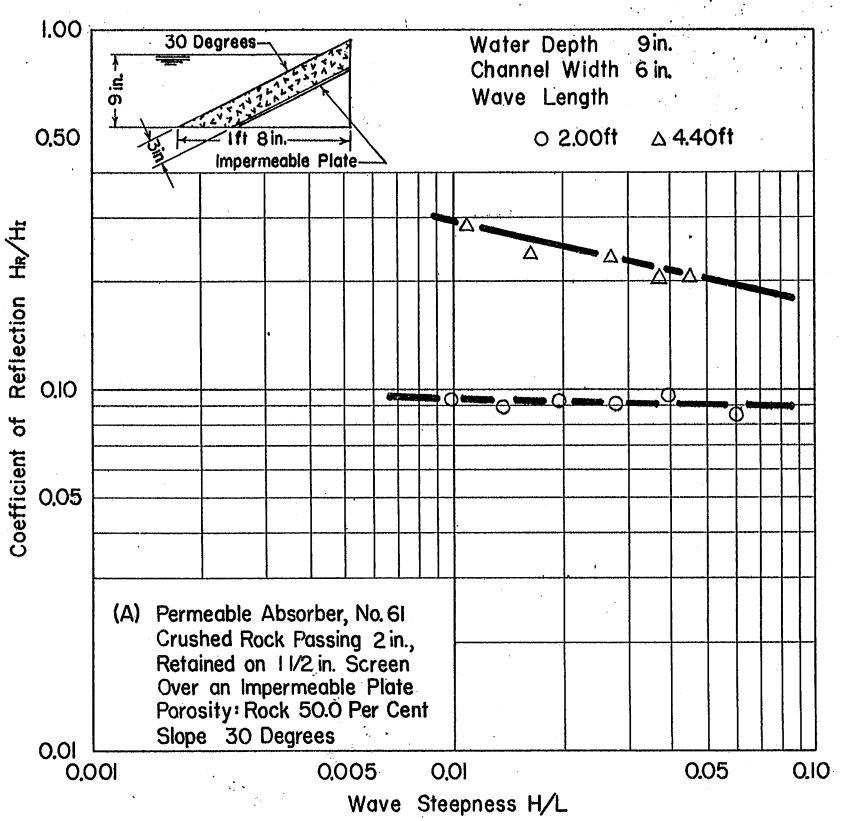

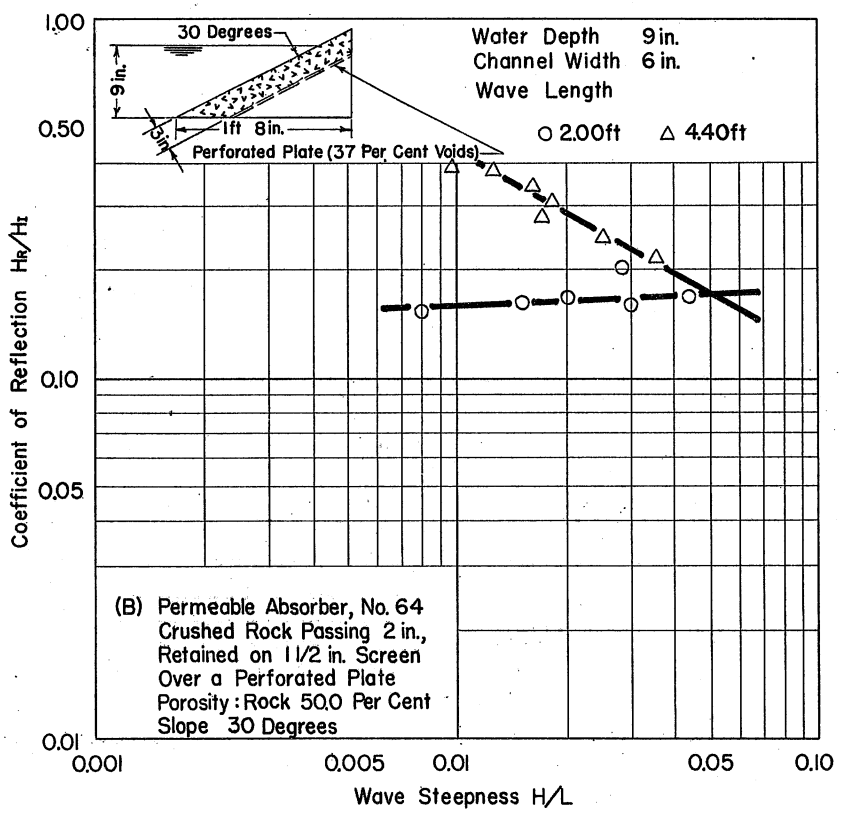

Fig. F-13 – Coefficient of Reflection for Permeable Absorbers Backed with a Perforated or an Impermeable Plate

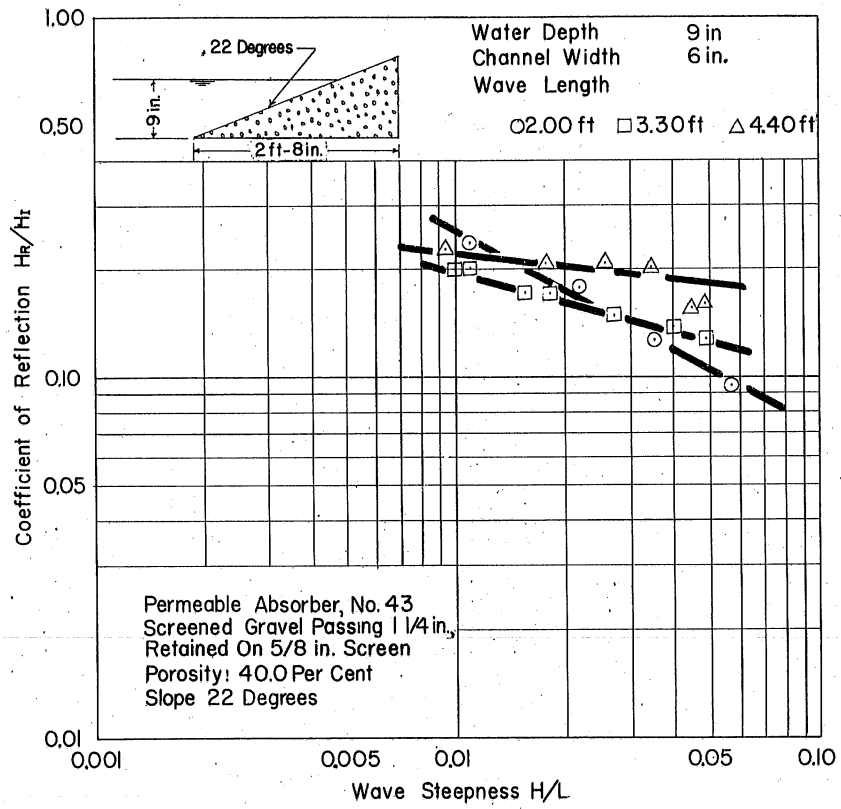

Fig. F-14 - Coefficient of Reflection for a Gravel Absorber

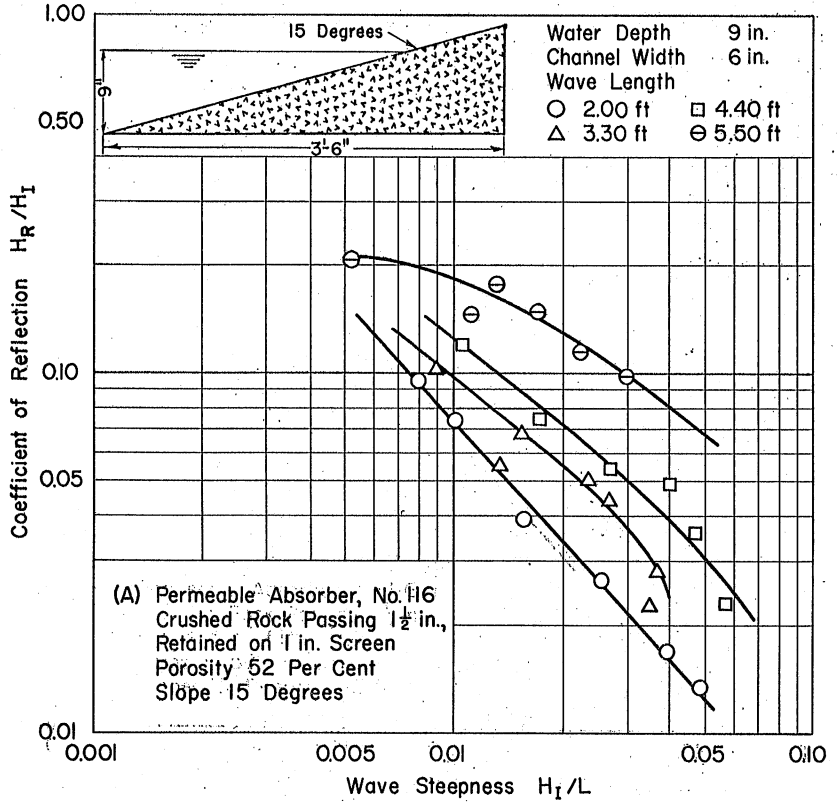

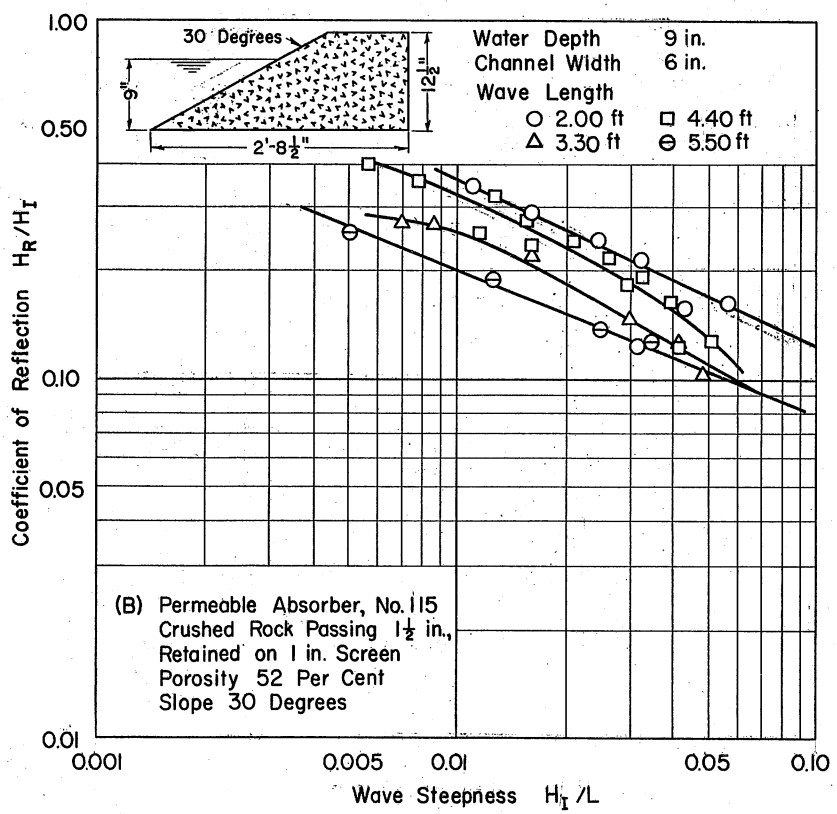

Fig. F-15 – Coefficient of Reflection for Crushed-Rock Absorbers-- Surface Slope 15 and 30 degrees

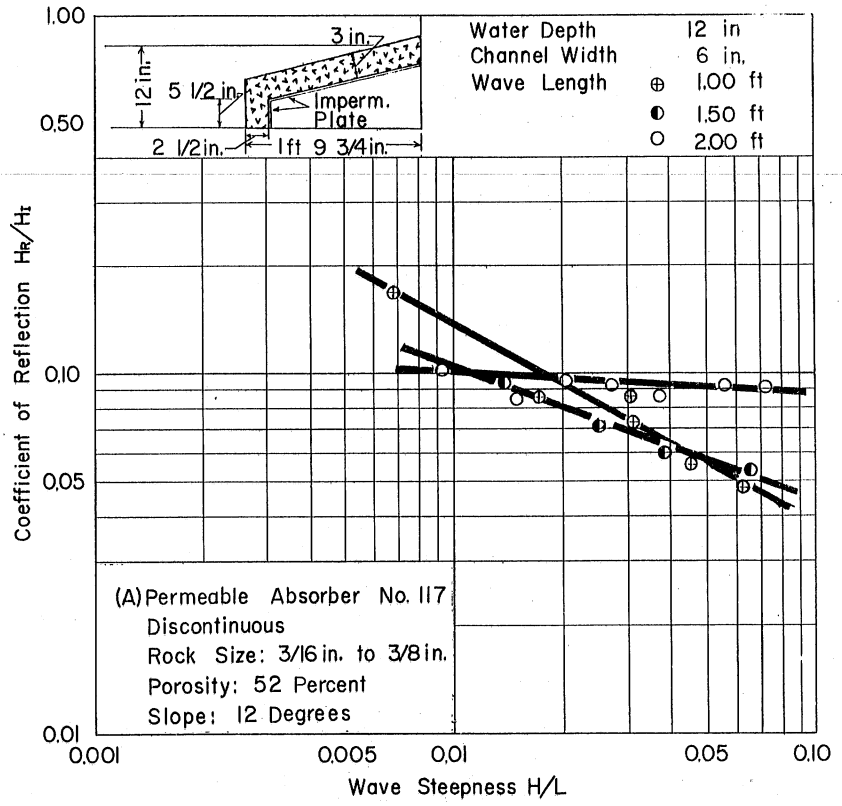

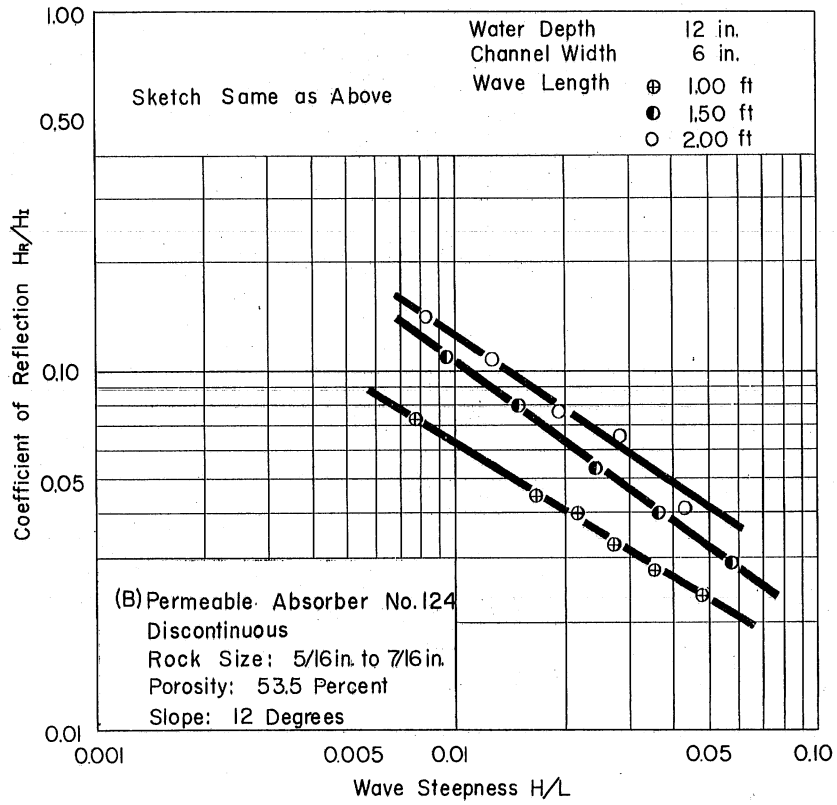

Fig. F-16 – Coefficient of Reflection for Discontinuous Crushed-Rock Absorbers

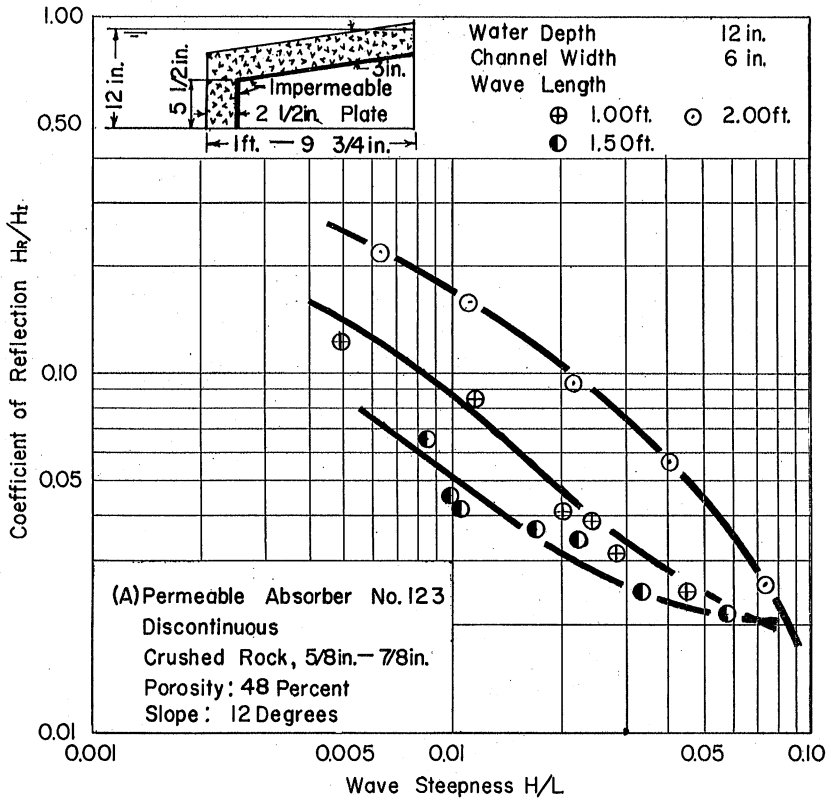

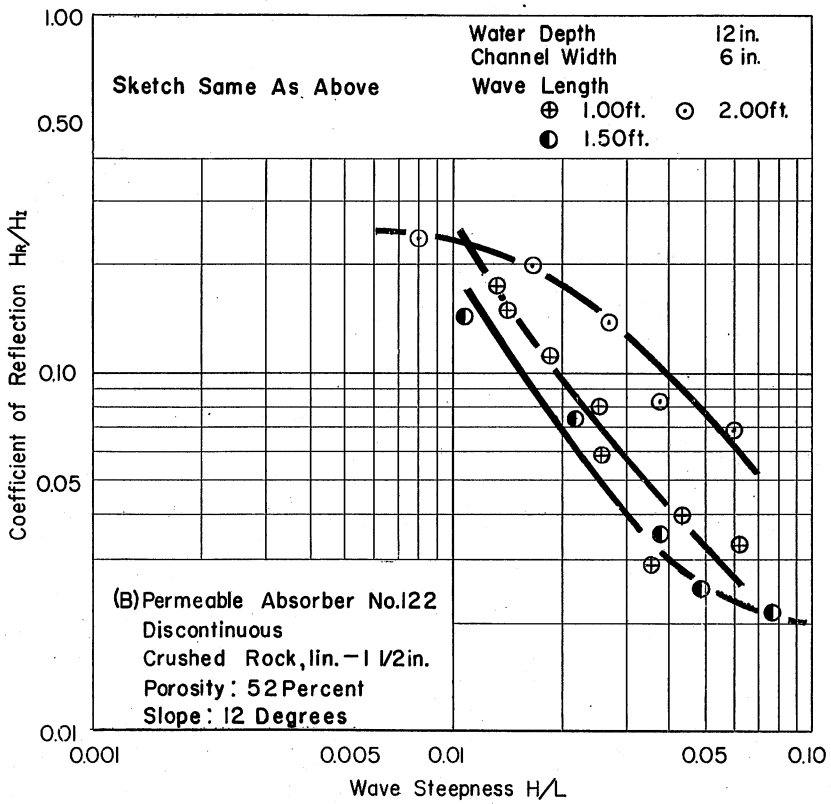

Fig. F-17 - Coefficient of Reflection for Discontinuous Crushed-Rock Absorbers

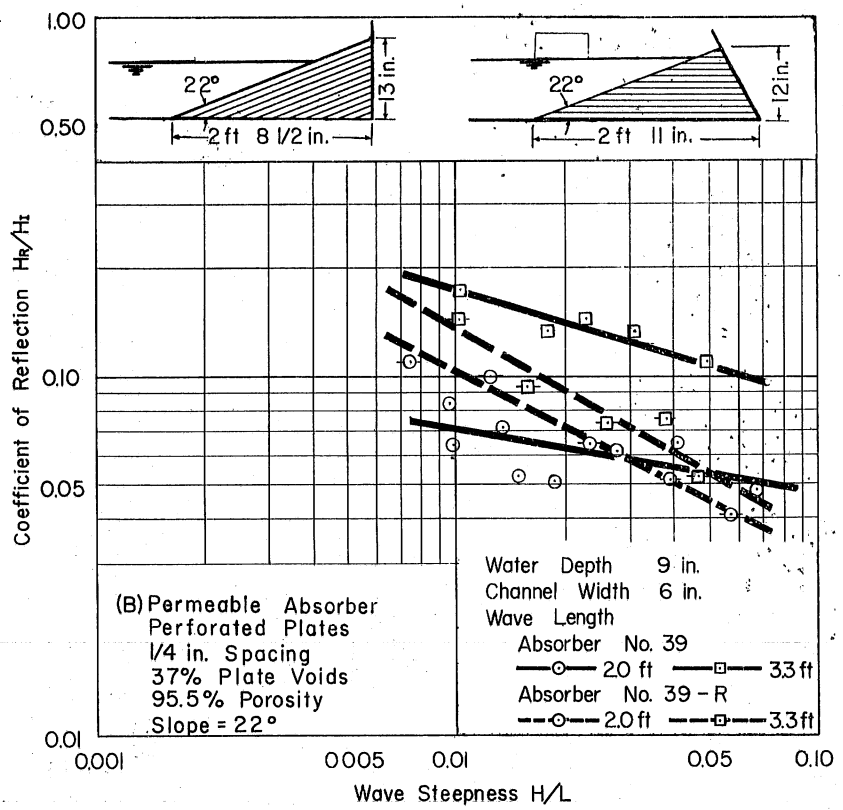

Fig. F-18 - Comparison of Two Perforated-Plate Absorbers

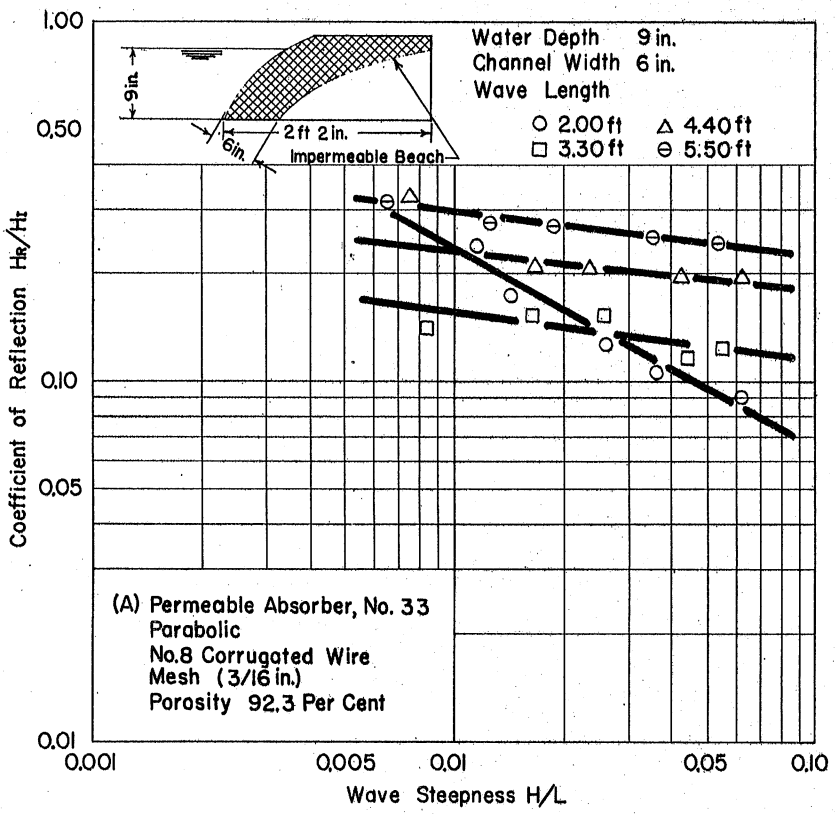

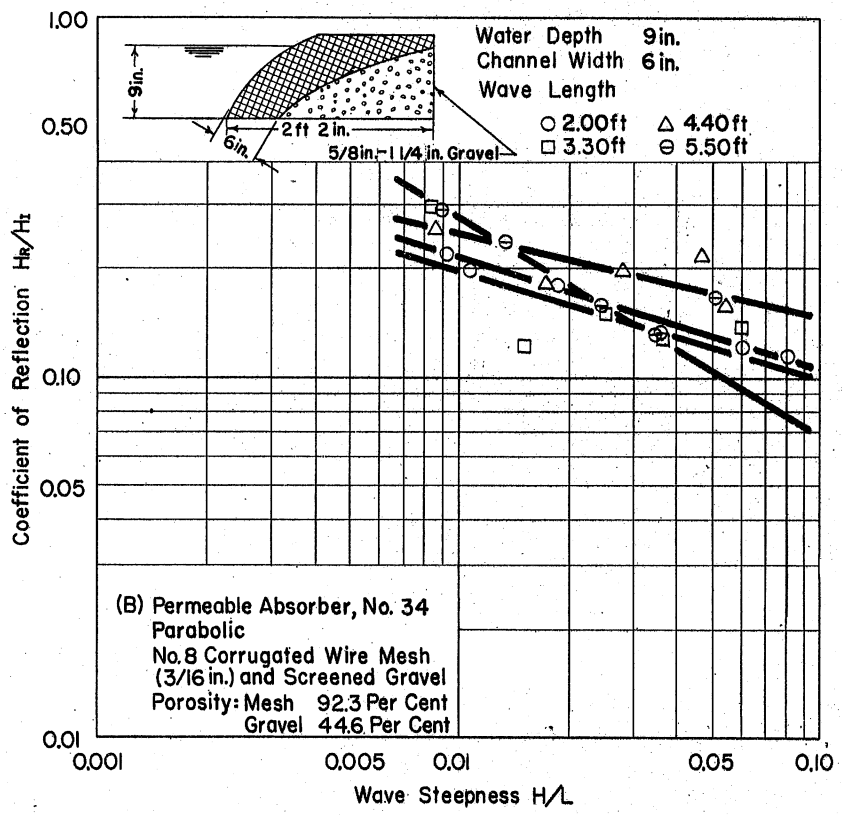

Fig. F-19 – Coefficient of Reflection for Short Parabolic-Type Absorber

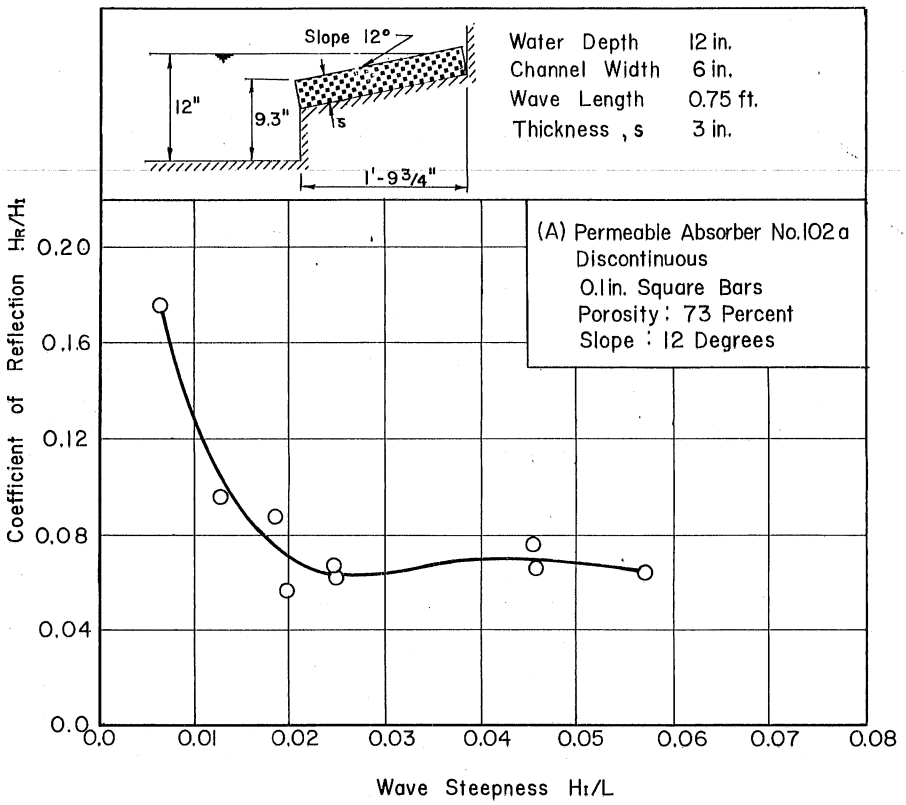

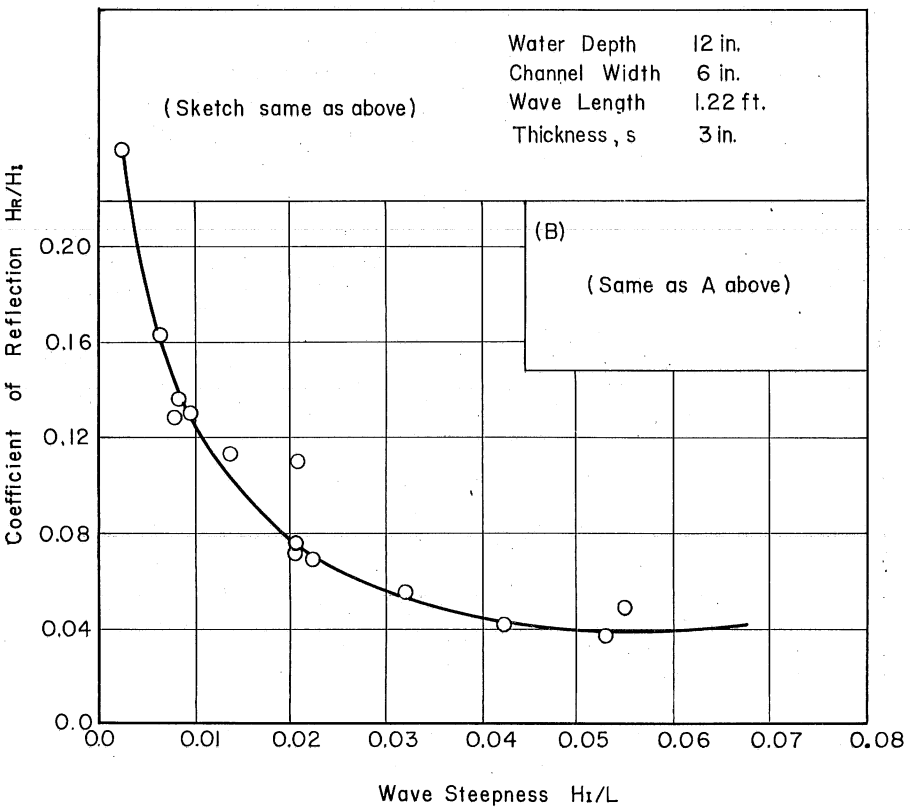

Fig. F-20 - Coefficient of Reflection as a Function of Wave Steepness for Various Wave Lengths for a Bar-Type Absorber. (a) L = 0.75 ft, (b) L = 1.22 ft

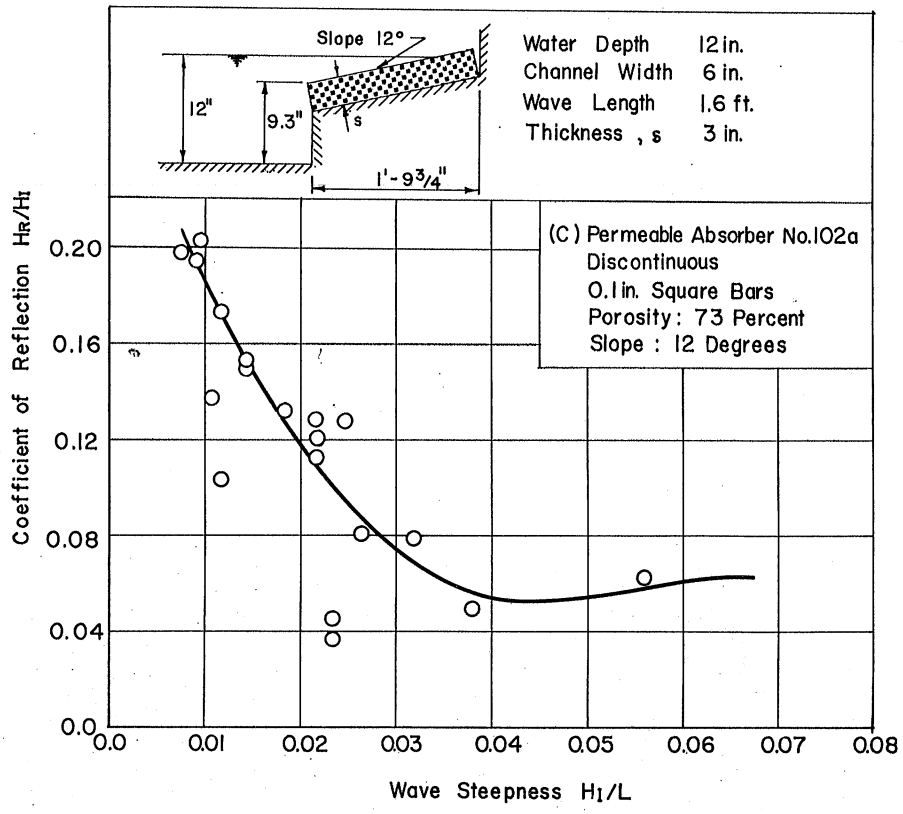

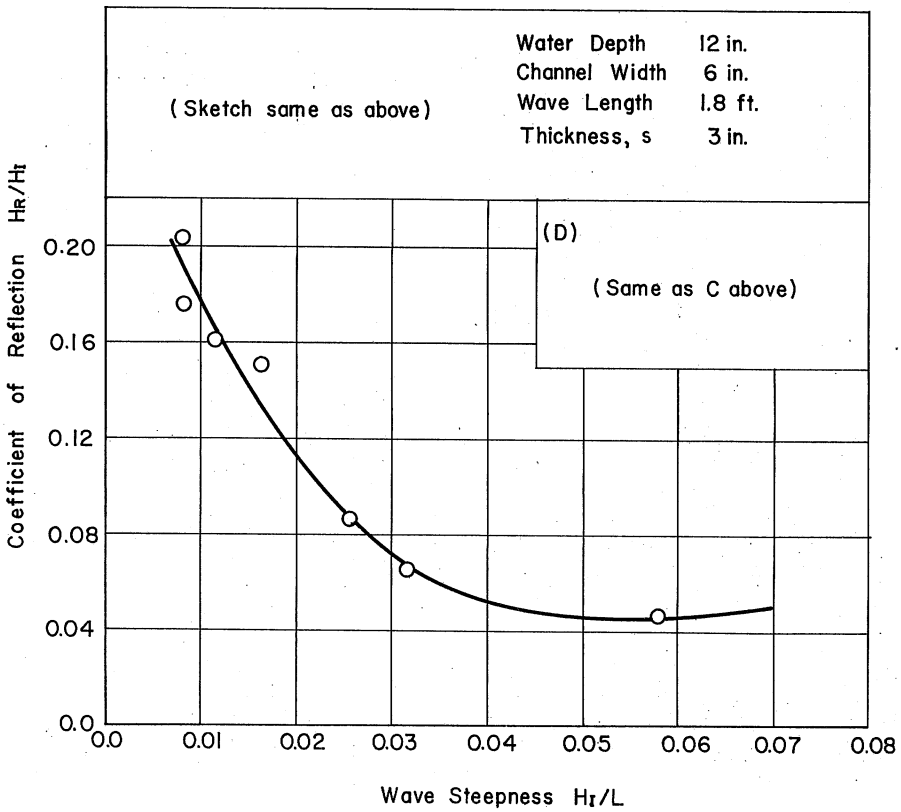

Fig. F-20 – Coefficient of Reflection as a Function of Wave Steepness for Various Wave Lengths for a Bar-Type Absorber. (c) L = 1.6 ft, (d) L = 1.8 ft

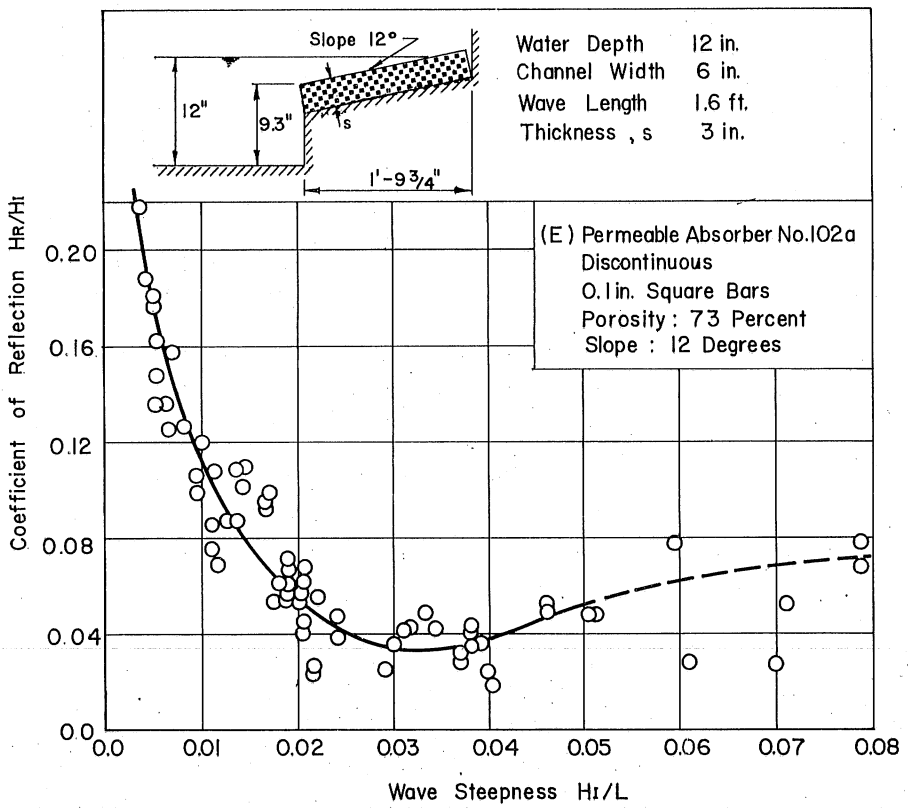

Fig. F-20 – Coefficient of Reflection as a Function of Wave Steepness for Various Wave Lengths for a Bar-Type Absorber. (e) L = 1.6 ft

DISTRIBUTION LIST FOR PROJECT REPORT NO. 44
of the St. Anthony Falls Hydraulic Laboratory

Copies	Organization
20	Commanding Officer and Director, David Taylor Model Basin, Navy Department, Washington 25, D. C., Attn: Code 580.
11	Chief, Bureau of Ships, Department of the Navy, Washington 25, D. C., Attn: Project Records (Code 324). For distribution as follows: 5 - Project Records 3 - Research (Code 300) 1 - Technical Assistant to Chief of the Bureau (Code 106) 1 - Preliminary Design (Code 420) 1 - Hull Design (Code 440)
6	Chief, Bureau of Yards and Docks, Department of the Navy, Washington 25, D. C.
3	Chief, Bureau of Ordnance, Department of the Navy, Washington 25, D. C. Attn: Underwater Ordnance (Code Re6a).
3	Chief, Bureau of Aeronautics, Department of the Navy, Washington 25, D. C., Attn: Aero and Hydrodynamics (Code DE-3).
3	Chief of Naval Research, Department of the Navy, Washington 25, D. C., Attn: Fluid Mechanics (Code N426).
1	Director, Naval Research Laboratory, Washington 25, D. C., Attn: Code 2021.
1	Commanding Officer, Office of Naval Research, Branch Office, The John Crerar Library Building, 86 East Randolph Street, Chicago 1, Illinois.
1	Commanding Officer, Naval Ordnance Laboratory, White Oak, Silver Spring 19, Maryland.
1	Commander, Naval Ordnance Test Station, 3202 East Foothill Boulevard, Pasadena, California.
1	Commanding Officer and Director, Underwater Sound Laboratory, Fort Trumbull, New London, Connecticut.
1	Hydrographer, Department of the Navy, Washington 25, D. C.
1	Superintendent, U. S. Naval Postgraduate School, Monterey, California, Attn: Librarian.
1	Office of Ordnance Research, Department of the Army, Washington 25, D. C.
1	Director, Waterways Experiment Station, Box 631, Vicksburg, Mississippi.

Copies	Organization
1	Office of the Chief of Engineers, Department of the Army, Gravelly Point, Washington 25, D. C.
1	The President, Beach Erosion Board, 5201 Little Falls Road, N. W., Washington 16, D. C.
1	Director of Research, National Advisory Committee for Aeronautics, 1724 F Street, N. W., Washington 25, D. C.
1	Director, Langley Aeronautical Laboratory, National Advisory Committee for Aeronautics, Langley Field, Virginia.
1	Director, Hydraulic Laboratory, Bureau of Reclamation, Denver Federal Center, Denver, Colorado.
1	U. S. Geological Survey, Department of the Interior, Washington 25, D. C., Attn: C. G. Paulsen, Chief, Hydraulic Engineer.
1	Documents Service Center, Armed Service Technical Information Agency, Knott Building, Dayton 2, Ohio.
2	Chief, National Bureau of Standards, National Hydraulic Laboratory, Washington 25, D. C.
2	Newport News Shipbuilding and Dry Dock Company, Newport News, Virginia. For distribution as follows: 1 - Senior Naval Architect 1 - Supervisor, Hydraulic Laboratory
9	British Joint Services Mission, Navy Staff, P. O. Box 165, Benjamin Franklin Station, Washington, D. C.
3	The Naval Member, Canadian Joint Staff, 2001 Connecticut Avenue, N. W., Washington 8, D. C.
1	Professor M. L. Albertson, Department of Civil Engineering, Colorado A & M College, Fort Collins, Colorado.
1	California Institute of Technology, Hydrodynamics Laboratory, Pasadena 4, California, Attn: Dr. R. T. Knapp.
1	California Institute of Technology, Hydrodynamics Laboratory, Pasadena 4, California, Attn: Professor M. S. Plesset.
1	Columbia University, Department of Civil Engineering, New York 27, New York.
2	Dr. K. S. M. Davidson, Experimental Towing Tank, Stevens Institute of Technology, 711 Hudson Street, Hoboken, New Jersey.
1	Professor H. A. Einstein, Department of Engineering, University of California, Berkeley 4, California.

Copies	Organization
1	Professor W. S. Hamilton, Department of Civil Engineering, Northwestern University, Evanston, Illinois.
1	Dr. A. T. Ippen, Hydrodynamics Laboratory, Massachusetts Institute of Technology, Cambridge 39, Massachusetts.
1	Head, Department of Naval Architecture and Marine Engineering, Massachusetts Institute of Technology, Cambridge 39, Massachusetts.
1	Director, Woods Hole Oceanographic Institute, Woods Hole, Massachusetts, Attn: Dr. C. O. Iselin.
1	Dean M. P. O'Brien, Department of Engineering, University of California, Berkeley 4, California.
1	Dr. R. R. Revelle, Scripps Institute of Oceanography, La Jolla, California.
1	Dr. Hunter Rouse, Director, Iowa Institute of Hydraulic Research, State University of Iowa, Iowa City, Iowa.
1	Dr. V. L. Streeter, University of Michigan, Ann Arbor, Michigan.
1	Professor J. K. Vennard, Department of Civil Engineering, Stanford University, Stanford, California.
1	Librarian, John Crerar Library, Chicago 1, Illinois.
1	Librarian, Engineering Societies Library, 29 West 39th Street, New York 18, New York.
2	Library, California Institute of Technology, Pasadena, California.
1	Librarian, Massachusetts Institute of Technology, Cambridge 39, Massachusetts.
1	Librarian, Library of Congress, Washington 25, D. C.
1	Librarian, School of Engineering, University of Texas, Austin, Texas.
2	Director, Naval Ordnance Research Laboratory, Pennsylvania State College, State College, Pennsylvania.
3	Serials Division, University of Minnesota Library, Minneapolis, Minnesota.